Universidade de Aveiro Departamento de Engenharia Mecânica
Ano 2012/2013

Gonçalo José Rodrigues Costa

EXPERIMENTAL INVESTIGATION OF EDM PARAMETERS ON MACHINING AlMg10 15%SiC COMPOSITE BASED ON TAGUCHI METHOD

Universidade de Aveiro Departamento de Engenharia Mecânica
Ano 2012/2013

Gonçalo José Rodrigues Costa

EXPERIMENTAL INVESTIGATION OF EDM PARAMETERS ON MACHINING AlMg10 15%SiC COMPOSITE BASED ON TAGUCHI METHOD

Dissertation presented to the Faculty of Machine Manufacturing and Industrial Management of Gheorghe Asachi Technical University of Iasi for the fulfillment of the requirements to accomplish the Master degree in Mestrado Integrado em Engenharia Mecânica, tutored by Professor Doctor Margareta Coteata, Professor from Faculty of Machine Manufacturing and Industrial Management of Gheorghe Asachi Technical University of Iași

"Knowledge is acquired by experience, everything else is just information"

Albert Einstein

The jury

president

Prof. Dr. Laurentiu Slatineanu
professor from Faculty of Machine Manufacturing and Industrial Management of Gheorghe Asachi Technical University of Iași

Prof. Dr. Oana Dodun
associated professor from Faculty of Machine Manufacturing and Industrial Management of Gheorghe Asachi Technical University of Iași

Prof. Dr. Laurentiu Ghenghea
associated professor from Faculty of Machine Manufacturing and Industrial Management of Gheorghe Asachi Technical University of Iași

Prof. Doutor Nicolae Seghedin
Associated professor from Faculty of Machine Manufacturing and Industrial Management of Gheorghe Asachi Technical University of Iași

Prof. Doutor Constantin Carausu
associated professor from Faculty of Machine Manufacturing and Industrial Management of Gheorghe Asachi Technical University of Iași

Prof. Doutora Margareta Coteata
professor from Faculty of Machine Manufacturing and Industrial Management of Gheorghe Asachi Technical University of Iași

EXPERIMENTAL INVESTIGATION OF EDM PARAMETERS ON MACHINING AlMg10 15%SiC COMPOSITE BASED ON TAGUCHI METHOD

Master Thesis

Student Name: Gonçalo José Rodrigues Costa
Study Programme: Master Study Programme of Mechanical Engineering

Supervisor: Prof. Dr. Margareta Coteata

Iasi, June 2013

Acknowledgment

The author wishes to express his deepest sense of gratitude and indebtedness to his thesis supervisor Prof. Dr. Margareta Coteata, lecturer, at the Department of Machine Manufacturing Technology within the Faculty of Machine Manufacturing and Industrial Management of “Gheorghe Asachi” Technical University of Iasi, Romania, for providing precious guidance, inspiring discussions and constant supervision throughout the course of this work. Her timely help, constructive criticism, encouragement during the investigation and conscientious efforts made it possible to present the work contained in this experimental investigation.

The author also would like to thank Prof. Dr. Laurentiu Slatineanu, professor, at the Department of Machine Manufacturing Technology within the Faculty of Machine Manufacturing and Industrial Management for his invaluable advice and criticism during the investigation.

The author also would like to tank Professor Ioan Carcea, for his kindness into provide the composite material samples used on the experiments.

The author also would like to tank laboratory operator Adrian Bucovei, for his help on the preparation of the workpiece.

The author is also thankful to all the staff members of the department of Mechanical Engineering of Aveiro University, and also thanks to his classmate’s Rui Trovisco, João Aveiro, Nuno Mirante, Luis Pinho and Richard Carvalhais for the their help, friendship and companionship during his course.

The author would like to offer his great thanks to his girlfriend for her endless support, patience and love.

The author also would like to offer his great thanks to his sister, grandparents, uncles and all great friends that who supported during this journey.

The author feel pleased and privileged to fulfill his parent’s ambition and also is greatly indebted to them for bearing the inconvenient during his Mechanical Engineering Master course.

Palavras-chave: Eletroerosão, Taxa de Remoção de Material, Desgaste do Elétrodo, Sobre Corte Radial, Conicidade, Corrente de Pico, Servo Voltagem, Pulso on-time, Pulso off-time, Método de Taguchi, Análise da Variância.

Resumo

O objetivo do estudo é investigar os efeitos da corrente de pico, servo voltagem, pulso on-time e pulso off-time na perfuração por electroerosão da liga de Alumínio Magnésio reforçado com carbonetos de silício e determinar a sua influência num grupo de parâmetros de saída, que incluem a taxa de remoção de material, desgaste do elétrodo, sobre corte radial e conicidade. Para melhor entender o problema experimental e todas as questões que este inclui, em primeiro lugar, foi feita uma revisão da literatura que abrange todos os princípios, tecnologias e aplicações do processo de electroerosão. Os dados para esta pesquisa foram recolhidos no laboratório de tecnologias não convencionais na "Gheorghe Asachi" Universidade Técnica de Iasi. O design de experiencias foi escolhido através do metodo Taguchi, nomeadamente o array L9. O primeiro objetivo desta pesquisa é encontrar a combinação ideal dos níveis de parâmetros através do método de Taguchi. O segundo objetivo é encontrar a contribuição da cada parâmetro de entrada para cada parâmetro de saída usando o método de análise estatística Análise da Variância. Objetivo final é desenvolver um modelo matemático para prever os valores de saída experimentais, através do software GW-Basic. Os resultados mostraram que os parâmetros com uma maior influência sobre a taxa de remoção de material e desgaste dos elétrodos foram a servo voltagem e corrente de pico, com 49% e 24% em relação ao primeiro parâmetro e 84% e 10% em relação ao segundo. O sobre corte radial foi mais influenciado pela corrente de pico e pelo pulso on-time, com 29% e 35%. Relativamente a conicidade, os parâmetros com mais influência foram corrente de pico e o pulso on-time, com 47% e 33% em termos de contribuição. Além disso, os níveis de combinação ótima de parâmetros associadas com a taxa de remoção de material, desgaste dos elétrodos, sobre corte radial e conicidade foram também obtidos. As respostas em estudo podem ser previstas usando os modelos matemáticos com um erro médio de 2% para a taxa de remoção de material, 16% para o desgaste do elétrodo, de 2% para sobre corte radial e 2% para a conicidade.

Keywords: Electrical Discharge Machining (EDM), Drilling Electrical Discharge Machining, Material Removal Rate (MRR), Electrode Wear (EW), Radial Over Cut (ROC), Taper (T), Peak Current (PC), Servo voltage (SV), Pulse on-time (Ton), Pulse off-time ($Toff$),Taguchi Method (TM), Analysis of variance ($ANOVA$)

Abstract

The purpose of this study is to investigate the effects of $peak\,current$, $servo\,voltage$, $pulse\,on-time$ and $pulse\,off-time$ on electrical discharge drilling of an aluminum magnesium reinforced with particles of silicone carbide and determine their influence on a range of output parameters such as $material\,removal\,ratio$, $electrode\,wear$,$radial\,over\,cut$ and $taper$. To better understand the experimental problem and all issues that it includes, firstly, was done a literature review that covers all the electrical discharge machining principals, technologies and applications.The data for this research was collected on the "non conventional" machining technologies laboratory at "Gheorghe Asachi" Technical University of Iasi. The design of experiments was chosen by $Taguchi\,method$, namely, orthogonal array L_9.The first goal of this research is to find the optimum parameter level combination through the $Taguchi\,method$. The second goal is to find the contribution of the each parameter for each output using the statistic method $Analysis\,of\,variance$. Final goal was to find a mathematical model to predict the experimental output values, through a software *GW-Basic*. The results shows that the parameters with more influence on *material removal ratio* and *electrode wear* responses were *servo voltage* and *peak current*, with 49% and 24% regarding the first output and 84% and 10% the second. *Radial over cut* was more influenced by *peak current* and *pulse on-time*, with 29% and 35%, concerning the *tape*r, the parameters with more influence were also *peak current* and *pulse on-time* but with 47% and 33% of contribution. In addition, the optimal combination levels of machining parameters associated with *material removal rate, electrode wear, radial over cut* and *taper* were also drawn. Responses in study can be predicted using the Mathematical models with a average error of 2% for *material removal rate*, 16% for *electrode wear*, 2% for *radial over cut* and 2% for *taper*.

List of symbols and abbreviations

CI	Confidence interval
DF	Degrees of Freedom
EDM	Electrical Dischage Machining
EW	Electrode wear
EWR	Eletrode Wear Rate
HAZ	Heat Affected Zone
HB	Higher the Better
LB	Lower the Better
MMC	Metal Matrix Composite
MQL	Minimum Quantity of Liquid
MRR	Material Removal Rate
N_E	Effective number of experiments
OA	Orthogonal Array
OC	Over Cut
PC	Peak current
$PMEDM$	Powder Mixed Electrical Discharge Machining
Ra	Roughness
ROC	Radial Over Cut
SAF	Stabilized Aluminum Foam
SEM	Scanning Electron Microscopy
SV	Servo voltage
T	Taper

T_{off}	pulse off-time
T_{on}	pulse on-time
TM	Taguchi Method
V_P	Variance of parameter P
VRT	Volumetric Removal Rate
$WEDM$	Wire Electrical Dischage Machining
WR	Wear Ratio
WRR	Workpiece Removal Rate

Contents

List of Figures

List of Tables

Introduction

This thesis discuss the effect of certain EDM parameters on EDM drilling operation of a metal matrix composite material ($AlMg10\,5\%\,SiC$). Nowadays the challenge for production engineering is to development efficient production processes as well as new concepts for innovative, sustainable and high-quality products. One strategy to achieve these kinds of products is to focus on light weight concepts. These concepts are based on new materials with unique characteristics as well as low weight and high strength values. Here comes the role of EDM technology, since EDM is a "non contact" machining process, becomes easier achieve good results with this kind of technology in comparison with the conventional processes due the hardness of the material under study.

The issues related with EDM application on this process are the existence of ceramic particles, silicone carbide, that have low electrical conductivity, so they did not melt efficiently during the machining process and the removal of material in the composite occurs as a result of matrix melting and vaporizing around the ceramic particles. The lowest knowledge about this specific material is also an issue for this investigation.

To better understand this phenomena, preliminary experiments were done, based on the literature review and on the standard programs form the used machine, *Sodick AD3L*.

Regarding the organization of this thesis, it has two parts. The first part is a literature review of the EDM technology, principals, applications and machinery. The second part is the experimental work. As previous described several preliminary experiments were done to understand the effect of certain parameters. The design of experiments for the final experiments is based on the orthogonal array L_9, from *Taguchi method*, and the results obtained are analyzed by the method analysis of variance, $ANOVA$. Finally were done the confirmation test to validate the *Taguchi method* and was found the mathematical model to predict the experimental output values, through the *GW-Basic* software.

Part I

Literature Survey

1 History of Electrical Discharge Machining EDM

The basis of EDM can be traced as far back as 1770, when the English chemist Joseph Priestly discovered the erosive effect of electrical discharges or sparks. After that, in 1930s, the machining of metals and diamond with electrical discharges was done. However, it was only in 1943 at the Moscow University where two Russian scientists, B.R. and N.I. Lazarenko explored the destructive properties of electrical discharges for constructive use. They developed a sparking machining process with an electrical circuit that used many of the same components as the automobile ignition system. This process became one of the standard EDM systems in use throughout the world. Since the Lazarenko EDM system used resistors and capacitors, it has become known as a resistor-capacitor (R-C) circuit for EDM [1].

Simultaneously, in America, three employees came up with the same results by using electrical discharges to remove broken taps and drills from hydraulic valves. With a reference to this work, the vacuum tube EDM machine and an electronic circuit servo system that automatically provided the proper electrode/work piece spacing (spark gap) for sparking, without contact between the electrode and the work piece.[2] In 1952, due to his interest for spark erosion machining, the manufacturer Charmilles created the first machine using this machining process, which was presented for the first time at the European Machine Tool Exhibition in Milan in 1955.[3]

$WEDM$was first introduced to the manufacturing industry in the late 1960s. The development of the process was the result of the search for a technique to replace the machined electrode used in EDM. In 1974, D.H. Dulebohn applied the optical-line follower system to automatically control the shape of the component to be machined by the $WEDM$ process. By 1975, its popularity was rapidly increasing, as the process and its capabilities were better understood by the industry.[26]

In 1980s with the initiation of Computer Numerical Control (CNC) in EDM brings remarkable advancement by improving the efficiency of the machining operation. EDM

machines have become so stable with the regular improvement in the process, so that these can be used for long interval of time under monitoring by an adaptive control system. This process enables machining of any material, which is electrically conductive, irrespective of its hardness, shape or strength. The improvement of *EDM* have since then been intensely sought by the manufacturing sector yielding enormous economic benefits and generating keen research interests.[2]

Few years later appeared the first reference to dry *EDM* in a 1985 NASA Technical report. It was briefly reported that argon and helium gas were used as dielectric medium to drill holes using tubular copper electrode. Further details are however not available. Later in 1991, Kunieda et al. showed that introducing oxygen gas into the discharge gap improves the material removal rate (*MRR*) in a water-based dielectric medium. It was in 1997 that the feasibility of using air as the dielectric medium was first demonstrated by Kunieda et al.. [61]

2 Introduction of *EDM*

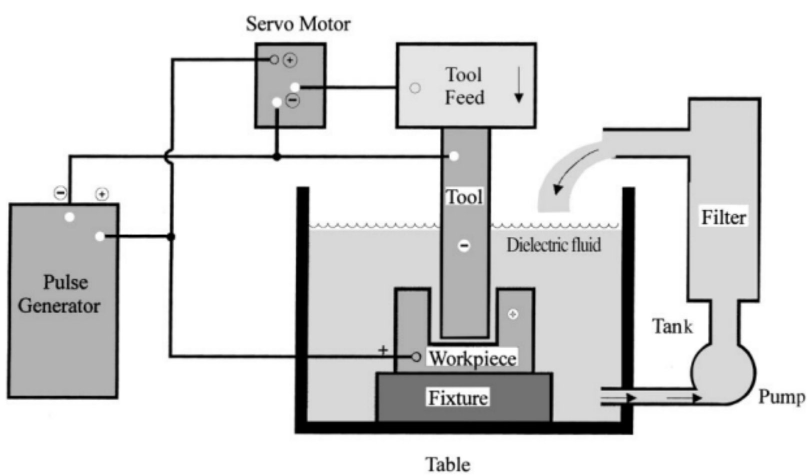

Figure 1 – Setup for Electrical Discharge Machining[25]

EDM is basically a "non conventional" or "non traditional" machining process. The basic principal followed is the conversion of electrical energy into thermal energy through a series of discrete electrical discharges occurring between the electrode (tool) and workpiece immersed in a dielectric fluid. The Fig.1 represent a typical Die-sinking *EDM* setup.

The insulating effect of the dielectric which is used in EDM process is very important because it avoids electrolysis of the electrodes during the EDM process. Spark is initiated when high voltage is applied between the electrode and workpiece at smallest point distance. Metal starts eroding from both the surfaces of workpiece as well as electrode. At the end sparks spread over the entire workpiece surface leads to its erosion, or machining to a shape which is mirror image of the tool.[2]

The biggest advantage of EDM is that there isn't direct contact between the electrode and the component during machining, and therefore no deformation occurs, even for thin components. However, due to the rapid heating and cooling effects induced by the machining process, a thermally affected zone will form on the surface of the component. The structure of this layer is quite different from the parent material. Indeed, it is the portion of the base metal that was not melted during brazing, cutting, or welding, but whose micro structure and mechanical properties were affected. Thus, the thickness of the thermal damage surface layer depends on the surface temperature distribution, which can be computed by the thermal properties of the workpiece material and cutting parameters.[4]

3 Electric Principals of EDM

3.1 Pulse characteristics and parameters

3.1.1 Peak Current

The peak current, one of most important parameters in $EDM,$ is measured in units of amperage and is the amount of power used in discharge machining. It is a preset level that the current reaches during each pulse on-time. High current values will improve the MRR sacrificing the surface finish, as show in Fig.2 and tool wear rate. Fortunately with the advent of new electrode materials like graphite, it is possible work with high voltages without much damage on the electrode tool.

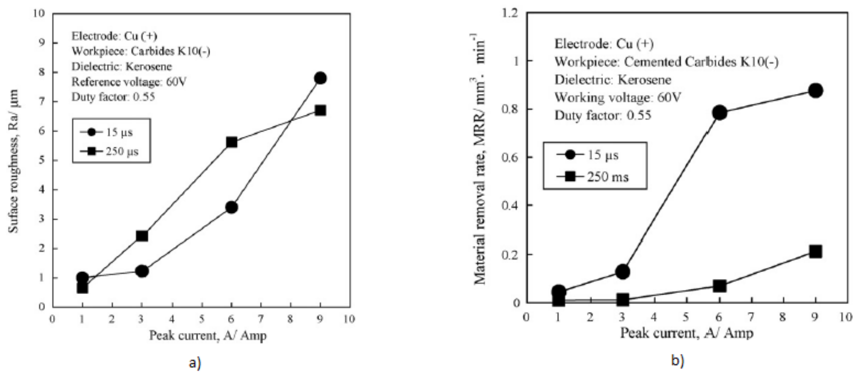

Figure 2 – Effect of Pulse Current on Removal Rate and Surface Roughness[35]

$$E = VIT \tag{1}$$

Note that:
V : Voltage $[Volt]$,I : Current $[Ampere]$,T : Time $[sec]$

3.1.2 Frequency

Frequency is the measurement of the number of times the current is turned on and off. For finishing operations, the frequency would be considered high frequency, because it will have many cycles per second with shorter on and off-time ($20\mu s$ for each) [6]. As previously mentioned, the shortening on and off times sacrifices the material removal rate to improve the surface roughness and surface finish as desired in finishing operations.

On the other hand, in roughing operations the on-time is extended to achieve higher rates of material removal rate. Usually on-time takes average values as much as $100\mu s$ and off-time as $20\mu s$.[6]

3.1.3 Pulse On-time and Off-time

The pulse on-time and off-time are expressed in units of μs and these two pulses complete one cycle as shown in Fig.3. The work is done during the pulse on-time, so, the duration of the pulse, the number of cycles per second (frequency), and the time in which the spark is sustained (duty cycle) have a crucial role on the process. Metal removal is directly proportional to the amount of energy applied during the pulse on-time, consequently, with bigger duration of on-time better the MRR, because the crater will be broader and deeper.

However the MRR can not be increased only by increasing the pulse on-time duration, is also necessary a combination of peak current. According to [Anand Pandley et. al] this is due to the reason because of short pulses cause less vaporization, where as long pulse duration causes the plasma channel to expand rapidly. This expansion of plasma channel cause less energy density on the work material, which is not sufficient to melt and vaporize the work material. It was also concluded by the researchers that with increase of pulse duration, surface roughness decreased, hardness of work material, crack length, crack width and the thickness of recast layer increased.[15]

During the pulse off-time no machining takes place and it allows the melt material to vaporize and to remove from the spark gap. The off-time is liable to the speed and stability of the cut. The smaller off-time faster the operation, however short off-time causes erratic cutting due no debris removal from the spark gap by the flow of dielectric fluid.

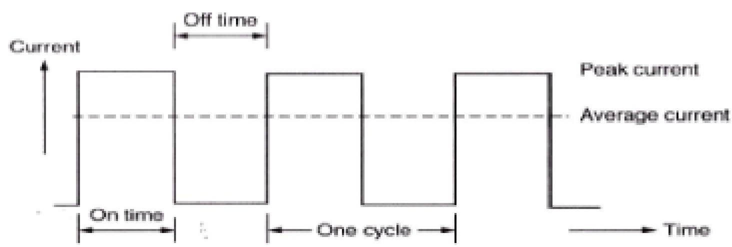

Figure 3 – Typical *EDM* pulse[16]

In the pulse current, if time T is substituted to an intermittent one with frequency, Eq.1 is expressed to the following

$$E_p = V_p I_p t_{on} \frac{1}{t_{on} + t_{off}} \tag{2}$$

Note that:

V_p : Voltage of a single pulse, I_p :Current of a single pulse, t_{on} :pulse on-time, t_{off} :pulse off-time

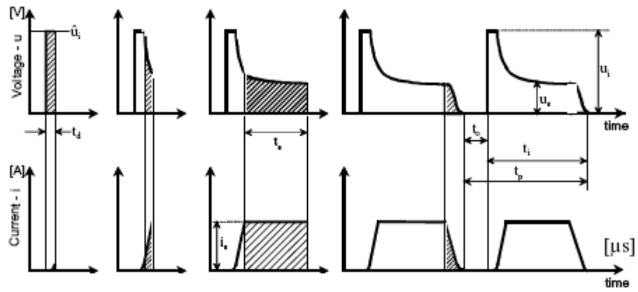

Figure 4 – Characteristics of current and voltage pulses[72]

Nomenclature:
$\hat{u}_i - open\, circuit\, voltage,\, V$
$u_e - discharge\, voltage,\, V$
$t_d - ignition\, delay\, time,\, \mu s$
$t_e - discharge\, duration,\, \mu s$
$t_i - pulse\, duration,\, \mu s$
$t_{p-}pulse\, cycle\, time,\, \mu s$

3.1.4 Servo voltage

EDM-servo systems make use of the electrical characteristics of the dielectric fluid for their operation. The dielectric fluid, firstly, acts as an insulator until the open-circuit voltage and the spacing between the electrode and workpiece reach the ionization point. Then, the dielectric changes to a electrical conductor, causing the voltage drop from the open circuit voltage to sparking voltage .

Since the machining-voltage range is constant for a particular dielectric fluid, a voltage in this range is selected as a reference for controlling the servo system. The reference voltage is compared to the actual machining voltage measured between the electrode and workpiece. The difference between the reference voltage and the actual electrode workpiece voltage is used to command the electrode-servo system such as[1]:

- to advance the electrode, for any electrode-to-workpiece machining voltage that is greater than the servo system's operational voltage range.

- to hold the electrode, for any electrode-to-workpiece machining voltage in the acceptable servo system's range.

- to retracts the electrode, for any electrode-to-workpiece machining voltage that is less than the servo system's operational voltage range.

For this last case, this offers the benefit of opening the electrode-to-workpiece spacing so that machining debris will have a larger opening to exit the sparking area, ensuring a clear sparking area[1].

3.1.5 Duty Cycle

It is a percentage of the on-time relative to the total cycle time. This parameter is calculated by dividing the on-time by the total cycle time (on-time pulse off-time)

$$DutyCycle = \frac{on - time}{totalcycle_{time}} \cdot 100 \qquad (3)$$

3.1.6 Polarity

The polarity of the electrode can be either positive or negative. Both, anode and cathode, will be eroded because of the high temperature action, more precisely, due the impact of electrons and positive ions into the electrode surface, trough the plasma channel. On EDM process with short spark times ($30\mu s$), should be used the called positive machining,in other words, the workpiece should be anode and electrode should be cathode. In this case, for the electrons, its easy to get high speed due of its small quality and high accelerated speed causing a bigger erosion on the anode in comparison with the positive ions. For them its more difficult reach a higher speed in a short period of time due your bigger quality and lower accelerated speed. On the other hand, with bigger spark times ($300\mu s$), should be used the process called negative machining, with reverse polarity in comparison with the previous case, because in this case, the positive ions can be accelerated to a high speed and due the bigger kinetic energy will cause a bigger erosion on the cathode[18]. However, according with many literature, in general , polarity is determined by a experiments and is a matter of tool material, workpiece material, current density and pulse length combinations.[19] The next Fig.5a), b) shows the difference between polarity on the crater size and electrode surface on the Fig.5 c), d).

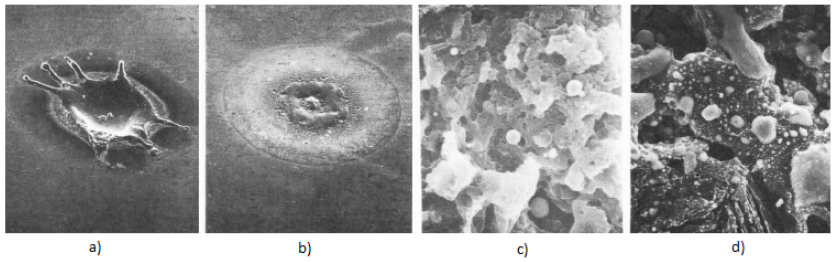

Figure 5 – SEM micrographs of the crater and the electrode surface a) Crater shape with electrode polarity(-) b) Crater shape with electrode polarity(+) c) Electrode surface with electrode polarity (-) d) Electrode surface with electrode polarity (+) [17]

3.2 Types of Power Supply

The Power supply must provide the most efficient possible machining energy for the different operations. Wish operation requires a certain type of voltage wave, different spark on/off times, that are generally related with the intensity and frequency, as can be seen in next subsection.

3.2.1 Relaxation Generator

The Relaxation Generator or also called Lazarenko-type Generator, is basely an RC Circuit, as shown in Fig.6, constituted by a capacitor C that is charged by the source E through a resistor R. When the voltage on the capacitor and the gap has a proper size, the capacitor release the discharge through the gap. This cycle is repeated after a certain time, that depends of the time that capacitor need to recharge. This type of circuits may have more than one resistor or capacitor, this allows the operator can select a bigger range of spark on/off time.

However the RC circuit allows a good surface finishing by sacrificing the material removal rate (MRR), that mean there was a peak in current at the instant of spark initiation followed by a rapid rate of decline, because of that this generator is used normally for the finishing process that requires short time sparks.

On the contrary, if the peak in current was to higher, this can causes a spark with a much higher temperature than that needed to remove the material, and resulted in a thermal damage to the electrode.[37, 9]

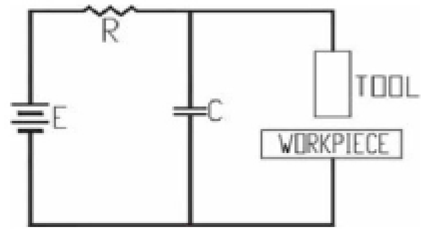

Figure 6 – Relaxation Generator[37]

3.2.2 Pulse Generator

The pulse generator is compound by a electrical source E, a pulse generator in combination with a electronic interrupter. The Fig.7 shows a simple pulse generator without resistive limitation. With this type of generator the operator can control the spark on/off time and this is a big advantage of this generator. The pulse generator allows the selection of machining conditions for a particular operation. Normally this type of generator is used for roughing operations. This type of generator can be completed with more components as can be seen in the next subsection. The wave from this type of generator can be seen in the next subsection on Fig.8 a). [9, 38]

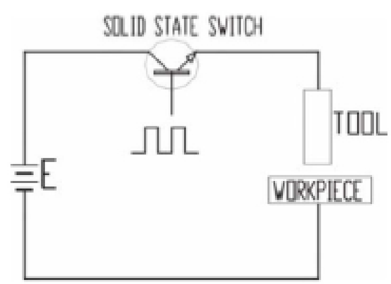

Figure 7 – Pulse Generator[37]

3.2.3 Hybrid Pulse Generator

As mentioned in the previous subsection, the pulse generator circuit can be completed with more components as capacitors and resistive limitation of the current between pulse generator and working area. In this case, we will have a hybrid pulse generator. This type of generator promotes a slightly different wave called trapezoid wave as shown in Fig.8 b). The trapezoidal wave occurs due to capacitor, that means, the presence of the capacitor causes the voltage does not grow nor decreases in a so abruptly, then it causes a more stable process. Nowadays, the most of the *EDM* machines use a hybrid pulse generator.[9, 38]

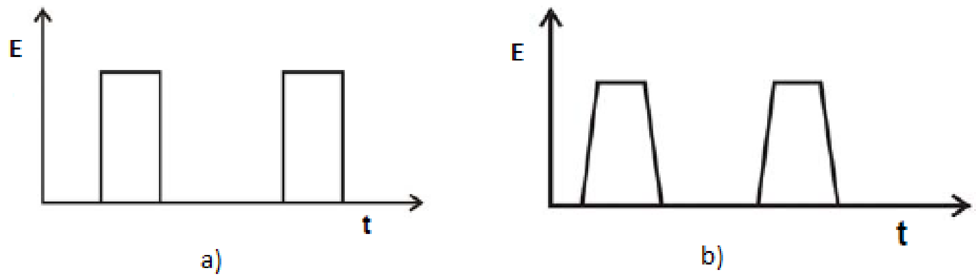

Figure 8 – a) Wave from Pulse Generator; b) Wave from Hybrid Pulse Generator [38]

4 Phenomena

4.1 Mechanism of Material Removal in *EDM* Process

The following steps represent the evolution of the electric field in the gap, which in turn, depend on the voltage, current intensity, and electrical resistance of the dielectric fluid.

The electrode is brought near the workpiece, with a certain polarity applied, generally the electrode is the negative pole and the workpiece the positive pole. Between them there is dielectric fluid that acts as an insulating oil. Even though a dielectric fluid is a good insulator, a large enough electrical potential (pulse of magnitude about 20 to 120 V and frequency on the order of 5 kHz [12]) can cause the fluid to break down into ionic (charged) fragments, allowing an electrical current to pass, between the most closed peaks of the electrode and tool, as shown Fig.9 a)

The application of the electric field, can causes the polarization and a particular orientation of the molecules and ions found in the dielectric medium. To notice this is a progressive phenomena and with the decrease of the medium resistance the electrons and ions start to move faster and promotes the appearance of a high conductivity column [11],as shown Fig.9 b)

When the medium resistance achieve a small value, the current strength takes high values (107 to 108 A/sec) [9] and a spark occurs typically with a duration between 0.1 to 2000 μs

[12]. This amount of current strength promotes the vaporization and decomposition of the dielectric surrounding the conduction column, due an additional heating caused by a strong magnetic field that compresses the current beam, as shown Fig.9 c)

The occurrence of the plasma channel, with high enough temperatures, (8000-12000^{o}C)[12] and heat fluxes up to 1017 W/m^2[12], is capable to melt and evaporate small portions of the workpiece and electrode. Owing to this thermal effect, this process is able to machine the hardest and toughest electric conductivity materials, as shown on Fig.9 d)

If maintaining the current intensity and voltage difference constant , the removal material achieves the biggest value coinciding with the maximum expansion of the gas bubble as high as 200 atmospheres [12] causing micro-blasts and chemical reactions on the dielectric fluid. This is the moment of switching off the current and the voltage, as shown on Fig.9 e)

With the disappearance of the spark, the generation of heat ends, and the evaporated metal solidifies in to the dielectric fluid, one can now be remove the chips and debris from the machining gap, as shown on Fig.9 f)

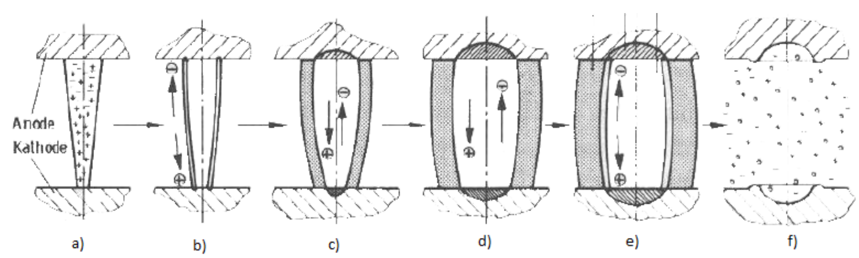

Figure 9 – Schematically Representation of MMR Phenomena in EDM Process[36]

The equation of material removal rate (MMR) can be produce by the multiplying Eq.2 by machining property. Hence the expression can be written as follows:

$$MRR = \alpha V_p I_p t_{on} \frac{1}{t_{on} + t_{off}} \tag{4}$$

The constant α is the removal constant of material. This constant is the removal volume of a material per unit electric power.

4.2 Phenomena in the Dielectric Medium

The phenomena in dielectric medium also called skin effect and pinch effect is directly related with the compression or expansion of the ionized column. The first phenomena is called Skin effect, and occurs due a significant variation of the voltage and current. These variations are responsible for the shock wave appearance. The wave shock front is very close or even coincidence with the wall of the ionized column. This fact is due to the divergent character of the electrodynamic forces. Thereafter the current intensity stabilizes, the electrodynamics forces change their direction and a ionized column compression occurs. This phenomena is called Pinch effect. In this moment an intense melting and vaporization of the electrode materials found in contact with the plasma column are produced, generating a new increasing of column diameter. Finally a new skin effect occurs due other great variations of the voltage and current intensity at the discharge end.[9]

4.3 Recast Layer and Heat Affected Zone (HAZ)

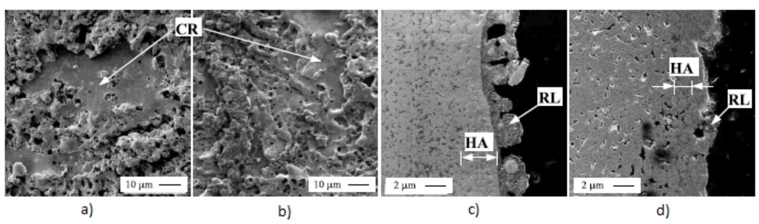

Figure 10 – SEM micrographs of the crater (CR),recast layer (RL) and heat affected zone (HA), a) CR 14μs pulse on-time, b) CR 5μs pulse on-time, c) RL and HA14μs, d) RL and HA 5μs [22]

These Phenomena occur due the high temperatures of the discharge and promotes some metallurgical changes in the surface layer of the workpiece. The surface integrity highly affects the performance, life, and reliability of the components[20]. The most important parameter that affects the thickness of these layers (recast layer and heat affected zone) is the pulse on-time. The recast layer, shown in Fig.10c), b) is a thin layer of about ($25\mu m - 50\mu m$)[21], and it happens because the molten material from the workpiece is not flushed out quickly and it will re-solidify and harden due to cooling effect of the dielectric and get acceded to the machined surface. This layer is extremely hard, brittle and porous and may contain micro cracks. Below the previously mentioned layer there is the heat affected zone, as shown in Fig.10c), d), this layer is approximately $25\mu m$ tick and is formed due to rapid heating and cooling cycles during theEDM process. This layer's main characteristics as thermal residual stresses, grain boundary weakness and grain boundary cracks. This last characteristic is visible in Fig.11.

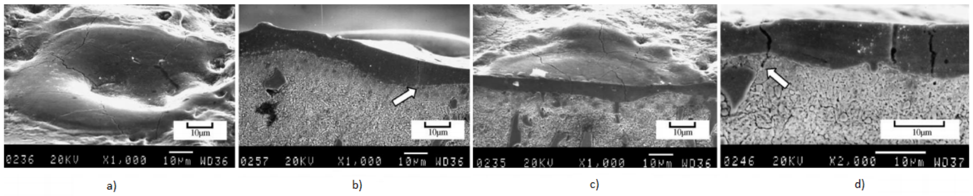

Figure 11 – SEM photographs of cracking show: (a) micro-cracks on the EDMed surface ($4A/15\mu s$); (b) crack initiates at its surface ($4A/15\mu s$); (c) crack terminates within the white layer ($8A/15\mu s$); (d) crack penetration into the parent material ($6A/15\mu s$) [76]

4.4 Secondary Discharge

The secondary discharge phenomena is directly related with the pressure of the dielectric flow, capacity to acts as heat sink of the same. This factor is further studied in the section 8. In this stage, the main objective is understand the secondary discharge phenomena. In order to obtain a good result, the successive discharge sparks should be randomly distributed over the machined surface which does not occur with this phenomena, as shown in Fig.12a).

Briefly, the dielectric fluid should cooling the electrode and the workpiece. It acts as an effective isolator between the same in addition to removing the debris and chips from the spark gap. The phenomena under study, occurs specially, when the dielectric flowing through the electrode and tends to cool the electrode but the workpiece will be warmer after a certain period of time. Owing to this, the hot oil surrounding the material tends to heat up the side walls of the cavity, and these tends to expand slightly, closing in around the sides of the electrode[6]. This thermal effect in addition to the debris and chips passing by the cavity walls, allows two discharges to take place in the same spot of the machined surface, as shown in Fig.12b).

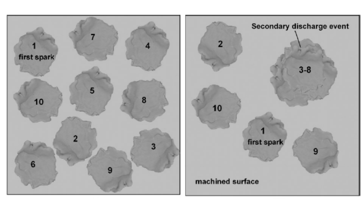

Figure 12 – Schematic illustration of locations of 10 successive discharge events. (a) The events are randomly distributed; (b) occurrence of secondary discharges[23]

5 Types of EDM by electrode

5.1 RAM or Die-Sinking EDM

As previous described EDM is a well-established machining option for manufacturing geometrically complex or hard material parts that are extremely difficult-to-machine by conventional machining processes. The non-contact machining technique has been continuously evolving from a mere tool and die making process to a micro-scale application machining alternative attracting a significant amount of research interests.

This process is the most widely used techniques for the fabrication of die and mold cavities which are finally used for mass production of metals and polymer products by replication such as die casting, injection molding, and other applications.

The electrode is moved toward the work piece, in a presence of dielectric fluid, until the gap is small enough so that the impressed voltage is great enough to ionize the dielectric. Short duration discharges are generated in a liquid dielectric gap, which separates tool and work piece. The material is removed with the erosive effect of the electrical discharges from tool and work piece. [5, 9, 13]

Technical aspects and more information about Die-sinking EDM process was previous described in last sections.

5.2 Wire Cut EDM

Wire electrical discharge machining ($WEDM$) is a thermal machining process capable to achieve accurately machining parts with varying hardness or complex shapes, that are very difficult to be machined by the conventional machining processes[26]. Moreover with improvements such as advances in wire, ability to work with larger pieces and the most important CNC, the wire EDM came to be accepted as a reliable process in several fields such as fabrication of the stamping and extrusion tools and dies, fixtures and gauges, prototypes, aircraft and medical parts, and grinding wheel form tools[7]. The spark theory behind the wire EDM is basically the same as that of the Ram EDM process previously described. In wire EDM, the conductive materials are machined with a series of electrical discharges that are produced between an accurately positioned moving wire (the electrode) and the workpiece as shown in Fig.13

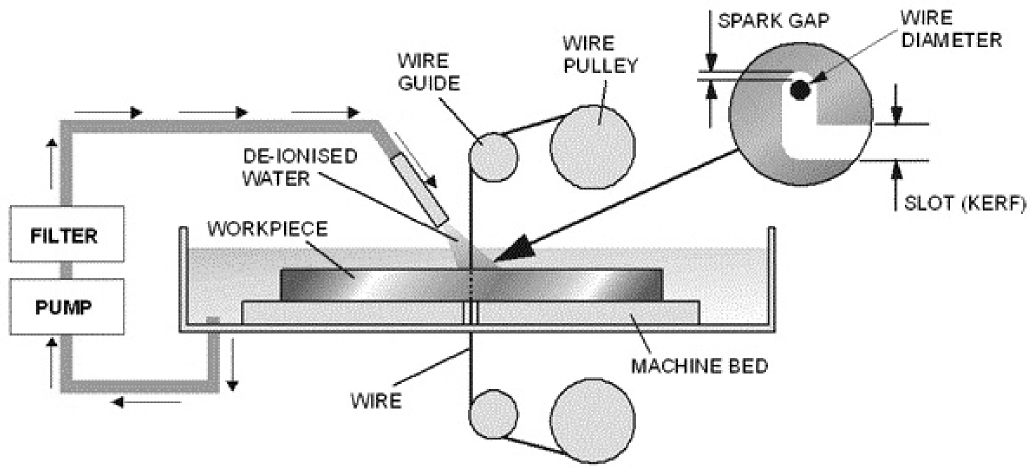

Figure 13 – Schematic Illustration of Wire EDM[29]

However in some cases, low electric conductive material can also be machined [27]. In the process under study the wire does not touch the workpiece, so there is no physical pressure on the workpiece and clamping pressure required is too small, in comparison with other machining process, thereby preventing damage or distortion to the workpiece. The $WEDM$ process leaves no residual burrs on the workpiece, which reduces the need for subsequent finishing operations. [13]. In fact, these complex shapes and exceptional high accuracy is due to the use of microprocessors that control a thin wire continuously feeding through the workpiece. These microprocessors can constantly maintains the gap size between 0.025 and 0.05 mm, obtained a varying degree of taper ranging from 15ºC to 30ºC to respectively 100 mm to 400 mm thick workpiece besides allowing the machines can work without a permanent operator. However, in order to achieve a desired quality some parameters as pulse-on time, pulse-off time, table feed rate, flushing pressure, wire tension and wire velocity should be chosen properly according to workpiece properties, so that a better performance can be obtained [26]. The $WEDM$ use the deionized water as dielectric fluid, as can be seen in the subsection “Common dielectric fluids”. The Fig.14 shows the influence of certain parameters on the surface roughness.

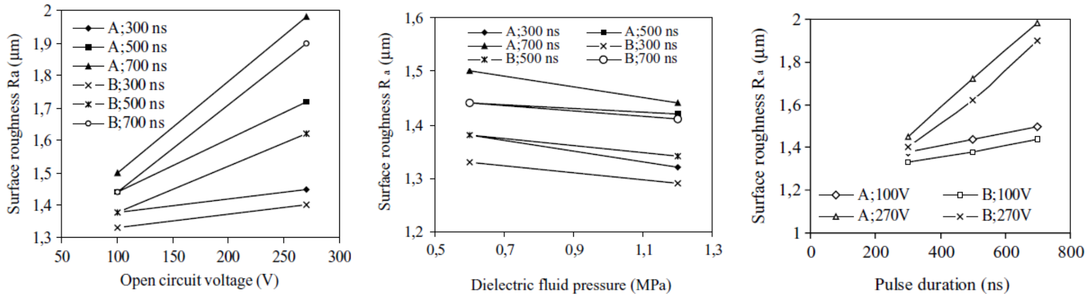

Figure 14 – Influence of certain parameters on the surface roughness[28]

5.3 Micro *EDM*

There are several micro-*EDM* technologies, such as micro-wire *EDM*, micro-*EDM* die sinking, micro-*EDM* drilling, and micro-*EDM* milling, to be applied to manufacture metal micro-features. In micro−*EDM* die sinking, more than one tool electrode is usually required when fabricating high-accuracy micro-features with complex cross section due to severe wear of the tool electrode. Generally, these tool electrodes are very difficult to be produced by the conventional techniques such as micro milling, micro turning, micro grinding, micro wire *EDM*, and wire electro discharge grinding. Thus, electro-forming is frequently used as the main method to fabricate these complex three-dimensional tool electrodes for micro-*EDM* die sinking process.[43]

Micro *EDM* is a micro machining process for the fabrication of micro cavities with advantages, such as high precision machining of conductive materials regardless of material hardness it being a thermal process, negligible force due to its non-contact nature.[64]

5.4 *EDM*Drilling

*EDM*drilling is a machining process that is known to be capable of drilling burr-free holes in a wide range of materials regardless of their hardness as long as the material is electrically conductive. In micro-hole drilling, the most common technique involves making the electrode from a high temperature material such as tungsten (W), either by circular grinding with a diamond abrasive wheel or by wire electrical discharge grinding. The diameter of the electrode is carefully matched to the size of hole to be drilled by considering the radial overcut of the*EDM* process. Other important parameter on the *EDM* drilling process is the flushing. Some authors proved that within a range of types of *EDM* drilling flushing as non-rotating (a), rotating (b) and rotating electrodes with injection flushing through the center of electrode (c), the forced flushing of (c) yields significantly higher material removal rates compared to the side flushing of (a) and (b).[50]

A rotating spindle holds the electrode, and a guide ensures the correct location is held during drilling. As the electrode creates a hole in the material, a high-pressure dielectric flush surrounds it. This high-pressure flush forces the eroded material to leave the hole quickly, enabling deeper holes to be made. As holes become deeper, maintaining the high-pressure flush becomes even more important because the removed material has farther to travel up the hole. If flushing conditions are poor, or if the pressure is not high enough, material can build up and will begin acting like an extension of the electrode. If this occurs, sparks will arc across the dielectric fluid and strike the workpiece in an unwanted area. This short-circuit, or DC, arc creates pitting on the workpiece and is the first indicator of poor flushing conditions.[59]

5.4.1 Geometrical and Accuracy variations at the hole

Taper on EDM drilling

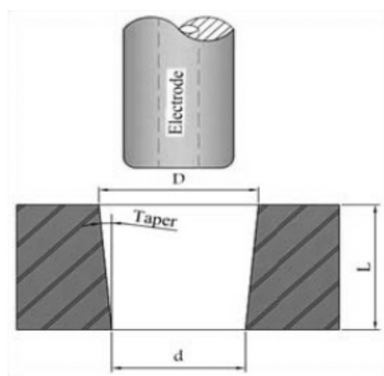

Figure 15 – Characteristics of Taper on EDM [49]

An important type of defect from hole drilling during EDM process is hole taper and hole accuracy. Therefore, in order to improve hole quality, some authors investigated optimum values of the process parameters experimentally such as voltage, feed rate, pulse on time, duty cycle, and the length of uninsulated tool.

In the EDM sparking hole drilling process, the viscous resistance in the narrow discharge gap causes difficulty in the removal of debris and bubbles from the working area, abnormal discharges are occurred and resulting in extensive electrode wear. Moreover, the debris moved by pressure flow of dielectric fluid make taper on the workpiece. The hole taper of workpiece from EDM process, which as shows in Fig.15, can be calculated by equation.[49]

$$Taper = tan^{-1}\frac{D-d}{2L} \tag{5}$$

Where:
D is hole entrances
d is hole exits
L is hole length

Holes with neck on EDM drilling

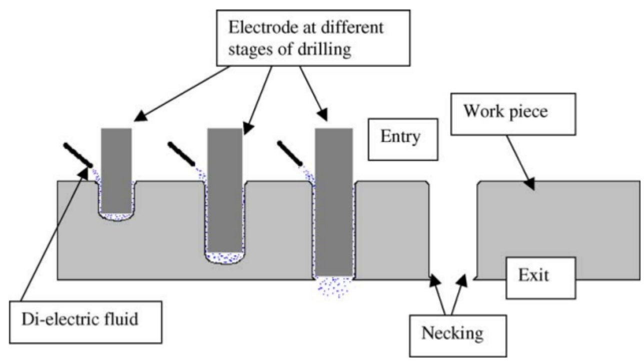

Figure 16 – Schematic showing development of a hole with a neck.[51]

On analyzing the type of hole typically produced by EDM it was seen that there were possibilities for improving the geometrical form of the hole. Straight or parallel walled holes generally have a neck at the end of the hole where final drilling takes place. Fig.16 shows a schematic of an EDM hole with a neck. The neck occurs due to the fact that, at the end of the drilling operation, the dielectric fluid can escape through the hole exit. This reduces the amount of erosion particles suspended in the dielectric and hence reduces lateral secondary erosion.[51]

5.4.2 Electrode orbiting

For deep holes, the bottom of the hole became increasingly uneven, which greatly reduced the machining efficiency. The orbiting of electrodes has additional advantages such as with orbital motion, the machine can perform the roughing and finishing cut with the same electrode. It also makes the flushing of the dielectric fluid less critical. Besides, while the electrode is inside the hole, it is possible to orbit the electrode and cut with the cylindrical surface of the electrode, which avoids the taper at the entry of the hole, in addition to to achieve fine surface finish and showed that the electrode wear can be reduced.[50]

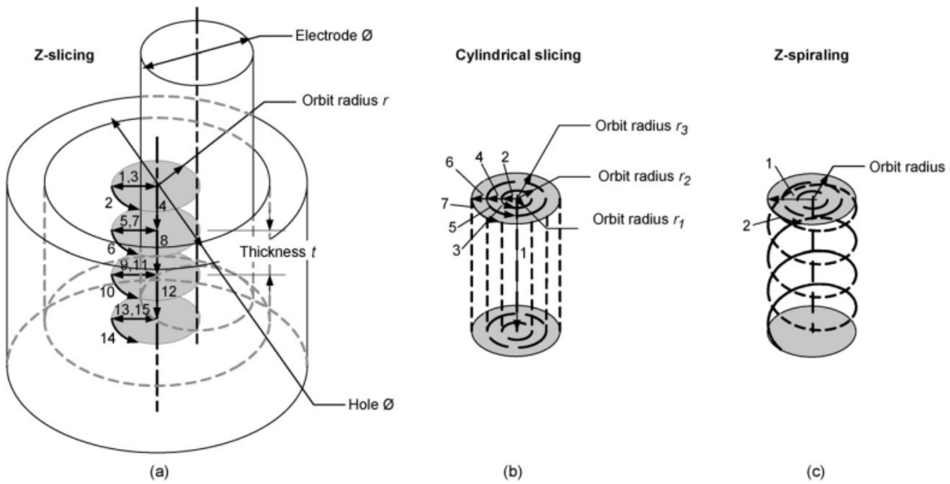

Figure 17 – Electrode orbiting strategies: slicing the hole into cylinders of thickness t and radius r (a), slicing the hole into cylindrical shells of radius r (b), and spiraling into the hole with radius r (c).[50]

The basic idea behind electrode orbiting is to actuate the electrode on a controlled, circular trajectory. If the orbiting motion is created with a device that allows the radius to be con-trolled electronically, the motion can be integrated into the EDM machine's control system for tight process control. The device used in this work is a flexure-based, 2-axis stage. Both axes are driven by linear piezoelectric motors and position feedback is provided by linear encoders.The orbital motion is then created by circular interpolation of the 2 axes and is controlled by the Profile 24P control system.

By integrating the orbiting motion into the machine control system, a number of different cutting motions are possible.The first scenario divides the depth into a number of cylindrical slices of thickness t, and removes the material contained in each slice by first plunging into the center of the cylinder. This is followed by a linear move outward towards the hole surface. The remaining material is then removed by a single, circular sweep. The machining parameters that can be varied in this setup are the thickness t of the slice and the radius r of the orbit.Another possibility would be to divide the material to be removed into a center cylinder, which is removed by plunging to the full depth of the hole and cylindrical shells, which are removed by orbits with gradually increasing radii. A third possibility would be to overlay a constant feed along the axis of the hole with the orbiting motion. The resulting spiral motion would continue until the final depth of the hole. The parameters that affect this technique are the plunge feed per revolution and the orbital radius.[50]

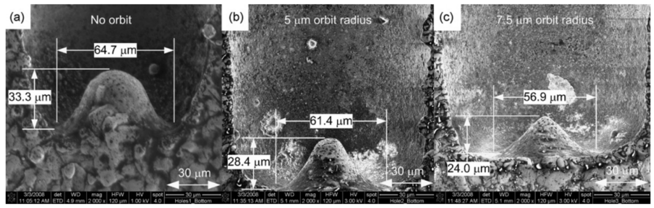

Figure 18 – Comparison at 2000× magnification of bottom surfaces drilled with no orbit (a), 5 m orbit (b), and 7.5 m orbit radius (c).[50]

5.5 Advantages of EDM over other Micro Drilling Technologies

One of the key benefits of EDM drilling is extremely deep holes can be created on electrically conductive surfaces. In standard drilling methods, the ratio between the hole diameter and depth is significantly low (1:5 or 6). The performance of EDM machines are not constrained by the hardness of the work pieces. MicroEDM drilling has advantages over other micro drilling technologies as [75]:

- Compared with conventional milling processes, the walls of micro EDM drilled holes have less or no burrs. Burr-free EDM drilling process is especially suited for machining difficult holes (an example would be drilling holes in turbine blades). When machining speed and discharge energy of EDM machines are controlled, small holes can be drilled in work pieces with high levels of accuracy

- EDMmachines have long needles as the tool electrode which are used for drilling deep holes in work pieces. For instance, the aspect ratio of EDM drilled structures can be as high as 10:1 (hole depth versus hole diameter). Conventional machining processes are not ideal for drilling deep micro holes.

- Micro EDM drilling is a non-contact micromachining process. Therefore, work piece surfaces and discharge electrodes are free from any mechanical pressure during machining. This property is also advantageous in machining curved and jangled structures or ultra thin surfaces.

- While drilling holes in angled or curved surfaces, drill bits of conventional drilling machines tend to break if torque conditions are not carefully controlled. In EDM

drilling, there is no need for torque control since discharge electrodes never contact with work pieces.

- EDM drilling machines can be used to drill materials such as soft copper and aluminum that produce gummy chips when machined.
- The non-contact EDM drilling process is suited for drilling deep straight holes in work pieces, as opposed to conventional methods in which the drill bits tend to drift during deep hole drilling.

6 Types of Medium

6.1 Wet EDM

The principals of the wet EDM are previous described on the subsection Die-sinking EDM. In this chapter worth retaining that the nature of the fluid used on the process is the major differentiator with respect to the types of medium. In wet EDM the two electrodes are submerged only in liquid dielectric fluids. The most common liquid used on this process are hydrocarbon fluids and deionized water, as detailed further on, in the subsection common dielectric fluids.

The environment and human health are big concerns when referring wet EDM and were also reflected in the studies regarding the "non-conventional" machining processes. The environmental problems related to the EDM methods refer to the mineral oils that are typically used as dielectric medium. These oils generate toxic fumes and can produce fire hazards.[41]

Cheke et al. [40] studied a comparison of process performance of wet EDM with near-dry EDM, and has proven, wet EDM more beneficial for roughing process in a given range of input variable. At high energy input low spark frequency were obtained with wet EDM which improve the flushing condition resulting higher MRR and rough surface as compared to near-dry EDM.

Nevertheless, the wet EDM was also applied in wire cut EDM (stainless steel), showing a better surface integrity than the dry EDM. The better surface integrity can be attributed to the cooling effect of the dielectric fluid. That means, during the wet EDM, the adhesion of machining debris onto electrode workpiece interface after successive erosion is reduced by the flushing effect of the dielectric fluid between the electrode and workpiece.[39]

6.2 Dry *EDM*

Dry electric discharge machining (*EDM*) is an environment-friendly modification of the oil *EDM* process in which liquid dielectric is replaced by a gaseous medium. It is characterized by simplicity, low viscosity of dielectric helping better debris evacuation, low wear of tool electrode, thin white layer on machined surfaces. Dielectric wastes generated during the oil *EDM* process are very toxic and cannot be recycled. Also, toxic fumes are generated during machining due to high temperature chemical breakdown of mineral oils. The use of oil as the dielectric fluid also makes it necessary to take extra precaution to prevent fire hazards. In the dry *EDM*, since the viscosity and the electrical permittivity of the gaseous dielectric being lower than the liquid dielectric, the machined surfaces in dry *EDM* could experience lesser pressure (thermal and mechanical shocks) and reduced discharge energy. Therefore, it is anticipated that the surface integrity characteristics of the dry EDMed surfaces could be relatively better than the liquid EDMed surfaces.[63, 62]

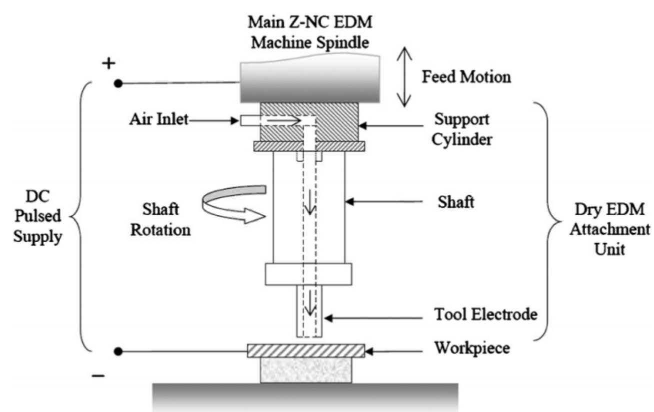

Figure 19 – Schematic diagram of the experimental set-up.[61]

High velocity gas flowing through the tool electrode into the inter-electrode gap substitutes the liquid dielectric. The flow of high velocity gas into the gap facilitates removal of debris and prevents excessive heating of the tool and workpiece at the discharge spots. Providing rotation or planetary motion to the tool has been found to be essential for maintaining the stability of the dry *EDM* process. Tubular tools, as shown in Fig.19 are used and as the tool rotates, high velocity gas is supplied through it into the discharge gap. Tool rotation during machining not only improves the process stability by reducing arcing between the electrodes but also facilitates in the flushing of debris. [61]

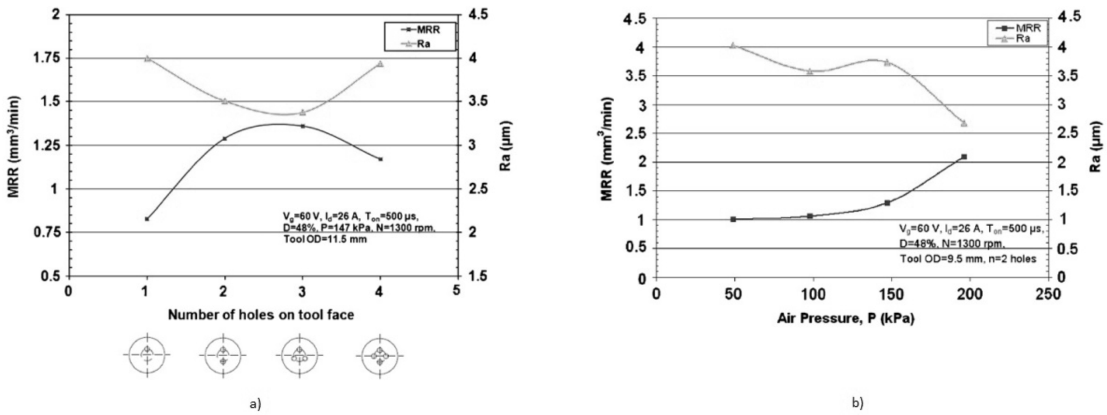

Figure 20 – Effect on MRR and Ra: a) number of holes for air flow in the tool electrode, b) air pressure [61]

Dry EDM has also been successfully implemented in wire EDM operations. Some studies have recently reported that oxygen gas and copper tool combination leads to a high MRR in dry EDM and nitrogen gas–water mixture dielectric and graphite tool combination leads to high surface finish in near-dry EDM. However, the current literature in the field is insufficient in order to make dry EDM a commercially viable process. Suitable process models for accurately predicting the process performance (such as MRR, surface finish and electrode wear rate (EWR) for a given set of input parameters are still not available. A limited knowledge base in parametric analysis makes it difficult to choose input process parameter values for obtaining a high performance.[61]

6.3 Near Dry EDM

Near dry EDM, commonly used in the EDM drilling and $WEDM$, is the alternative method to achieve the high speed machining process with the best surface finish, and have a simple concept, mixing of a minimum quantity of liquid (MQL) with the compressed air or gas in a dielectric medium (air-mist and oxygen-mist). In this process the dielectric medium doesn't react with the erode materials, as a result doesn't producing the harm-full smells (carbon monoxide, nitrogen oxide, xylene, formaldehyde and toluene) to the operators during the dielectric decomposition. Generally the air-mist dielectric medium improve the surface finish while oxygen-mist improves MRR because oxygen-mist accelerate the thermal process due to oxidation in the cutting zone, although for some near dry EDM drilling operations is used water–air mixture, because achieved better hole consistency with almost no taper, as shown in Fig.21 [30]

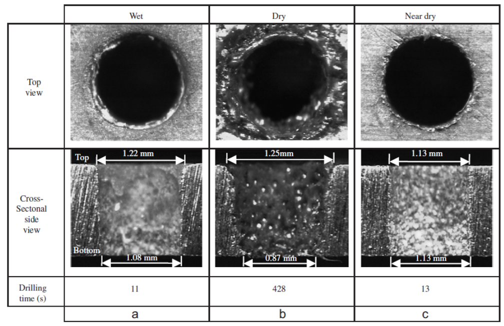

Figure 21 – Optical micrographs on holes drilled on 1.27mm Al6061: (a) wet, (b) dry, and (c) near dry EDM conditions ($i = 10A$, $t_{on} = 10\mu s$, $t_{off} = 70\mu s$, $u = 60V$).[8]

A presence of liquid phase in the gas environment promote a stable machining process at low discharge energy input due the changes in the electric field, thus making discharge easier to initiate and creating a larger gap distance. The fact of the dielectric properties can be tailored in order to achieve various machining needs is other big advantage of near dry EDM. However there is some other important parameters taking into account as gap-voltage, pulse-width, air-mist/oxygen-mist pressure and discharge current.[31]. The great disadvantages of near dry EDM are higher thermal load on the electrode, which leads to wire breakage in wire EDM and increases electrode wear in EDM drilling. Finally, doing a comparison between the three types of medium, near dry EDM has lower material removal rate at low discharge energy and generates a smaller gap distance when compared to wet EDM. On other hand compared with dry EDM, it has higher material removal rate (MRR), sharper cutting edge, and less debris deposition, as shown in Fig.22.[8]

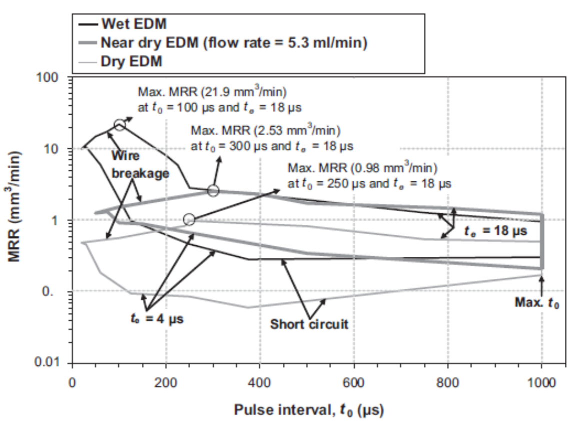

Figure 22 – Comparison of the boundaries of feasible MRR envelopes for wet, dry, and near dry wire EDM ($i = 25A$, $u = 45V$)[8]

6.4 Powder Mixed Electrical Discharge Machining ($PMEDM$)

Powder mixed electric discharge machining ($PMEDM$) is capable to improve MRR, the surface finish and surface quality to obtain near mirror like surfaces at relatively high machining rate. The near mirror surfaces has high resistance to corrosion and abrasion. This process consist in mixed some powders as aluminum, chromium, graphite, silicon, copper or silicon carbide and others into the dielectric fluid. In greater detail, a voltage is applied, the spark gap filled up with additive particles, subsequently the gap distance between tool and the workpiece increased. The powder particles get energized and arrange themselves under the sparking area in different types of arrangements. The particles in the discharge gap can be classified in four types: reciprocating motion, adhesion on either electrode, stagnation like a cluster in the gap and stagnation like a chain connecting the electrodes.[32][2][33]

As regards, the types of powders shows best results in different types of material. Fig.23 shows SEM micrographs of $OHNS$ die steel, $SKH-54$, after machining with tungsten powder, graphite powder, and silicon powder mixed in the dielectric respectively. As seen in Fig23 a) the tungsten powder failed on try to achieve a mirror finish on the $SKH-54$ workpiece , however the Fig23 b) and c) shows a mirror finish on the $SKH-54$ material by the graphite and silicone powder.[2]

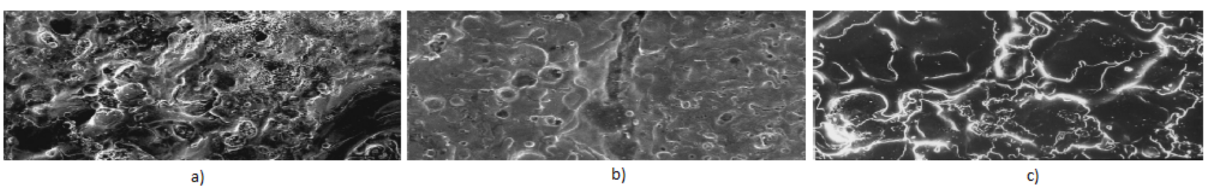

Figure 23 – SEM micrographs of OHNS die steel after machining with different powders, a) tungsten powder b) graphite powder c) silicon powder[2]

A proper choice of certain parameters as electrode polarity (negative polarity on tool) and pulse parameters should be considered.

In order to obtain a stable process it is necessary a distribute discharge locations, which depend mainly upon powder concentration, as shown in Fig.24 and its distribution, bubbles, dielectric flow,and surface irregularities of the workpiece. [33]

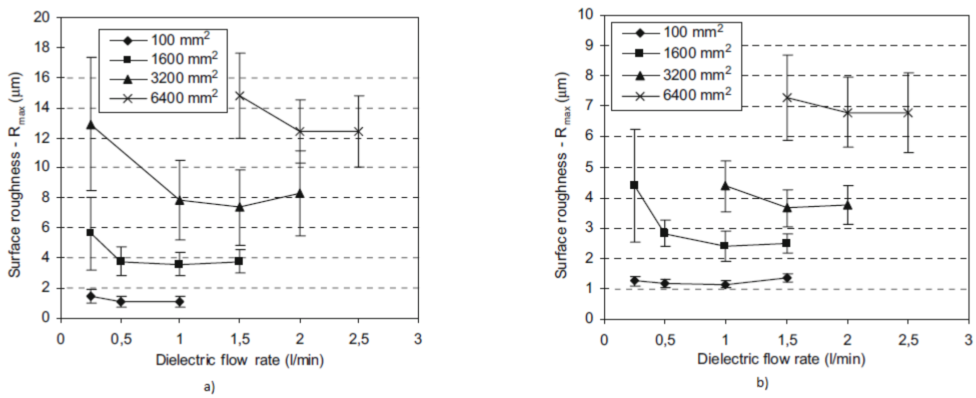

Figure 24 – Dielectric flow rate influence on the surface roughness for several electrode areas. a) Conventional dielectric condition (0 g/l), b) PMD-EDM dielectric condition (95% confidence interval; silicon powder 2 g/l)[34]

7 Tool Material (Electrode)

7.1 Characteristics of Electrode

The main objective of the electrode is to transmit the electrical charges and to erode the workpiece as a desired shape. However different electrode materials have different results on the machining.

As mentioned in [38], the most important characteristics of electrode materials are:

- High melting point - high melting point leads to less tool wear due to less tool material melting for the same heat load
- High electrical conductivity - electrons are cold emitted more easily and there is less bulk electrical heating
- High thermal conductivity - for the same heat load, the local temperature rise would be less due to faster heat conducted to the bulk of the tool and thus less tool wear
- Higher density - for the same heat load and same tool wear by weight there would be less volume removal or tool wear and thus less dimensional loss or inaccuracy
- Easy manufacturability
- Cheap cost

7.2 Materials of Electrode

There are two principal groups of electrode materials: Metallic(brass, copper, tungsten and zinc) and Metalloid (graphite). Some electrodes materials are combined with other metals in order to cut more efficiently and improve MMR (Material Removal Ratio) and decrease the wear, for example, brass/zinc , tellurium/copper, copper/tungsten and silver/tungsten. Initially, brass and steel was the only electrode materials due yours high wear and they were really available and inexpensive. Later , operators increased wear ratio by using copper and its alloys.

The improvement in equipment made EDM one reasonable choice for the machining processes, the problem was, copper has a melting point approximately 1083 ºC (1980 F), while temperatures in the spark gap must exceed 10000 ºC (18064 ºF), this causes too high a wear rate in relation with metal removal rate.[6]

Graphite appears slowly on the market , however with certain developments, graphite becomes an electrode material with a big MMR in comparison with wear. Graphite belongs to the "Metalloid" group, which means, graphite does not melt in the spark gap, but goes directly from solid state to gas. This process is called "Sublimation". The sublimation temperatures are approximately 3500 ºC (6332 ºF), because of that, graphite is a much more efficient electrode material in comparison with copper, due the high resistance to heat in the spark gap.[6] Tungsten has a similar melting point to graphite, but it’s far harder to machine.

Table 1 – Electrode Materials Melting Points [6]

MATERIAL	SPECIFIC GRAVITY	DEGREES FAHRENHEIT	DEGREES CENTIGRADE	CONDUTIVITY *
Aluminium	2.70	1220	660	63.00
Cobalt	8.71	2696	1480	16.93
Copper	8.89	1980	1082	97.61
Manganese	7.30	2300	1260	15.75
Molybdenum	10.20	4757	2625	17.60
Nickel	8.80	2651	1455	12.89
Carbon Steel		2500	1371	12.00
Titanium	4.50	3308	1820	12.73
Tungten	18.85	6098	3370	14.00

* Condutivity values are based on silver = 100.00

Graphite is much easier to machine or grind, there are no resulting burrs to remove, in comparison with the " metallic" electrodes, but in the beginning it is not easily accepted because is considered "too dirty", in other words, when it is machined, graphite does not create chips, but create black dust. This black dust it's not a benefit for the shop or the machines because of the abrasive characteristics of graphite that cause premature wear into the machines and if the dust is not cleaned during the machining of the electrodes, it will blanket the entire shop. To solve this problem a vacuum system should be used. [7]

7.3 Metallic vs. Metalloid

The major advantages of the metallic electrodes are : high strength, machining "safety", low cost, mirror finishes, good characteristics for wire cuts and discharge dressing . On the other hand, the major disadvantages are: high wear, slow machining speeds and occurrence of burrs and low grindability index.

In the case of Metalloid, the principal advantages are: good wear resistance, high material removal ratio, high strength, good machinability (no existence of burrs) and it can be abraded or ultrasonic machined. The main disadvantages are: high cost, difficult machining conditions , black dust from machining, lower "safety " index and wire cuts slowly.

7.4 Electrode Wear (EW)

The wear of the tool electrodes is not completely eliminated, but with today's level of technology it can be reduced to small values. In EDM, the tool wear problem is very critical since tool shape degeneration affects directly the final shape of the die cavity. In addition, the cost of a part manufactured by the EDM method is determined mainly by the tool cost, which consists of the raw material cost of the tool, the tool production cost and the number of tools required for operation, generally 70% of the final price. There are three types of tool wear, front wear, edge wear and side wear . Firstly presented, the front wear is the percentage ratio of the amount of electrode material lost from the bottom end of the electrode, to the depth of the cavity burned ($h_a$in Fig.25). Secondly the edge wear is the percentage ratio of the length lost (measured in the burn direction, usually Z) of a 90 degree external corner on the electrode, to the length of the corresponding sharp internal corner produced in the cavity. It should be noted that corner wear is almost always significantly greater than end wear, because the corner is being attacked by a multitude of sparks from many directions simultaneously. Besides, it should also be noted that edge wear is dramatically affected by the included angle of the electrode external sharp corner, since corner wear is a function of the surface-to-volume ratio of the corner condition. Finally the side wear, is represented by the tool side surface taper angle (βin Fig25.). In many research works, side wear is neglected since it has a very small angle. The other geometrical tool wear characteristics; namely, edge wear and front wear, are much more evident than side wear and are largely responsible for the degeneration of the tool shape and eventually the workpiece geometry.

In today's technology, the new EDM machine tools and pulse generators can reduce the wear ratio below 1% (called as "no wear" case) by setting the machining parameters in accordance with the machine tool manufacturers catalogs. At the "no wear" case, the side wear and the frontal wear of the tool electrode are very low but the tool edge wear is still at large quantities.[43, 42, 44]

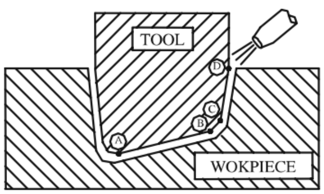

Zone	Descriptive Parameter	Wear Type
AB	Φ, h_a	Front Wear
BC	r	Edge Wear
CD	β	Side Wear

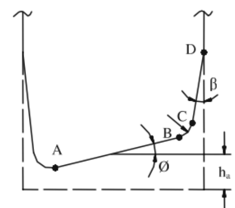

Figure 25 – Geometrical Wear Characteristics [44]

Tool wear is generally expressed by means of tool wear rate (EWR) , wear ratio(WR) and Workpiece removal rate (WRR) [44]

$$EWR[mm^3/min] = VRT/t_m \tag{6}$$

$$WRR[mm^3/min] = VRW/t_m \tag{7}$$

$$WR[\%] = (EWR/WRR) \times 100 \tag{8}$$

Note that:
VRT is volumetric removal from tool $[mm^3]$
ERW is volumetric removal from workpiece $[mm^3]$
$t_m$is the machining time $[min]$

7.4.1 Electrode Wear in Die-Sinking *EDM*

As mentioned earlier on subsection Die-sinking EDM, this process is the most widely used technique for the fabrication of die and mold cavities. However in any replication process, it is expected that the quality mold will faithfully duplicate its shape and surface texture. On account of that, inaccurate duplications cause problems in assemblies, final finishes, dimensional and geometrical tolerances. The process performance for the intricate areas such as sharp or pointed corner, flat or pointed areas of electrode, is obviously different because of different concentration of heat and current density that promotes the electrode material is also melted and vaporized (EWR). Due to this wear, electrodes loose their dimensions resulting inaccuracy of the formed cavities, nevertheless the electrode wear can be reduced in several ways, such as, using different electrode materials for roughing and finishing operations, sensing the electrode wear, providing compensation and strengthening the surface of the electrode with high wear resistance coating.[45]

Table 2 – Influence of the Electrode Shape an Current Intensity on the Wear Parameters[45]

Input			Response			
Ex. No	Shape *	Current (A)	*MRR*	*EWR*	*WR*	R_a (μm)
1	○	2.5	7.14	0.114	0.016	0.16
2	□		6.35	0.152	0.024	0.19
3	Δ		5.36	0.177	0.033	0.21
4	◊		5.12	0.266	0.052	0.22
5	○	3.5	10.4	0.271	0.026	1.24
6	□		9.5	0.323	0.034	1.27
7	Δ		8.92	0.410	0.046	1.27
8	◊		8.23	0.502	0.061	1.36
9	○	6.5	29.1	6.700	0.230	2.45
10	□		28.9	7.798	0.270	2.66
11	Δ		28.1	8.155	0.290	2.87
12	◊		27.6	10.76	0.390	3.23

The Tab.2 shows the influence of the electrode shape and current intensity on the material removal rate (MMR), electrode wear rate (EWR) and wear ratio (WR) on Die-Sinking EDM. As shown in Tab.2 the diamond shaped electrodes MRR were minimum because it has the largest peripheral length compared to the other electrodes which results more heat loss to the surrounding and finally causes low MRR. A round shaped electrode undergoes less wear, because of no vulnerable sharp corner at the sparking tip and the same is verifying for the WR, as shown in Fig.26. Finally, the influence of the shape of electrodes on surface roughness is found to be insignificant. [45]

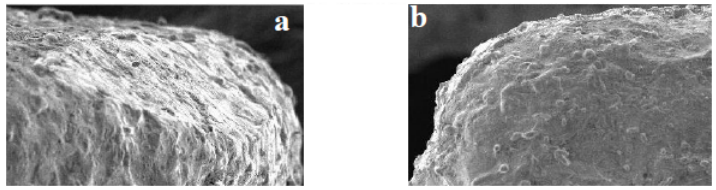

Figure 26 – SEM micrographs of electrode wear due to die sinking EDM with 2.5 A current for (a) round and (b) diamond shape configurations[45]

7.4.2 Electrode Wear in Micro-EDM

As previous described, the tool degeneration affects the final shape of the die cavity. In order to solve this problem one solution is to repeat the processing several times using new or reground micro-electrodes until the required profile of holes is obtained. Obviously, it is impracticable because of being rather time-consuming and difficulty in predicting the number of electrodes required. Application of the uniform wear method, the real-time wear compensation method and the method of enhancing loss speed of electrode to ensure contour integrality is effective only to a certain extent. However, these methods rely on rules about the loss of the electrodes caused by wearing, which are very difficult to be precisely estimated beforehand as the processing conditions change irregularly all the time.

7.5 Over cut (OC)

The over cut is defined as the gap distance between the electrode and the workpiece surface (see Fig. 27). The OC greatly affects the precision and accuracy of the workpiece dimensions and because of that becomes important when the component tolerance requirements are strict for making high precision tools and dies. However, the OC and the final workpiece dimensions are difficult to predict due to the non-linear, complex relationship among the electrode wear, the electrode diameter, electrical discharging parameters, and the machine positioning accuracy.[52]

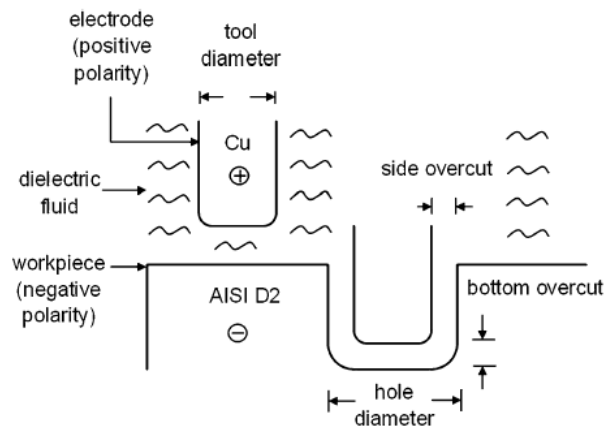

Figure 27 – Illustration of the overcut for a die-sinking process[52]

Many studies have shown that the over cut is associated with many variables, including electrical discharging parameters, such as discharge voltage, current, duty cycle, and pulse duration, the control circuit, the electrode, workpiece properties, and the working fluid. In a batch die-sinking EDM process, the spark hole dimensions vary even under fixed machining condition due to the inevitable, uncontrollable *OC* and progressive tool wear.

Some authors has studied the effect of operating parameters on the radial over cut (*ROC*) and found that the radial over cut increases at high current and on-time ratings, worsening the spark hole dimension accuracy. Others parameters have been investigated such the effects of discharge current, pulse duration, duty cycle, and voltage on radial over cut in the *EDM* of AISI D2 steel with copper electrode and was found that the discharging current and pulse duration are linearly proportional to the means of the radial over cut.

In micro-*EDM* process, was found that a small spark gap and gap stability are needed to obtain good spark hole dimensional accuracy and good performance.

Nerveless a lot of research has been conducted on the relationship of the *OC* with the geometric dimensional variables such as electrode wear and diameter of spark hole in the *EDM* process. Since the over cut and the other dimensional variables strongly influence each other, the coupling effects among the dimensional variables should be taken into consideration to accurately describe the over cut and its variation.[52]

8 Dielectric Fluid

8.1 Characteristics of Dielectric Fluid

The dielectric fluid is one of the most important parameters on EDM. In the past, oils has been used as a dielectric fluids but only in the last two decades, did they have any scientific approaches to the composition, capability with the environment and people, and more recently research about health and safety concerns. Furthermore dielectric has great importance into to the material removal rate and surface integrity. The dielectric strength is a very important parameter because it define the maximum electric field strength that he can stand without breakdown, for the gap distance is an important parameter as well.

The other important role is that the dielectric fluid acts as an insulator, until it ionizes and allows a current to flow through the gap, between the electrode and the workpiece. In order to obtain a good melting , solidification , and heat transfer among to the workpiece, it must have a good heat capacity, thermal conductivity and viscosity, which means, the dielectric must be capable to cool the electrode and workpiece to a reasonable work temperature, and also re-solidify the vaporized material into "chips"(thermal conductivity) and constrains the expansion of plasma channels and improve the explosive forces of the discharges(viscosity).[9]

A high chemical stability and passivity, a low volatility , good filter-ability, minimum odor and a low cost are also important parameters for the good performance of dielectric fluid. The Flash point and non-toxic vapors are the parameters directly related with the operation safety. In case of the flash point, the temperature of the dielectric fluid should never exceeds the temperature at which the vapors of the fluid will ignite 74 ºC (165 ºF).[7]

8.2 Dielectric Fluid Subsystems

The dielectric fluid subsystems is compound by a reservoir where is stored the dielectric fluid, a systems in charge over pressure control, pumps , valves, plumbing and filters that remove the debris and chips of the dielectric fluid.

8.3 Common Dielectric Liquid Fluids

Usually there are three major groups of dielectric fluids, petroleum or hydrocarbon fluids, deionized water and for specific operations emulsions and solutions of water and oil as you will see later on.
The hydrocarbon fluids (Kerosene and Paraffinic) are used by die-sinker machines, because

they provide a controlled environment to surround the sparking area, since they do not change their characteristics during the sparking. They break down into hydrogen and carbon.[1] The deionized water as its name implies, doesn't have impurities in its constitution and this fact promotes its electrical conductivity. Even so the deionized water absorbs material, that surrounds it, and that change its characteristics and affects the capacity to repeat the sparking process with the same purity of the fluid. Because of that and other reasons like low viscosity, good cooling efficiency, capability to see the working area the deionized water is used in the wire-cut machines. They need a fresh and high-flow jet of new fluid surrounding the working area. [1]

However, for specific EDM applications, water in oil emulsions, aqueous glycol solutions, distilled water containing borax, kaolin or acid boric are used. In a specific case to machine titanium , the choice is silicone fluids mixed with petroleum oils.[9]

8.4 Common Dielectric Gas Fluids

Compressed air it the most common gas used. However some studies have recently reported that oxygen gas and copper tool combination leads to a high MRR in dry EDM and nitrogen gas–water mixture dielectric and graphite tool combination leads to high surface finish in near-dry EDM.

9 Flushing Method

9.1 Characteristics of Flushing

According to the literature the most important parameter to a successful EDMing is flushing.[6]

The process of flushing consist into introduce "fresh" dielectric fluid to the cut, cool the electrode and the workpiece and flushes away the chips and debris from the spark gap.

In order to save time and money the EDMer should study the shape, cavities, details, surface area, corners, "dead areas", side draft, turbulence, cavitation, gas evacuation, "secondary discharge" and analyze the best way to flush the electrode. This principle goes by the name of "designing around flushing ".[7]

One of the main objectives of flushing is to avoid the danger of arcing in the gap, namely when the cavity contains too many erode particles because the insufficient removal of the same. This allows the current pass through the accumulated particles, occurrence of the arcing that promote new cavities wish can destroy the integrity of the workpiece. This occurs normally in the finishing operations, since the gap size is smaller than the roughing operations.

An efficient flushing requires a good balance between volume and pressure. For instance the high pressure can cause excessive electrode wear, due the high pressure which shakes the erode particles surrounding the electrode and this causes wear on the same.

Normally in finishing operations, a high pressure flushing is necessary due the smaller arc gap, this promotes a proper fluid flow, to cool the tool and workpiece and to remove the erode particles. By contrast the roughing operations requires low pressure and high volume of fluid owing your larger arc gap.

The flushing pressure revolves around 3 to 5 psi (0.2 to 0.33 bars).[7]

9.2 Types of Flushing

9.2.1 Pressure Flushing

The pressure flushing or injection flushing is the most common and preferred method, due to simplicity and easiness. In this process the operator can visualize the amount of oil that is being used and this fact is extremely important to monitor the flushing process.

There are two ways of flushing the working area, one through the electrode as show in Fig.28a) another through the workpiece, briefly, in this operations the oil is introduced through holes, previously drilled, in the electrode itself or for holes in the workpiece where the cavity will be.

The major concern in flushing operations through the electrode, are the studs or spikes that remains from the electrode flushing hole, for instance, if the stud achieve substantial dimensions, it can affects the proper flushing[6] .

In order to remove the studs, there are different ways such as, by hand, by a portable grinder, with another electrode or if the machine has a orbiting capabilities. Normally when the suds are removed by, for example, finishing electrode, the holes are drilled in different locations, in comparison with roughing electrodes, to ensure that the studs will be removed.

In order to prevent long studs, the flushing holes generally are drilled on an angle, but this technique may have some implications, for example, they can prevent a proper flushing , by directing oil away from needed areas.

In addition to flushing through the electrode, there is a flushing through the workpiece. This kind of flushing is done by a flushing "pot" or plenum chamber beneath the workpiece and is especially useful in moldmaking because the predrilled ejector and core pin holes already existing in the cavity[13].

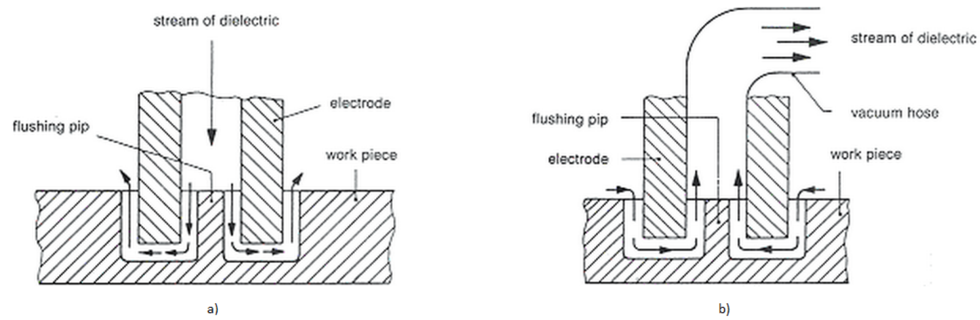

Figure 28 – Types of Flushing a)Pressure Flushing through the Electrode b) Suction Flushing[14]

9.2.2 Suction Flushing

In suction or vacuum flushing the eroded particles are sucked out of the working area (gap between the electrode and workpiece), through the electrode as shown in Fig. on this pageb) or the workpiece, usually, is used when the accuracy and straightness of cavity side walls are imperative.

Two important aspect from suction flushing are the fact that the oil is sucked from the work tank not from the clean filtered oil, and maybe the most negative aspect, the operator cannot visualize the oil stream.

This process reveals good results when the workpiece has wall tapering ,it is efficient to minimize secondary discharges and has a efficient cutting when the worktank is clean.

However careful attention it's required about the flushing pressure and gas removal. As a consequence of a high pressure can occurs , slow machining times, excessive corner wear and the electrode can be pulled from its mount, or workpiece from the magnetic chuck. In addiction if the gases aren't sufficiently removed this can cause a electrode explosion[13].

9.2.3 Combined Flushing

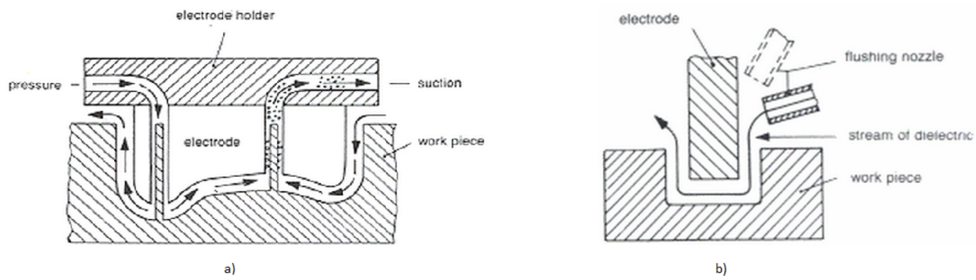

Figure 29 – Types of Flushing a)Combined Flushing b) Jet Flushing [14]

9.2.4 Jet Flushing

In fact this process is the least efficient , generally is used for shallow cuts and due to size or shape restrictions. Jet flushing as shown in Fig. on the current pageb) is done by tubes or flushing nozzles and is a " mechanical assist" process, this means, it needs to be aided by a time pulse or jump of the advancing axis. This motion, return stroke of the advancing electrode, promotes cool and fresh dielectric fluid to be drawn into to the cavity area "diluting" the contaminated oil. [6]

The biggest concern about this process is the danger of not removing the particles from the working area, this can causes trapping particles in the corners and on "dead areas", which may well be responsible for the occurrence of DC arcing.

Nevertheless, the non-appearance of studs is a big advantage of this process.

9.2.5 Pulse Flushing

Actually, there are three types of pulse flushing : rotary flushing, vertical flushing, orbiting flushing. Sub meant that, in this three types of pulse flushing the working area , is submerged in dielectric fluid and can be aided by nozzles to help to remove the eroded particles.

For a better understanding of the three types, in rotary flushing , the electrode rotates in the cavity; in vertical flushing, the electrode moves up and down and this motion causes a "pumping effect" that helps the flow of dielectric fluid; in orbiting flushing, the electrode is smaller than the cavity and this allows the orbit motion of the electrode inside the cavity, thus allowing the removal of the eroded particles.

10 Performance

10.1 Accuracy

The values of shape accuracy ranging from $1\mu m$, in micro EDM, to $3\mu m$ in die-sinking and wire cut EDM, with a repeatability accuracy ranging from $\pm 0.002mm$ to $\pm 0.05mm$ in the various types of EDM.[77, 78, 80, 81]

The surface finish (Ra) ranging from $0.05\mu m$, in micro EDM, to $2.5\mu m$ in die-sinking EDM. [81, 79]

10.2 Precision

The values of precision ranging from $1\mu m$, in micro EDM, to $15\mu m$ in die-sinking and wire cut EDM.[81, 79]

11 Advantages vs Disadvantages

The advantages of EDM include: machining of complex shapes that would otherwise be difficult to produce with conventional cutting tools, extremely hard material to very close tolerances, very small work pieces where conventional cutting tools may damage the part from excess cutting tool pressure, there is no direct contact between tool and work piece. Therefore delicate sections and weak materials can be machined without any distortion, a good surface finish can be obtained and very fine holes can be easily drilled.[57]

Some of the disadvantages of EDM include: the slow rate of material removal, the additional time and cost used for creating electrodes for ram/sinker EDM, reproducing sharp corners on the workpiece is difficult due to electrode wear, specific power consumption is very high. Power consumption is high, OC is formed, excessive tool wear occurs during machining and electrically non-conductive materials can be machined only with specific set-up of the process.[57]

12 Applications

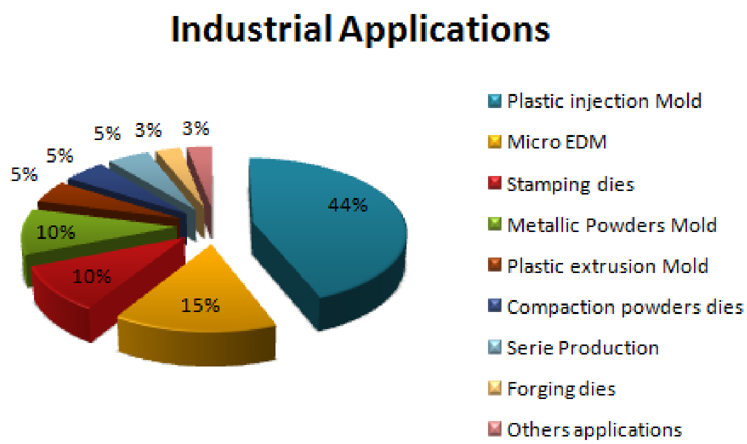

Figure 30 – Graphic Industrial Applications[82]

12.1 Industrial Applications

Automotive industries

This is one of the many applications on automotive industry, a high volume production fuel injector with 7, 8, 9 and 12 holes (see Fig.31) at multiple spray angle, hole height and spacing. The improved design with multiple smaller holes leads to better fuel dispersions in the cylinder, higher rate burning, increased power, reduced pollution. High quality hole no burrs, no taper, no micro cracking, excellent surface quality. [53] Gears, clutch components, and many other engine parts are obtained with *EDM* technology too.

Figure 31 – Examples of fuel injectors [53]

Plastic injection mold making

EDM is a machining process used to create plastic injection mold with intricate and complex shapes. The use of *EDM* in injection molding tooling is so essential that it is almost impossible to imagine a modern shop without and *EDM* machine. Many of today's products simply could not be produced without it. Some equipments as cell phones, calculators, IPods, cameras, medical devices and the endless amounts of high tech equipment that are made out of plastic and can not be produced without this technology as shown in Fig.32a)[54]

Wire cut *EDM* is widely used to machine various molds, such as punch die, squeezing die, powder metallurgy mold, bend mold, plastic mold(see Fig.32b)). Among these different kind molds, cutting punch die take a great share, to precious punch die machining, wire cut *EDM* machining is a indispensable technology. By adjusting different compensation value while programming, wire cut *EDM* can cut terrace die, punch plate, stripper plate and etc, it is easy to meet the requirement of mold fitting clearance and machining accuracy.[65]

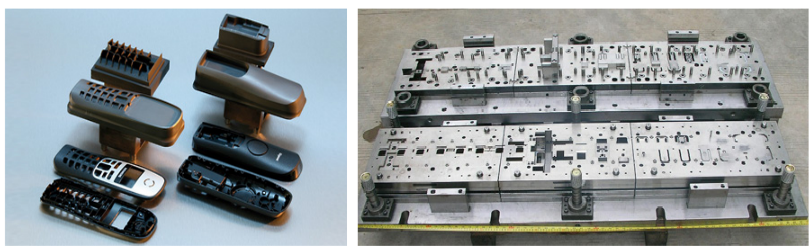

a) b) 9

Figure 32 – Examples of EDM applications on plastic injection molds: a) cell phones plastic mold b) plastic mold [55][65]

Die-sinking stamping and forging applications Sinker *EDM* is a versatile machining method, that can perform jobs ranging from making holes, to sinking complex surfaces, all with the ability to hold very close tolerances. Sinker *EDM* machining is used for more complex shapes and it uses machined electrodes to erode the desired shape.

Because it can create intricate and complex parts, *EDM* machining is advantageous over other machining techniques. It can also machine hard materials and machine extremely small parts. The work piece does not get deformed through *EDM* machining; the finished product will not have burrs or heat damage. Also, through *EDM* machining, internal cavities can be cut because electrodes can rotate about two-three axis.

Common applications for *EDM* machining include die casting dies and forging dies. It can also be used for manufacturing engine parts such as titanium as shown in Fig.33

Figure 33 – Examples of die-sinking stamping and forging applications [56][66]

12.2 Other Applications

12.2.1 Aerospace

Electrical discharge machining is capable to manufacture all sizes of production parts such, holes, slots, shaped holes, and micro holes for larger aerospace blades, vanes, rings, burner for aircraft, helicopter, jet and missile. From rocket guidance systems to unmanned flight hardware, to drone surveilance and gyroscopes.

The main reason for that choice is the capacity with high temperature alloys and exotic metals used for aerospace applications as Kovar, Invar, Inconel, Niobium, Scandium and much more.[47]

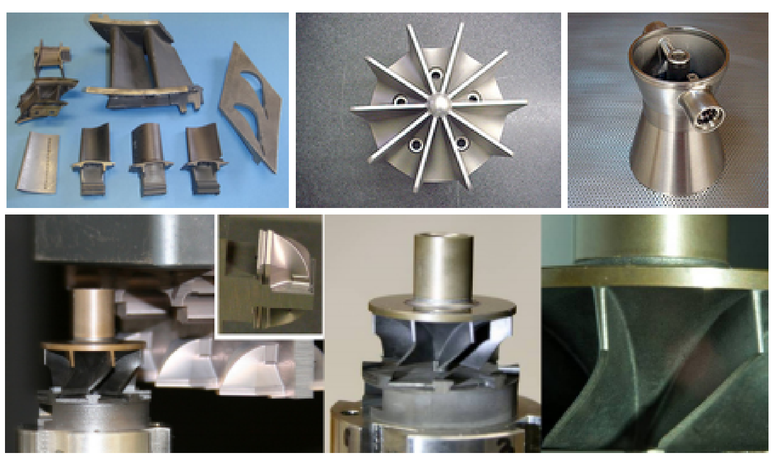

Figure 34 – Examples of aerospace applications[53][69][68]

12.2.2 Medical

Medical hardware continues to be a growing segment. The *EDM* process is chosen due to the increasingly complex geometries, hardness of materials and tight quality requirements of the latest generation of orthopedic components such medical staplers, retainers for medical tests, surgical blade, and all kind of prosthesis included micro bolts and screws. *EDM* can produce features not easily achieved with conventional machining methods. These features include narrow precision slots, contour shapes, and dead-stop holes.[46]

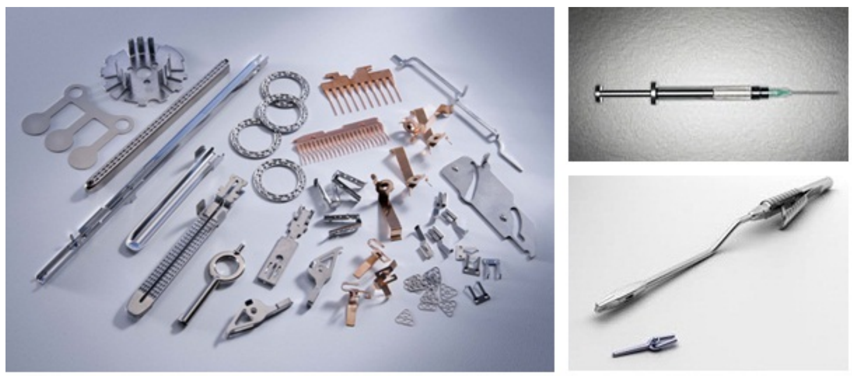

Figure 35 – Examples of medical applications[47][67]

12.2.3 Military

EDM machining process are ideal for military machining, creating military components and subprime individual components (see Fig.36) for larger companies that supply completed equipment, vehicles, etc. for military use. Also creates parts and components used in Rolls Royce's jet engines, which are used on a number of US fighter jets.[48]

These military machining projects include[48]:

- General Atomics' highly advanced, unmanned MQ-1 Predator drones
- Boeing's B-52 Stratofortress bombers
- McDonnell Douglas' F-15 Eagle fighter jets
- General Dynamics' F-16 Fighting Falcon fighter jets
- McDonnell Douglas' F-18 Hornet fighter jets

- Lockheed-Martin's F-35 Lightning II fighter jets

These defense components are made up of numerous and exotic materials described in the next section .[47]

Figure 36 – Example of military applications[47][69][70][71]

12.3 Types of Parts Obtained

12.3.1 Materials

In *EDM* process all the electrical conductive materials (see Fig.37) can be machined (Steel, Stainless Steel, Aluminum,pre-hardened steel) even as exotic materials such: Titanium, Inconel, H480, H4100, Ar236, AR400, AR500, Niobium, Molybdenum, Kevlar, Bullet-proof Glass, Waspaloy, Hastelloy, Kovar, Invar and Scandium.

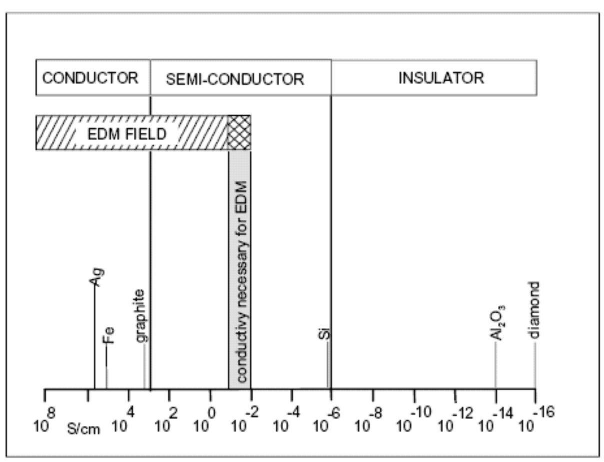

Figure 37 – Electric conductivity necessary for EDM [72]

12.3.2 Geometries

EDM is more capable to produce complex shapes comparatively with other machining processes. *EDM* can be used to machine a wide variety of materials with closer tolerances than conventional machining. Very small delicate pieces can be created without damage due to cutting pressure, and referred cost-effectiveness of small volumes. Other geometries such "blind" cavities, unlike stamping dies, small holes, burr-free sharp edges, extremely small parts that are difficult to fixture, small inside-corner radii, helical gears, hexes for special bolts and parts and internal splines.

Simple, flat shapes, which usually would be metal stamped, can be a job for Wire *EDM* when they require a superior quality edge. Wire *EDM* can produce complex, contoured shapes, freeing the designer, to design the complex configuration, in one piece rather than several.

12.3.3 Scale

After a survey among the main producers (Die-sinking and Wire*EDM*), the parts obtained have dimensions that can go from almost the size of the electrode, provided they can be fixed securely, until the maximum load capacity of the machine or to the dimensions of the worktable. In the last case the maximum workpiece dimensions can go until $2000 \times 1800 \times 395$ [mm] and the maximum workpiece weight can go until 4000 [kg].

For Micro *EDM*, the workpiece weight can go until 50 [kg] and is possible obtain parts with electrodes that can down to 45μm, in *EDM* micro drilling machines are generally available with electrodes as small as 50 μm. In addiction micro drilling operations can be precisely controlled to drill accurate holes with diameters ranging from 5 μm to 300 μm.[75, 81]

13 Sodick AD3L

"Since 1976, Sodick has manufactured over 55,000 *EDM* machines and over 30,000 linear motor driven EDMs. Sodick machines are used for the production of dies and molds and other various applications which cannot be produced by standard machining methods. Sodick EDMs enable the user to become the envy of their competition, as Sodick is committed to the highest quality standards.

As an *EDM* leader, Sodick has continuously conducted research and development that has resulted in machines with sophisticated and unique features. Continuous investments are also made in our three production facilities that have made it possible to manufacture all machine components to result in high-precision and high-performance machines. It is our highest aim that we continuously serve our customers by offering the most advanced machines to meet our customers' requirements and expectations."[83]

13.1 Machine tool

Table 3 – Machine tool parameters

Machine tool	
Work table size (W x D)	600 x400 mm
Work tank inner dimensions (W x D x H)	925 x 555 x300 mm
Work tank fluel level (min- max)	100 - 250 mm
work tank capacity	145 l
X axis travel	300 mm
Y axis travel	250 mm
Z axis travel	250 mm
Max thrust	50 kg
Max weight of workpiece	550 kg
Distance between from floor and table top	810 mm
Machine tool dimensions (W x D x H)	1,870 x 1,955 x 2,315 mm (incl. Power supply and dielectric tank)
Machine tool weight	3,200 kg (incl. Power supply)
Total power input	3 phases 50/60 Hz 13 kVA (incl. Dielectric cooling unit; option)
Air pressure	0,45 Mpa (Automatic Clamping chuck 0,65 Mpa)
Air flow	100NL/min

13.2 Dielectric tank

Table 4 – Dielectric tank parameters

Dielectric tank	
External dimensions (W x D x H)	800 x 1,705 x 2,125 mm
Weight (empty)	840 kg
Dielectric fluid	oil
Capacity	400 l
Filtration method	Replaceable paper filter (MF-240)

13.3 Power supply unit "LN1"

Table 5 – Power supply unit parameters

Power supply unit "LN1"	
Max. Machinig current	40 A
Discharging power supply unit	Optimum pulse control for TMM Power supply with SVC circuit
Power requirement	200/220 V 50/60 Hz
CNC unit	Multi-tasking OS, Sodick Motion Controller
User´s memory capacity	Editing: 100,000 blocks; Saving; 30 MB
Memory device	Hard disk, Floppy disk
Input format	FDD, Touch panel, Serial interface keyboard
Display type	15" TFT-LCD
Character set	Alphanumeric an symbols
Keyboard	Standard 101-key, Function key
Remote controller (option)	Jog, OFF ENT HALT, Clamp/unclamp, etc.
Position command	Incremental and absolute
Max. Input comand	± 999999.999 / ±999999.999 / ±999999.999
Machining conditions storage capacity	1,000 conditions (C000 - C999)
Offset settings storage capacity	1,000 conditions (H000 - H999)
Program sequence number assignments	N000000000 - N999999999
Subprogram nesting levels	50
Q command nesting levels	7
Number of coordinates	60
Simultaneous control axis	max 4 (LN10: max 8)
Min. Input command	0.1 µm
Min. Drive unit	0.1 µm
AJC speed	X, Y axis max 5 m/min; Z axis max 36m/min
Jog feed rate	3 m/min
Control System	Full closed loop (Linear scales)
Drive mechanism	Linear motor
Compensation	Pitch error/torque compensation for each axis
Editing	Editing during machining, multi-editing
Graphics	XY, YZ, ZX plane, 3D, graphics drawing during machining, back ground graphics drawing, etc.

Part II

Experimental Part

14 Objective of work

The objectives in the present experimental work on *EDM* drilling of a *MMC* ($AlMg10\,5\%\,SiC$), are to investigate and report to the influence of certain output parameters, such as *peak current*, *servo voltage*, *pulse on-time* and *pulse off-time*, on the responses of *material removal ratio* (*MRR*), *electrode wear* (*EW*) and *radial over cut* (*ROC*) and *taper* (*TAPER*), through the *Taguchi* method and *ANOVA*.

15 Material

15.1 Aluminum

Aluminum is the most abundant metallic element and third component of the earth's crust (8% weight) to oxygen (47%) and silicon (28%). In its natural state, aluminum is never found in the form of metal, it is very reactive always combined with other elements. The most common compounds are oxides (alumina) and hydroxides mainly from bauxite, silicates from clay and half case and the complexes water soluble forms sulphate, nitrates, chlorides in the presence of dissolved organics.

The aluminum metal is extracted from bauxite, which is named after the discovery of Baux-de-Provence town by Pierre Berthier in 1821. This aluminum oxide hydrate contains large amounts of alumina, Al_2O_3. Alumina, very hard compound having the appearance of a fine white powder, is isolated of bauxite by chemical process for the removal of impurities (Bayer process includes a treatment bauxite in an autoclave, followed by filtration, precipitation and calcination). Aluminum metal is then obtained by electrolysis of alumina mixed with cryolite (AlF_3, $3NaF$) and his properties can be seen in Tab.6

Table 6 – Aluminum Properties

Essential properties	Descriptions
Electrical resistivity (Ω.cm)	2,7 $\times 10^{-6}$
Melting point ($^\circ$C)	660
Thermal conductivity (W/m.K)	220
Specific heat (J/Kg.K)	904
Thermal expansion coefficient (1/ $^\circ$C)	24 $\times 10^{-6}$

Specific physico-chemical properties of aluminum make it a popular component in many sectors. The metallurgy of aluminum is based on the electrolytic reduction of alumina. The aluminum is used in various areas as building, transportation (automotive, aerospace, rail, aerospace), food (preservatives, colors, additives, etc..), packaging (beverage cans, food packaging), utensils of kitchen units, surgery: ceramics in orthopedic and dental surgery, orthopedic implants alloys and many other applications.

15.2 Metal Matrix Composite Foam $AlMg10\,5\%\,SiC$

The challenge for production engineering right now is the development of energy efficient production processes as well as new concepts for innovative, sustainable and high-quality products. One strategy to achieve these kinds of products is to focus on lightweight concepts. These concepts are based on new materials with unique characteristics as well as the substitution of approved materials, which can be done by adapting design aspects or by using materials with low weight and high strength values.

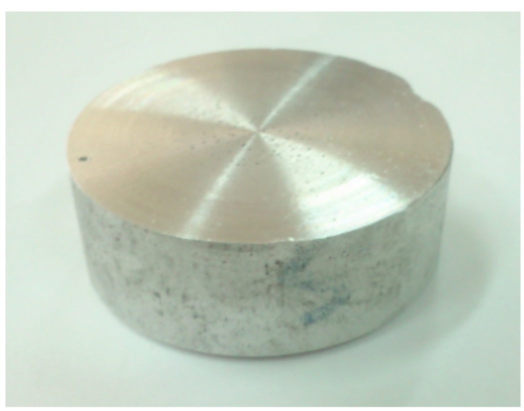

Figure 38 – Workpiece $AlMg10\,5\%\,SiC$

In this investigation the test material is a Stabilized Aluminum Foam (SAF). This material is versatile and cost effective material for use in a broad range of industry applications, combining the unique properties of SAF with a streamlined manufacturing process. SAF is used mainly on automotive industry increasing the performance of components by using the following characteristics: high mechanical energy absorption in all directions, excellent strength and stiffness to weight ratios, constant properties over temperature and moisture ranges, recyclable, notch insensitive (holes do not affect material strength), fire retardancy with no environmental degradation and acoustic and thermal insulating properties[87].

Table 7 – Workpiece dimensions

Dimensions	Measurements (mm)			
	1º	2º	3º	Average
Diameter	41,31	41,35	41,26	41,31
Length	15,12	15,16	15,15	15,14

In this particular SAF, the base material is a metal matrix, composed by aluminum alloy with ceramic particles added. The particles are necessary to stabilize the foam bubbles, shown in Fig.39, since, without the particles, the bubbles would form but then immediately collapse. The stabilizing particles slow the drainage of the aluminum in the cell walls and increase the apparent viscosity.

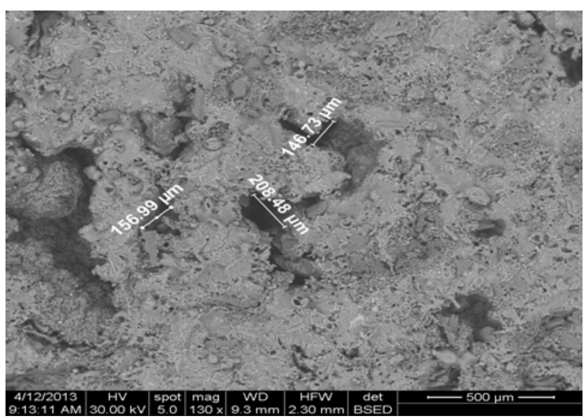

Figure 39 – SEM image highlighting porosity distribution and morphology of the composite structure formed. One can easily see a multitude of micro-porous globular structure as well as pores which have dimensions of the order of 150 µm having a mass distributed throughout the composite.

Other important characteristics of this material is the melting point, and the electrical conductivity, the melting point presents a value of 710 ^{o}C.

Table 8 – SAF composition

Component	Weight %	overall %
Al	42,1	80
Mg	4,4	7,6
Si	5,3	5
C	36,5	2,3
O	8,8	2,1
Ca	0,3	0,6
Fe	0,9	1,2
Cu	1,5	1,2

The Tab.8 shows the specific composition of the material in weight percentage and overall percentage. However the disposal of the elements is not homogenous in all material. To better understand this phenomena the Fig.40 shows the specific quantity of each element into a specific part of the foam.

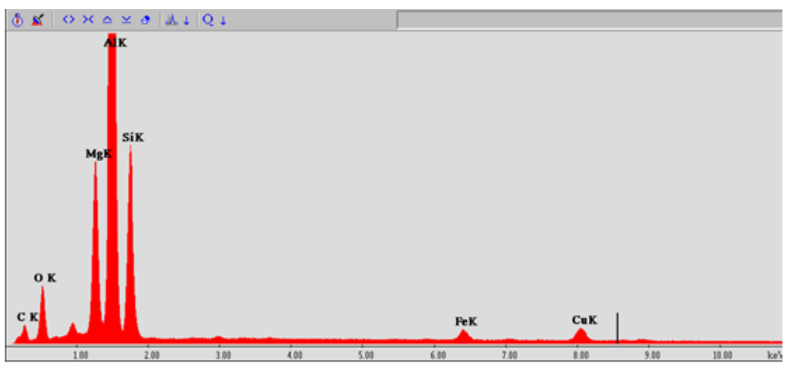

Figure 40 – Electron diffraction with images SEI EDX distribution maps outlining the main constitution of the composite. The colors are chosen in order to differentiate the distribution of the constituents on the basis of: Al.Si, Fe, Cu, Mg, O and C.

Fig.41 shows the specific location and quantity of each element into a specif part of the foam. The picture has color scheme, where is possible to see each element separately. The particles with a bigger size are the silicone (SiC) particles followed by the iron particles (Fe) and carbon particles (C).

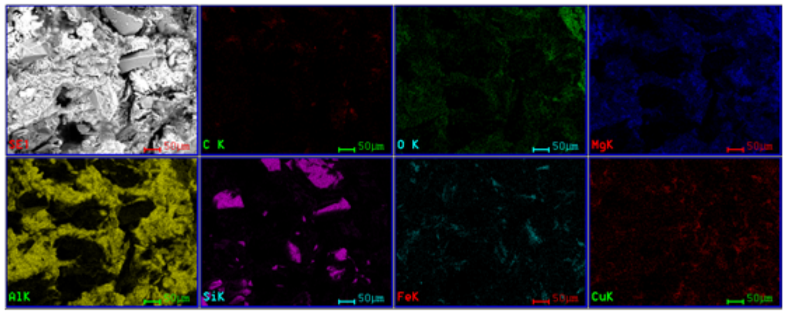

Figure 41 – Secondary electron image (SEI) in combination with EDX qualitative analysis to highlight the distribution map of aluminum and silicon, elements identified SEI image. One can easily observe SiC and diffuse distribution of pores in the matrix composite.

16 Methods

16.1 Taguchi Method

First appearance of Taguchi method was in 1960 in Japanese companies that used this method to greatly improve the quality of their products with great success. Since then it has been used for many companies which realized that the old methods for ensuring quality were not competitive with the Japanese new methods.

Dr. Genichi Taguchi developed his method based on several general steps as definition of a target value for a performance measure of the process, following by a determination of the design parameters affecting the process and their values, creation of arrays based on the parameters and their levels, conducting the experiments including the data collection on the effect of performance measure and finally, complete the process with the data analysis to determine the effect of the different parameters on the process performance and performing a validation test as shown on the diagram of the Fig.42.

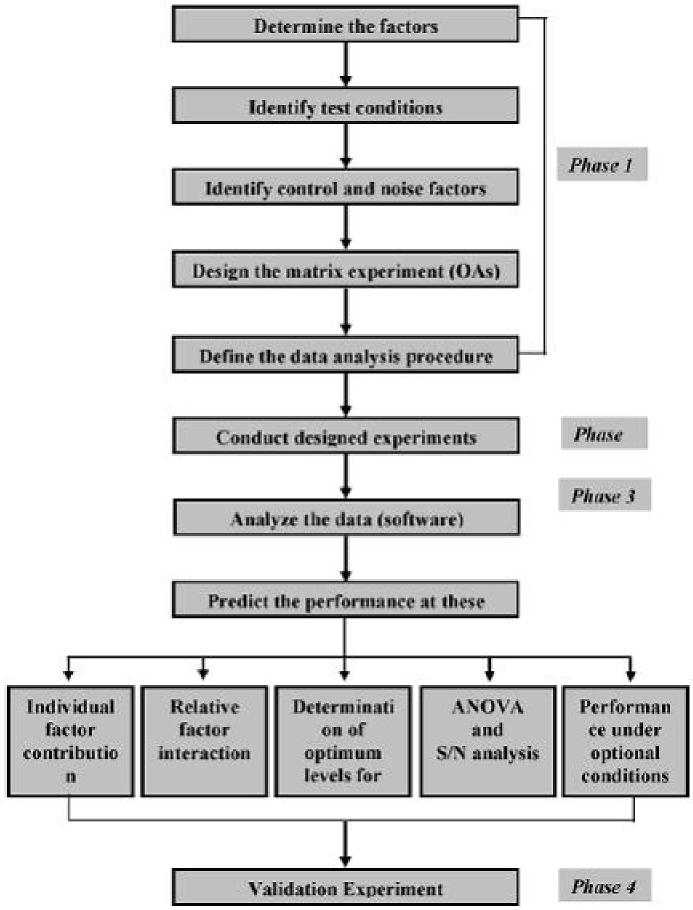

Figure 42 – Taguchi method diagram [97]

As previous mentioned the TM is based on performing evaluation or experiments to test the sensitivity of a set of response variables to a set of control parameters (or independent variables) by considering experiments in "orthogonal array" while Design of experiments only considering experiments in "fractional designs"or "full factorial designs".

Both arrays are represented by the Eq.9, however with different interpretations.

$$L = nl^{np} \tag{9}$$

where nl are the number of levels and np are the number of parameters.

Factorial designs are widely used in experiments involving several factors where it is necessary to study the joint effect of the factors on a response.

$$Fractional\, array\, 3^4 = 81\, runs \tag{10}$$

Otherwise orthogonal arrays are highly fractional orthogonal designs with an aim to attain the optimum setting of the control parameters. These designs can be used to estimate the main effects using only a few experimental runs as shown latter on.

The selection of a proper orthogonal array is based on the total number of degrees of freedom (DOF) that is calculated based on:

$$DOF = [(number\,of\,levels - 1) \times number\,of\,parameters] + 1 \tag{11}$$

To better understand the difference between the full factorial array and orthogonal array, the orthogonal array (3^4) applied on Eq.12 only needs 9 runs to evaluate the experiment, however the same full factorial array (3^4) needs 81 runs to complete the same experiment.

$$DOF = [(3 - 1) \times 4] + 1 = 9\,runs \tag{12}$$

A standard Taguchi $L_9(3^4)$ orthogonal Array (OA) was chosen for this investigation since it can operate four parameters: A (*peak current*) , B (*servo voltage*), C (*pulse on-time*), D (*pulse off-time*), each at three levels (1, 2, 3) as shown in Tab.9. Those three levels are sufficient to achieve considerable details of the effect of different parameter values on experimental results. The criteria used for choosing the three parameter levels is based on exploring a maximum range of experimental variables, avoiding to including the range which is already known. That range will be out of interest.[84, 85]

Table 9 – Standard L9 (3^4) Orthogonal Array used in Taguchi Method[84]

Run	A	B	C	D
1	1	1	1	1
2	1	2	2	2
3	1	3	3	3
4	2	1	2	3
5	2	2	3	1
6	2	3	1	2
7	3	1	3	2
8	3	2	1	3
9	3	3	2	1

Taguchi Methods use the S/N (signal-to-noise) ratio to analyze the test run results because the S/N ratio resulting in minimization of quality characteristics variation due to uncontrollable parameters. The S/N ratio is also used in Analysis of Variance (ANONA). The term S/N ratio is borrowed from signal processing technology, but has different meanings here. The standard S/N ratios can be customized to fit specific applications and new S/N ratios can be developed for particular applications. Selecting the proper S/N ratio depends on the physical properties of the problem, the engineering insight, the pursuing experiment results, etc.. [85]

According to Taguchi method a number of S/N ratios are available as "nominal the best", "the higher the better" (HB) and "the lower the better" (LB), but in this case the last two are the proper ones. In this work, the experimentally observed material removal rate *(MRR)* value is (HB), and the electrode wear (EW), radial over cut (ROC) and $TAPER$ values are (LB). Based on the Taguchi method, the S/N ratio calculation was decided as "the higher the better,HB" and "the lower the better, LB" as are given in the following equations:

$$HB: \quad \eta = -10log_{10}\left(\frac{1}{N}\sum_{i=1}^{N}{y_i}^{-2}\right) \tag{13}$$

$$LB: \quad \eta = -10log_{10}\left(\frac{1}{N}\sum_{i=1}^{N}{y_i}^{2}\right) \tag{14}$$

where denotes the S/N ratio calculated from the observed values (unit: dB), yi represents the experimentally observed value of the ith experiment, and N is the repeated number of each experiment.

16.2 *ANOVA*

The previous mentioned $ANOVA$ was first introduced by Sir Ronald Fisher and is a standard statistical technique to interpret the experimental results. The percentage contribution of various process parameters to the selected performance characteristic can be estimated by $ANOVA$. Thus information about how significant the effect of each controlled parameter is on the quality characteristic of interest can be obtained. $ANOVA$ for raw data has been performed to identify the significant parameters and to quantify their effect on the performance characteristic.[86]

In $ANOVA$, total sum of squares(SS_T) is calculated by [86]:

$$SS_T = \sum_{i=1}^{N}(y_i - \overline{y})^2 \tag{15}$$

where N is the number of experiments in the orthogonal array, in our case $N = 9$, y_i is the experimental result for the ith experiment and $\overline{y}$ is given by:

$$\overline{y} = \frac{1}{N}\sum_{i=1}^{N} y_i \tag{16}$$

The total sum of the squared deviations SS_T is decomposed into two sources: the sum of the squared deviations SS_P due to each process parameter and the sum of the squared error SS_E. SS_P can be calculated as:

$$SS_p = \sum_{j=1}^{t}\frac{(Sy_j)^2}{t} - \frac{1}{N}\left[\sum_{i=1}^{N} y_i\right]^2 \tag{17}$$

where P represent one of the experiment parameters, j the level number of this parameter P, t the repetition of each level of the parameter P,SY_j the sum of the experimental results involving this parameter P and level j. The sum of squares from error SS_E is:

$$SS_E = SS_T - SS_A - SS_B - SS_C \tag{18}$$

The total degrees of freedom is $D_T = N - 1$, and the degrees of freedom of each tested parameter is $D_P = t - 1$. The variance of the parameter tested is $V_P = SS_P/D_P$. Then, the $F - value$ for each design parameter is simply the ratio of the mean of squares deviations to the mean of the squared error ($F_P = V_P/V_E$). The percentage contribution ρ can be calculated as:

$$\rho_P = \frac{SS_P}{SS_T} \tag{19}$$

When the error of DOF is small or zero, which is the case when all columns of the OA are occupied and trials are not repeated, information regarding the error sum of squares cannot be determined. In addition, F ratios for the factors cannot be calculated because the calculations involve V_E. To complete the calculations, smaller factorial effects are added together (pooled) to form a new non-zero estimate of the error term (pooled error), this is known as a pooling-up strategy. The factors and interactions that are now significant, in comparison with larger magnitude of the error term, are now influential. Taguchi prefers this strategy as it tends to avoid the mistake (alpha mistake) of ignoring helpful factors[96].

16.3 Confirmation test

On Taguchi method the confirmation test is necessary and it is an important step. Once the optimal combination of EDM parameters is selected, the prediction and verifying of the expected response through the confirmation test it's must be done.

For determining the optimum S/N ratio value the following relation is used:[94].

$$\hat{\eta}_{opt} = \overline{\eta} + \sum_{i=p}^{p} (\overline{n}_{i,opt} - \overline{\eta}) \tag{20}$$

where $\overline{\eta}_{i,opt}$ is the mean S/N ratio for ith parameter at the optimal level, p is the number of parameters that significantly affect the quality characteristic. In order to statistically judge the closeness of the predicted ($\hat{\eta}_{opt}$) and observed value of S/N ratio (η_{obs}), the confidence intervals (CIs) values of $\hat{\eta}_{opt}$ for the optimal parameter level combination at 95% confidence band are determined. The CI is given by [95]:

$$CI = \pm\sqrt{\frac{F_{(1,n_2)} \times V_E}{N_E}} \tag{21}$$

where $F_{(1,n_2)}$ is the F value from the F table, Tab.42, Appendix 7, for factor DOF and error at the confidence level desired, V_e the variance of the error term (from $ANOVA$), and N_E the effective number of replications:

$$N_E = \frac{total\, number\, of\, parameters\, or\, S/N}{DOF_{of\, mean} + DOF_{all\, factors}} \tag{22}$$

where $DOF_{of\, mean}$ is always equal to 1 and $DOF_{all\, factors}$ is the value included in estimating the mean performance at optimum condition.

If the difference between $\hat{\eta}_{opt}$ and η_{obs} is within the CI value, then the EDM parameter level combinations are valid, as shown on Eq.23.

$$\hat{\eta}_{opt} - CI < \eta_{obs} < \hat{\eta}_{opt} + CI \tag{23}$$

17 Experimental Setup

The experiments were conducted using a *Sodick AD3L* electrical discharge machine. The electrode was fed downwards into the test piece under servo control of the EDM machine. The Fig.43 depicts the experimental setup of EDM machine.

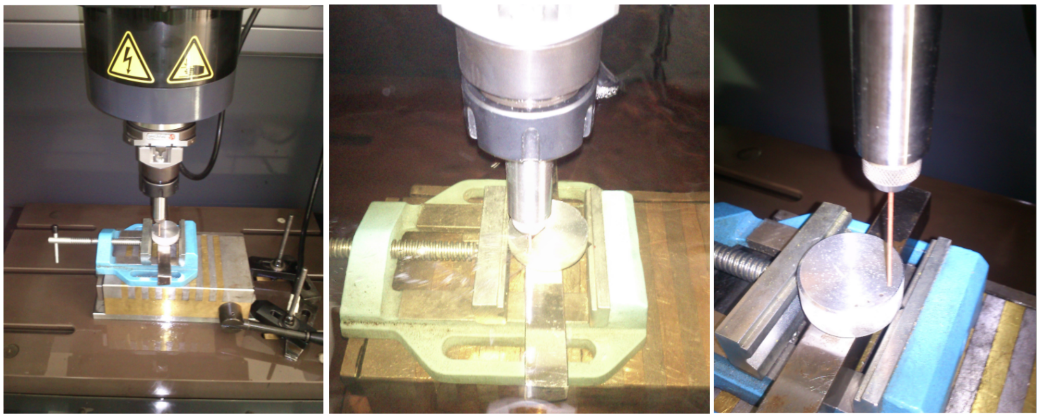

Figure 43 – Experimental Set up

A cooper electrode, Fig.44, with $1,40mm$ diameter was used to drill the test piece and its main characteristic can be seen in Tab.10. Water soluble dielectric fluid, $VITOL\,KS$,was circulated as the dielectric fluid. All the experiments have a predefined duration time of $35\,min$.

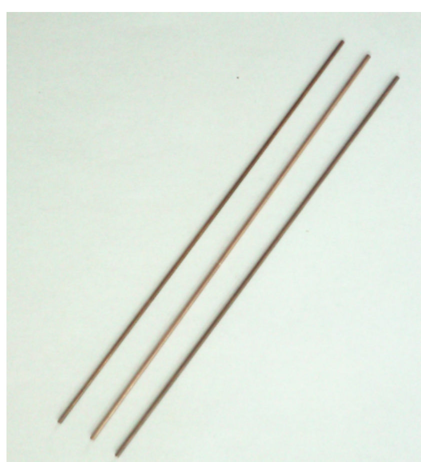

Figure 44 – Electrode tool used on the experiments

Before and after each experiment several parameters were measured as workpiece weight, electrode weight, electrode diameter, electrode length. At the final, also the top and bottom hole diameters are measured on a electronic microscope to later calculate the MRR, ROC and $TAPER$.

Table 10 – Essential properties of copper electrode

Essential properties	Descriptions
Specif gravity (g/cm^3)	8,94
Melting range (ºC)	1065-1083
Thermal conductivity (W/m.K)	388
Specif Heat (J/kg.K)	385
Electrical resistivity (Ω.cm)	1,7 $\times 10^{-6}$
Thermal expansion coefficient (1/ºC)	16,7$\times 10^{-6}$

To ensure the quality of the results, after each experiment the bottom part of the electrode tool was removed and kept. To remove the bottom part was used, firstly, a pliers as shown in Fig.45 2). However after this operation, the bottom face of the electrode was not plane, as shown on Fig.45 3), therefor,a grinding machine was used to achieve the plane electrode surface; after this operation some burrs were obtained on the electrode edge, as shown on Fig.45 5). These burrs were removed by a hand operation using a sand paper very carefully avoiding to damage the integrity of the cylindrical shape of the electrode tool.

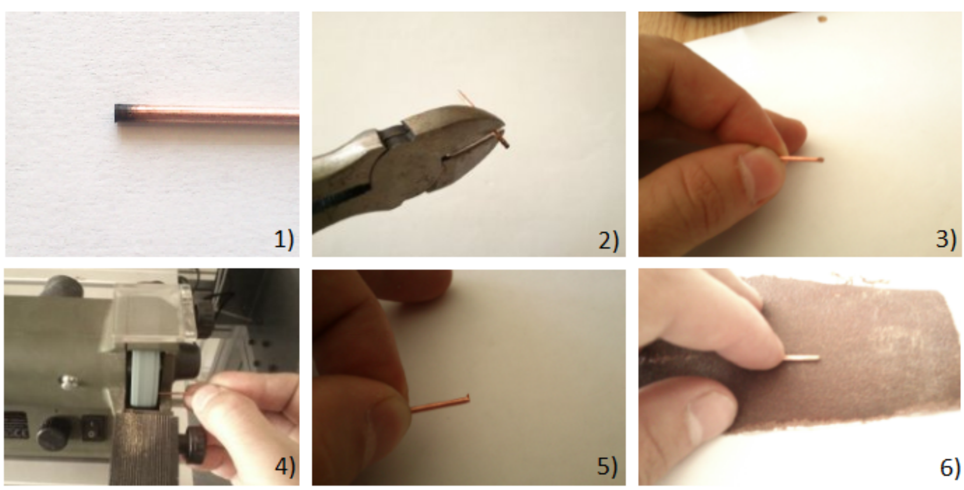

Figure 45 – All steps on the preparation of the electrode tool

To measure the bottom diameters and dept of the holes on the microscope, the test piece was cut longitudinally close to the holes axis. First, a cut about two millimeters distance from holes was made, with hand-help angle grinder machine, Fig.46 1), 2) and 3), showing the cutting and the clamping. Thereafter, the test piece was grinded and polished by hand until the holes axis were achieved ,Fig.464), 5) and 6).

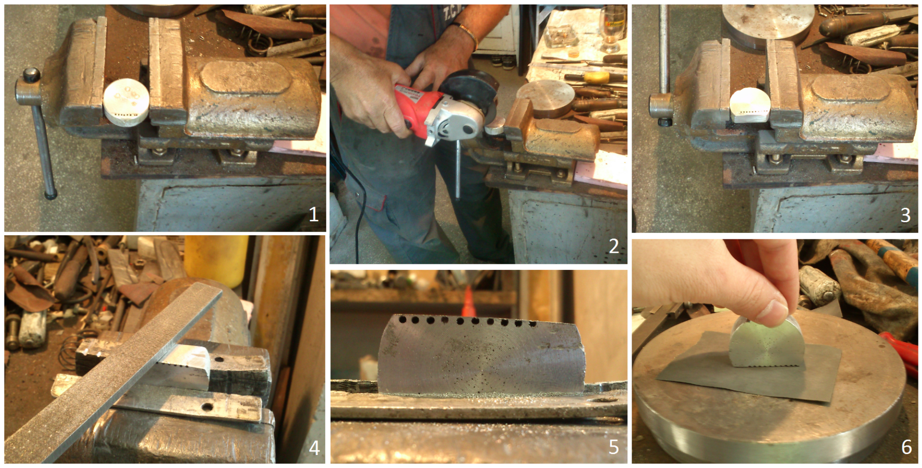

Figure 46 – All steps during workpiece preparation for measurements

The final aspect of the test pieces and electrode tips can be seen on Fig.47and Fig.48.

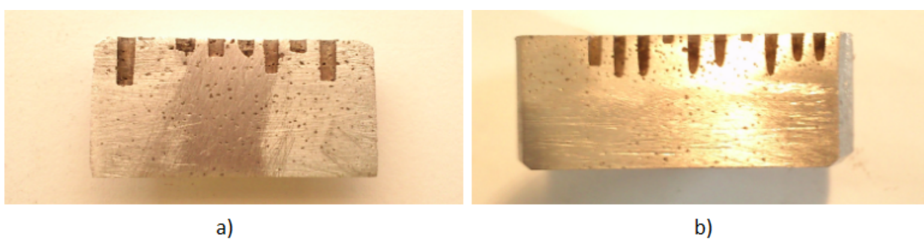

Figure 47 – Final aspect of workpieces, after the preparation for measurements on microscope: a) preliminary experiments and b) final experiments

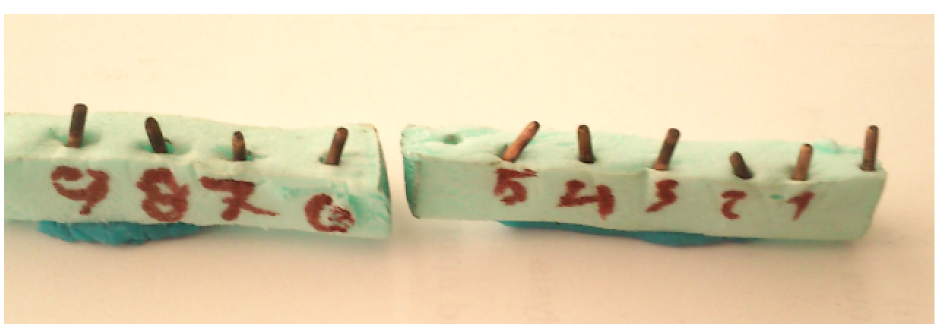

Figure 48 – Tips of the electrode tool used on the final experiment

18 Measurements and calculations

In order to eliminate the measurement errors, all measurements were done three times (electrode weight, electrode diameter, electrode length, workpiece weight and workpiece dimensions). The weights were measured on a analytical scale with a precision of $0,01\,mg$, as shown in Fig52. The value used for calculations was a average of the three previous obtained values. For the top and bottom diameter of the hole, another technique was used. The diameters of the holes were obtained with a non contact measurement system 2D made of a light microscope *Kestrel* model (produced by Vision Eng. The U.S.) and an microprocessor *Quadra Check 200* (produced by Metronics Inc. the U.S.). Two types of measurements were done, first were selected six points around the hole diameter and second were selected only three points around the hole diameter.

18.1 Material removal ratio (MRR)

Figure 49 – Microscope *Kestrel* model and an microprocessor *Quadra Check 200*

Material removal rate was expressed on (mm^3/min) and is the ratio of the hole volume on each experiment to the machining time, i.e. :

$$MRR = \frac{(V_h)}{t} \tag{24}$$

where V_h is a volume of the hole calculated as shown on the Fig.50 and Eq.25.

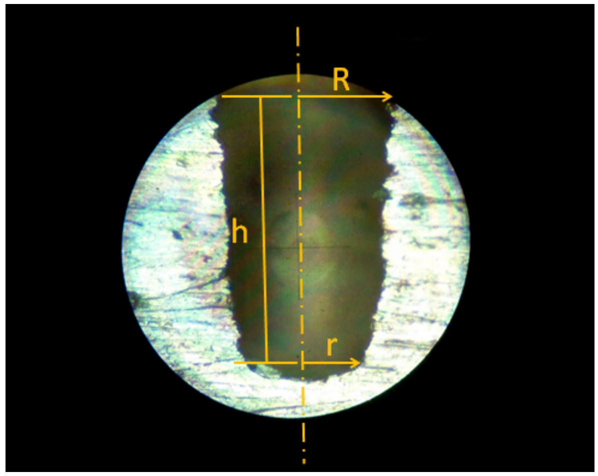

Figure 50 – View of the hole with different diameters on the top and another bottom surface(approximation to a cone frustum). .

$$V_h = \frac{\pi h}{3}\left[R^2 + Rr + r^2\right] \tag{25}$$

where:

h is the high of the hole,

R is a radius of the top and

r is a radius of the bottom.

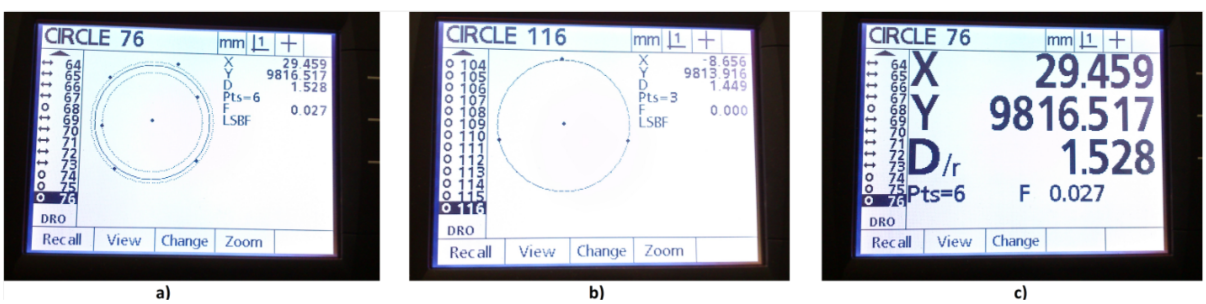

Figure 51 – Different diameter measurements from *Quadra Check 200 display*: a) six points measurement, b) three points measurements, c) display with results

18.2 Electrode wear (EW)

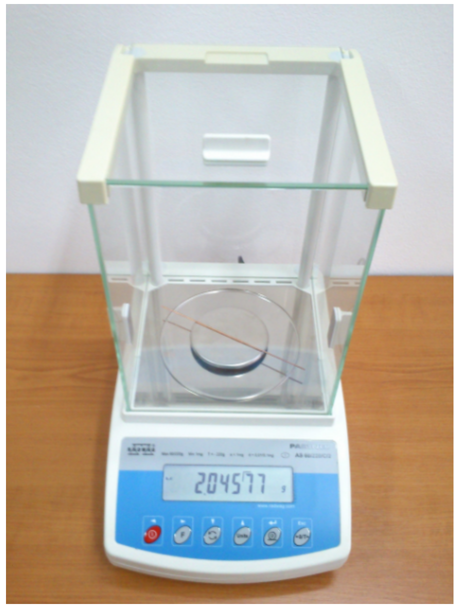

Figure 52 – Measurements of electrode weight on a *Radwag* analytical scale

Electrode wear was expressed on (mm^3/min) and is the ratio of the volume that the electrode lost during the machining to the machining time, i.e.:

$$EW = \frac{(V_t)}{t} \tag{26}$$

where V_t is the volume of the tool lost during the machining.

To calculate the volume lost during the machining, first was calculated the density of the electrode tool as shown on Appendix 8 and Fig.11, after, this value was related with the lost weight, shown on Fig.37 into Appendix 4, to achieve the value of the lost volume through the Eq.27.

$$V_t = \frac{L_w}{\rho_t} \tag{27}$$

where,

L_w is the lost weight of the electrode tool during the machining

ρ_t is the density of the electrode tool

Table 11 – Density calculated based on two samples of the electrode tool

Sample	Measurements (mm)		Calculations		Average $[mm^3/g]$
	Dimensions	Values	Volume	Density	
A	diameter	1,393	109,884	0,0088	0,00882
	length	72,103			
	weight	0,969			
B	diameter	1,393	42,757	0,00881	
	length	28,056			
	weight	0,377			

18.3 Taper ($TAPER$)

TAPER can be calculated from the expression:

$$T = tan^{-1}\left[\frac{d_{ht} - d_{hb}}{2l}\right] \tag{28}$$

where d_{ht} and d_{hb} are diameters of the machined hole at the top and bottom of the workpiece, and l the length of the machined hole.

18.4 Radial over cut (ROC)

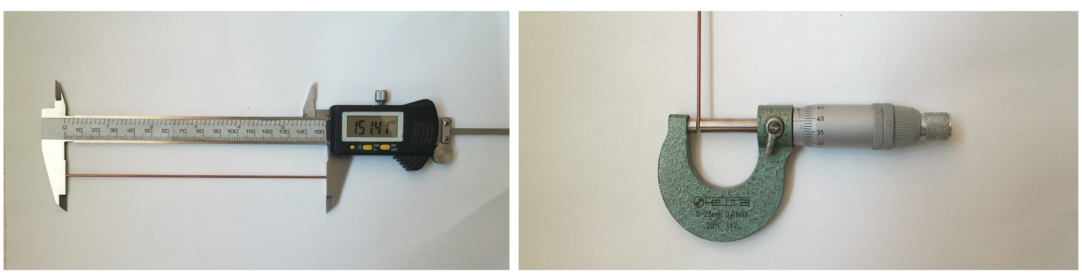

a) b)

Figure 53 – Measurements: a) electrode length with a caliper rule, b) electrode diameter with a micrometer

ROC is expressed as half of the difference of diameter of the obtained hole to the tool diameter, i.e.:

$$ROC = \frac{d_{ht} - d_t}{2} \tag{29}$$

where d_{ht} and d_t are the diameters of the hole and electrode tool

19 Preliminary Experiments

The preliminary experiments were used mainly to better understand the effect of some parameters before start doing the final experiments with the orthogonal array layout. The parameters values used in those experiments came from a research on several scientific articles about *EDM* on *MMC* material and standard programs from *LN Assist* software of the *Sodick AD3L* machine, for example, standard program to machine hard materials and normal aluminum. The chosen values can be seen on Tab.12.

Table 12 – Input parameters used on preliminary experiments

Experiment	Input parameters values								
	ON	OFF	IP	SV	C	UP	DN	J	S
1	100	100	5	40	0	11	20	5	42
2	10	10	5	40	0	11	20	5	42
3	5	10	5	40	4	11	20	5	42
4	5	10	5	40	0	11	20	5	42
5	5	10	5	40	4	9	15	10	32

The preliminary experimental layout has a specific order, that means, the experiments were not independent from each other. For example, the values for *pulse on-time, off-time, peak current,* and *servo voltage* on the first experiment were choose based on literature review, [90, 89, 91], and the remaining parameters were kept as a standard program to machine simple aluminum with copper electrodes. On the following experiment was choose small values for *pulse on-time* and *pulse of-time* based on several articles about EDM on hard materials, [88, 92]. The third experiment was based on the standard program from the machine for drilling hard materials and on a specific article, [93]. The main differences to the previous experiments were, the use of a capacitor with $0.047\mu F$ and a smaller value for a *pulse on-time*, the remaining parameters were kept constant. Next experiment was conducted without capacitor, and all renaming parameters constant. Finally, on the last experiment were used the standard program values were used for jump-up speed, jump-down speed, jump speed and servo speed, and kept constant the remaining parameters.

19.1 Preliminary experiment measurements

The Tab.13 and Tab.14 present bellow shows the average of all measurements done for top and bottom diameter, length of the hole and lost weight of the electrode tool. All measurements can be seen on Appendix 3.

Table 13 – Measurements of preliminary holes - average values

Experiment	Measurements (mm)		
	Top diameter	Bottom diameter	Hole length
1	1,6540	1,0600	2,043
2	1,5755	1,4505	1,633
3	1,5325	1,3530	4,677
4	1,5045	1,3745	2,048
5	1,4695	1,0735	3,943

Table 14 – Measurements of the tool lost weight on preliminary experiments - average values

Experiment	Lost weight (mm)
1	0,0006
2	0,0004
3	0,0024
4	0,0005
5	0,0018

19.2 Results

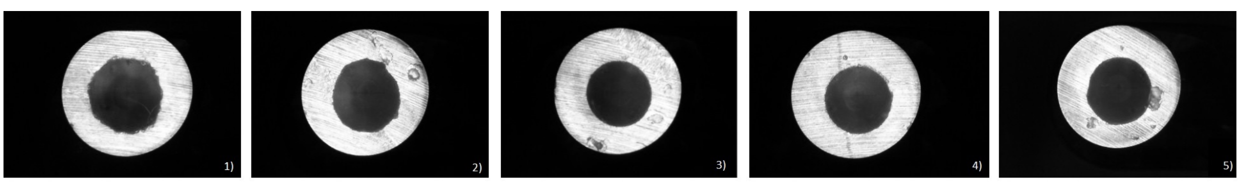

Figure 54 – Top hole diameters profile for the preliminary experiments

The values present on Tab.15, were calculated with the previous mentioned equations on the section *Measurements and calculations*.

Table 15 – Final results for preliminary experiments

Experiment	Output Parameters			
	MRR (mm^3/min)	EW (mm^3/min)	ROC (mm)	TAPER (degrees)
1	0,0857	0,0021	0,1303	8,3
2	0,0839	0,0015	0,0911	2,2
3	0,2186	0,0078	0,0696	1,1
4	0,0952	0,0016	0,0556	1,8
5	0,1441	0,0058	0,0381	2,9

In order to better understand the steps, the next calculations shows a example for the first experiment.

Value for MRR,

With Eq.25 and the values of top and bottom diameters and of the length hole,present on Tab.13, we obtained:

$$Vh = \frac{\pi \times 2,0425}{3} \left[\left(\frac{1,6540}{2} \right)^2 + \left(\frac{1,6540}{2} \right) \times \left(\frac{1,0600}{2} \right) + \left(\frac{1,0600}{2} \right)^2 \right] = 2,9997 \left[mm^3 \right]$$

With Eq.24 and the machining time of 35 min, the MRR is:

$$MRR = \frac{2,9997}{35} = 0,0857 \left[mm^3/min \right]$$

Value for EW,

With Eq.27, and the value of lost weight and density, presents on Tab.14 and Tab.11, the electrode lost volume is:

$$V_t = \frac{0,0006}{0,0088} = 0,0681 \left[mm^3 \right]$$

With Eq.26 and machining time of 35 min, the electrode wear is calculated:

$$EW = \frac{0,0681}{35} = 0,0021 \left[mm^3/min \right]$$

Value for ROC,

With Eq.29 and the values of top hole diameter, tool diameter before machining and hole of the dept, present on Tab.13 and Tab.11,

$$ROC = \frac{1,6540 - 1,3933}{2} = 0,1303 \; [mm]$$

Value for $TAPER$,

With Eq. 28 and the values of top and bottom hole diameter, and length of electrode tool, present on Tab.13,

$$TAPER = tan^{-1} \left[\frac{1,6540 - 1,0600}{2 \times 2,0425} \right] = 8,2500 \, [^{\circ}]$$

19.3 Analysis and discussion on preliminary experiments

The main goals for the preliminary experiments were: first experiment, test specific parameters alone as pulse on-time, with the remaining parameters constant; second, test several arrangement of parameters based on standard programs of the machine and finally, a compilation between the values from the literature and the standard values provide by the manufacturer of the machine. The data were used to graphically present the individuals output parameter values.

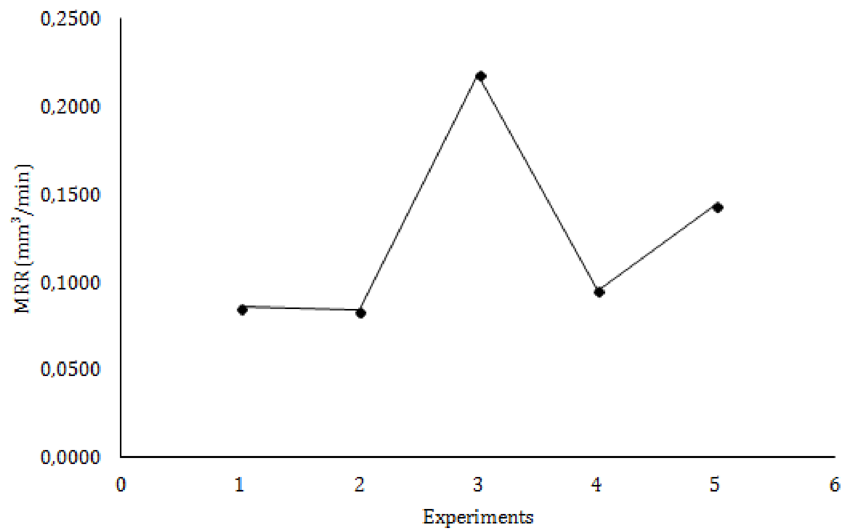

Figure 55 – Effect of factor levels on MRR

The Fig.55 and Fig.56 shows that MRR and EW have the same behavior, which means that they are directly proportionals. Bigger values for MRR are bigger values for EW as well.

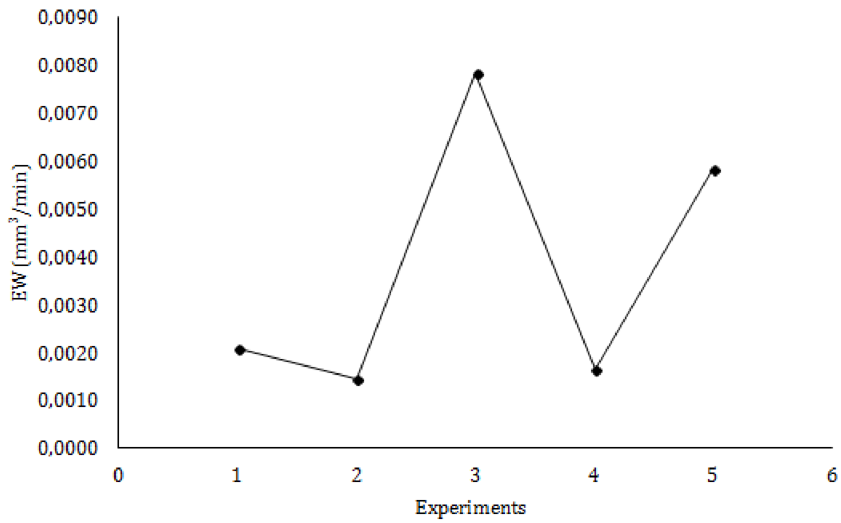

Figure 56 – Effect on factor levels on EW

As expected, MMR is not improved by big values of pulse on-time and off-time. On other hand, the big improvement for MRR, in third experiment, that can be explained by to the use of a capacitor with $0.047\mu F$, which implies an increase of EW too. The fifth experiment presents a reasonable values for MRR, the inconvenient problem for the fifth experimnet is related with the $TAPER$ which increases.

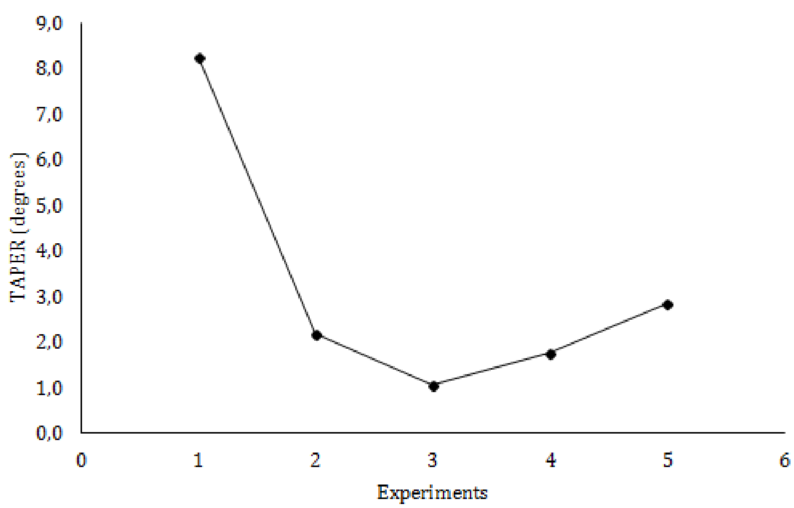

Figure 57 – Effect of factor levels on $TAPER$

In the Fig.57, it can be seen that the $TAPER$ values are decreasing along the experiments reaching a minimum oh the third experiment, then started to increase again until the fifth experiment.

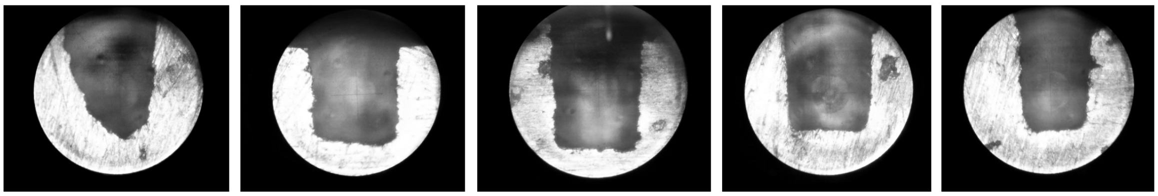

Figure 58 – Cross-section views of machined holes on preliminary experiments

As it can be observed on the Fig.58, after the first experiment the bottom of the hole is irregular, due to the low debris removal from the working area. After this first experiment , bottom surface of the electrode tool used to drill the first hole was covered by deposited debris, as one can see in Fig.59.

Figure 59 – Bottom surface of electrode used on first preliminary experiment

The following four experiments present regular bottom diameter holes, which implies smaller $TAPER$ values.

On the Fig.60, the ROC, is expressed as a decreasing line from the first to the fifth experiment. As can be seen on Tab.13, the values of top diameters decreasing as well as the ROC , once they are directly proportional values, as shown on Eq.29.

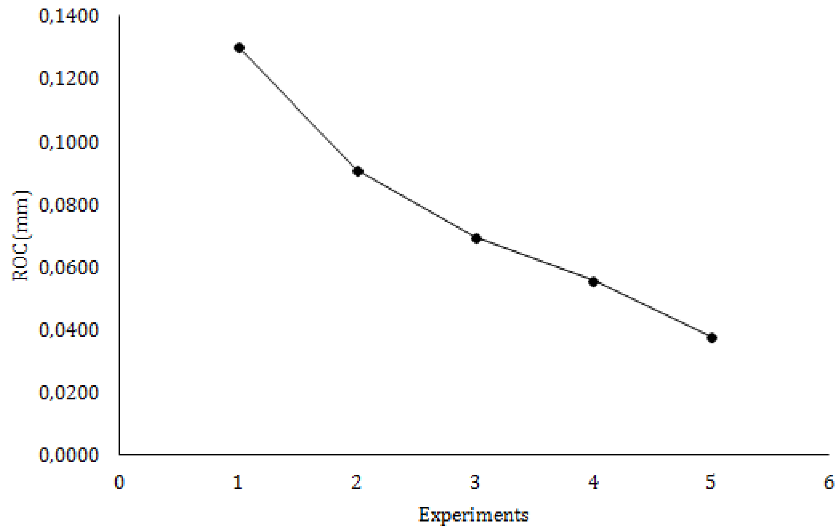

Figure 60 – Effect of factor levels on *ROC*

In order to realize the final experiments and to achieve the best results, small values of pulse on-time and off-time, a capacitor $(0,047\mu F)$, and standard values for jump-up, jump-down and jump speed as well as servo speed will be used

19.3.1 Conclusion of the preliminary experiments

Through the analysis of the preliminary experiments we can conclude that:

- Small values of pulse on and off-time improve all output parameters
- Using a capacitor improve the MRR and $Taper$
- Values of servo speed should not be to higher in order to obtain good results of *TAPER*

20 Experimental Layout

For the present experimental investigation, four different machining parameters, namely, *peak current, servo voltage*, *pulse on-time* and *pulse off-time* and their levels were fixed. For the above experiments, all remaining machining parameters were kept constant. The parameter values and their levels were chosen based on a previous research on several articles [88, 89, 90, 91, 92] related with the similar experimental objective and on the preliminary experiments. The remaining machining parameters can be seen on APPENDIX 5.

Table 16 – Machining parameters and their levels

Symbol	Machinning parameters	level 1	Level 2	Level 3
PC	Peak current (A)	5	10	15
SV	Servo voltage (V)	40	80	120
Ton	Pulse on-time (µs)	5	30	55
Toff	Pulse off-time (µs)	5	30	55

The Tab.17 shows a experimental layout, based on Taguchi method, orthogonal array L_9.

Table 17 – Experimental layout

Experiment	Machine settings			
	PC (A)	SV (V)	TON (µs)	TOFF (µs)
1	5	40	5	5
2	5	80	30	30
3	5	120	55	55
4	10	40	30	55
5	10	80	55	5
6	10	120	5	30
7	15	40	55	30
8	15	80	5	55
9	15	120	30	5

21 Final Experiments

21.1 Measurements

Table 18 – Measurements of the hole on final experiments

Experiment	Measurements (mm)		
	Top diameter	Bottom diameter	Hole length
1	1,473	0,930	3,446
2	1,540	1,140	5,097
3	1,460	1,342	0,891
4	1,478	0,958	3,768
5	1,538	0,999	4,461
6	1,426	1,194	1,037
7	1,521	0,989	4,680
8	1,504	1,108	4,876
9	1,607	1,468	3,492

Table 19 – Measurements of tool lost weight on final experiments

Experiment	Lost weight (mm)
1	0,01113
2	0,00691
3	0,00072
4	0,01863
5	0,02454
6	0,00290
7	0,02296
8	0,01980
9	0,00055

The values present on the Tab.18 and Tab.19 are the average values of all measurements that were done. As previous mentioned, all measurements were done three times for the weight of the electrode tool , bottom diameter and length of the hole. In relation of the top diameter of the hole was measured use first five points and then three points to get the right diameter value of the circumference, since as shown of Fig.61, sometimes the holes not present a good circularity. This process was better explain on the sub section *Measurements*. All measured values were included in APPENDIX 4.

21.2 Results of final experiments

Foe each experiment , during the measurements , photos of the enlarged views for top-diameters, cross-section holes and for electrode weared tips were done, as one can notice in Fig.62, Fig.63, and Fig.64.

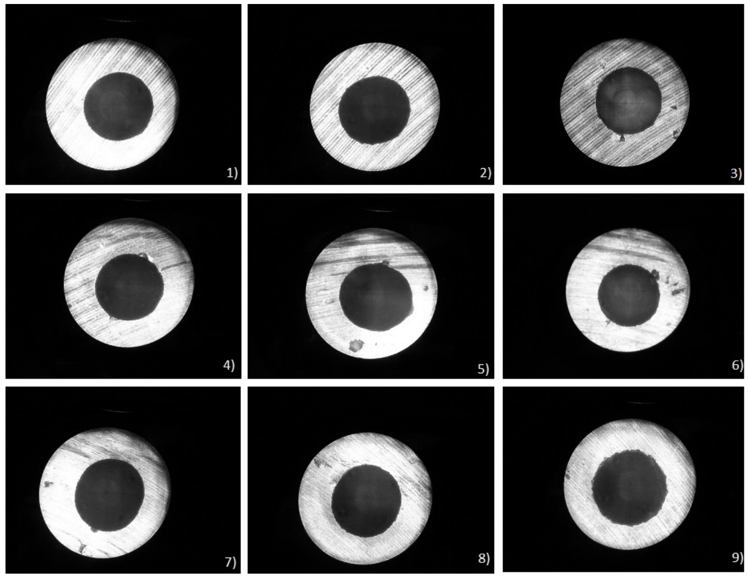

Figure 61 – Images on microscope of top hole diameters

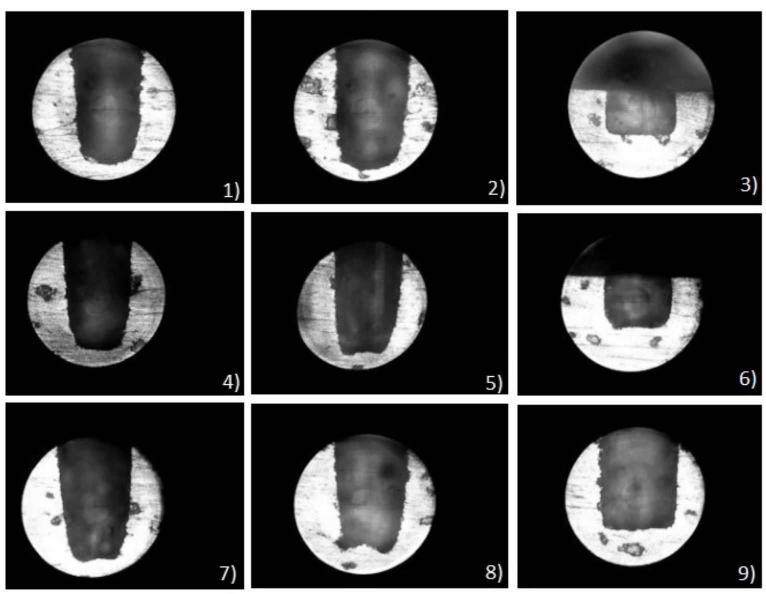

Figure 62 – Cross-section views of machined holes on final experiments

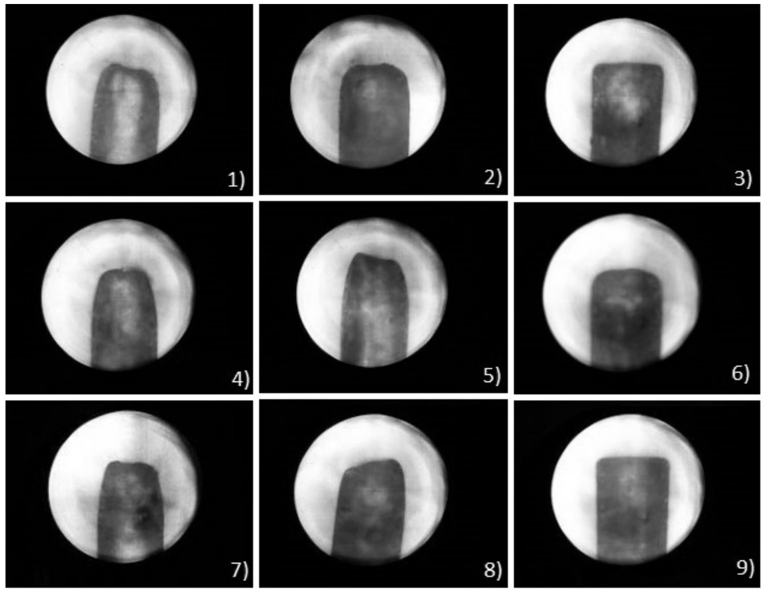

Figure 63 – Image on microscope of the electrode

The Tab.20, presented bellow, shows the orthogonal array arrangement and the values experimentally obtained.

Table 20 – Final results for material removal rate, electrode wear, radial over cut and taper

Experiment	Factor level				MRR	EW	ROC	$TAPER$
	PC	SV	Ton	Toff	(mm^3/min)	(mm^3/min)	(mm)	(degrees)
1	1	1	1	1	0,113	0,036	0,040	4,5
2	1	2	2	2	0,207	0,022	0,073	2,2
3	1	3	3	3	0,039	0,002	0,033	3,8
4	2	1	2	3	0,127	0,060	0,042	3,9
5	2	2	3	1	0,163	0,080	0,072	3,5
6	2	3	1	2	0,040	0,009	0,016	6,4
7	3	1	3	2	0,168	0,075	0,064	3,3
8	3	2	1	3	0,188	0,064	0,055	2,3
9	3	3	2	1	0,185	0,002	0,107	1,1

The MRR values obtained, shown on Fig.64, present a maximum for the second experiment, all parameters into level 2 with the exception of *peak current* into level 1, and minimum for the third experiment, all parameters into level 3 with the exception of *peak current* into level 1. The last three values of MRR are similar, both of the respective experiments with the higher value of *peak current*.

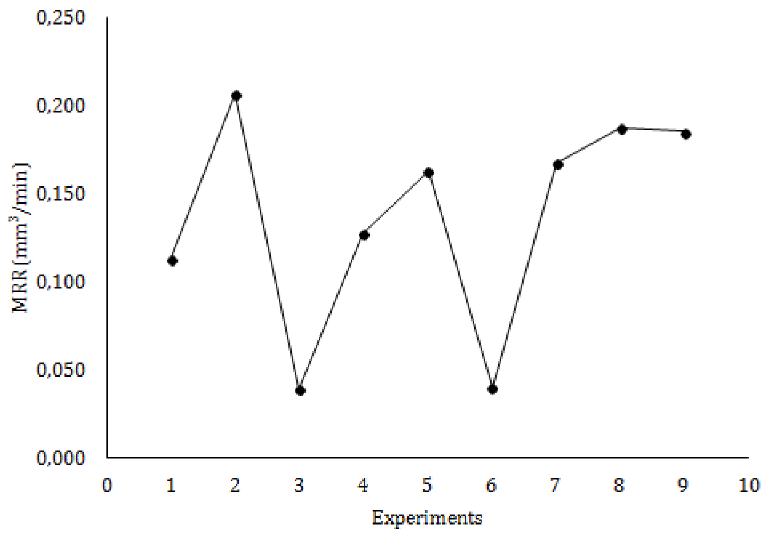

Figure 64 – Material removal rate on final experiments

Concerning the *electrode wear*, presented on Fig.65, it shows two minimum values, very close from each other, on the third and sixth experiments. Both of those experiments include on their experimental layout a big value of *servo voltage*. The maximum EW appears on the fifth experiment, which have a big value of *pulse on-time*.

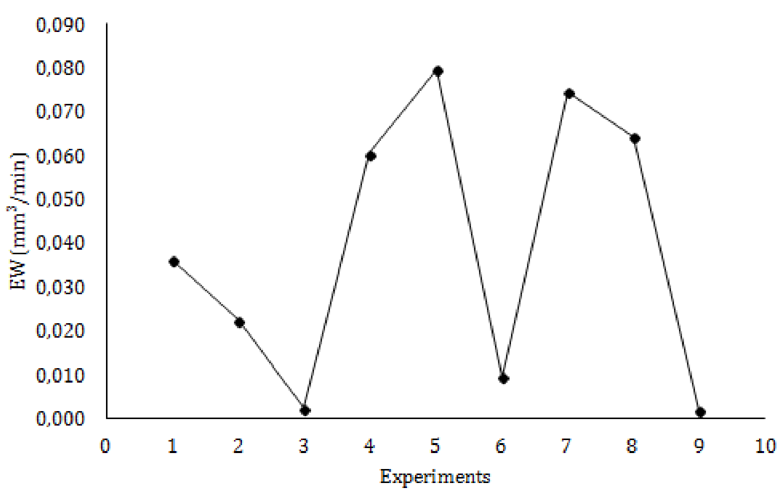

Figure 65 – Electrode wear on final experiments

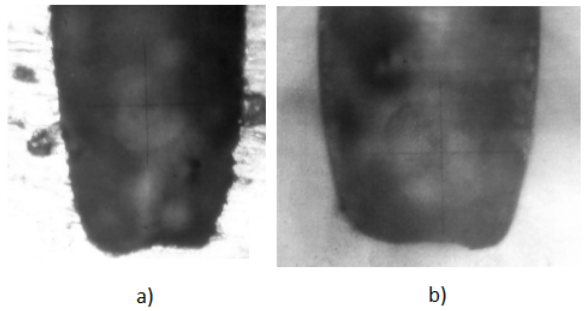

Figure 66 – Microscope images: a) hole and b) electrode tool

The Fig.66 a) and b) shows the bottom of the hole and the bottom surface of the electrode tool. As one can see the wear of the tool is directly related with the shape of the hole bottom.

Regarding the *radial over cut*, shown on Fig.67, the minimum appear on the sixth experiment, with a big value of *servo voltage* and small value of *pulse on-time*. The maximum *ROC* was obtained after the last experiment, with the bigger values of *peak current* and *servo voltage*, and a smaller value of *pulse off-time*.

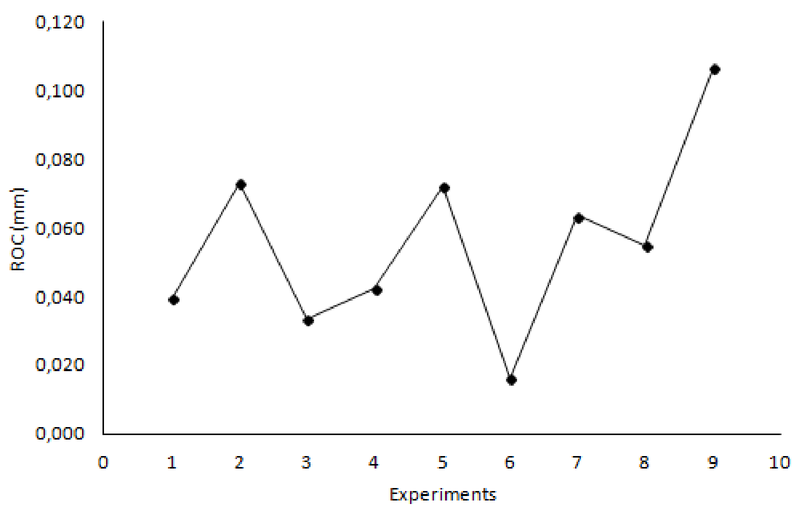

Figure 67 – Radial over cut on final experiments

The *taper* values, shown on Fig.68, present their maximum on the sixth experiment, with bigger value for *servo voltage* and smaller for *pulse on-time*. In other hand, the minimum appear on the last experiment with smaller values for *pulse off-time* instead of *pulse on-time*.

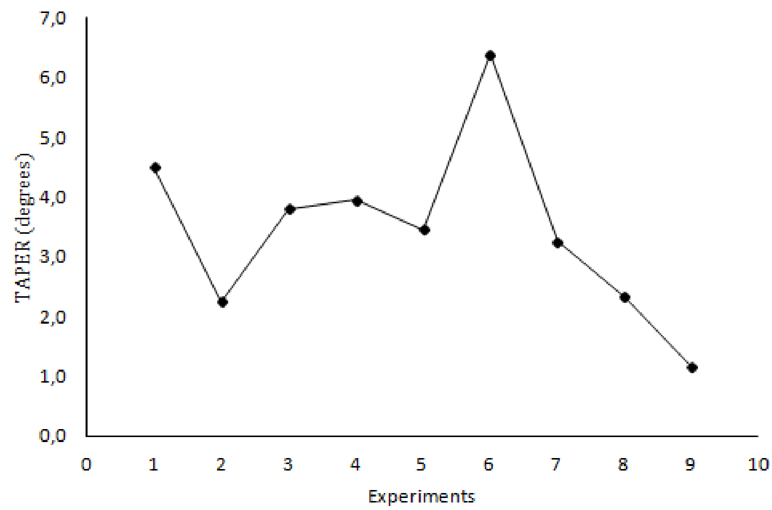

Figure 68 – Taper values on final experiments

As shown on Fig.69 and Appendix 9, the *machining speed* was not constant along the experiment. In beginning of the machining operation the machining speed has high values and then start to decrease. Probably the material homogeneity is responsible for this phenomena, since this is repeated for all nine experiments. Another possible explanation can be given by the debris evacuation decreasing as the electrode gets deeper in the material.

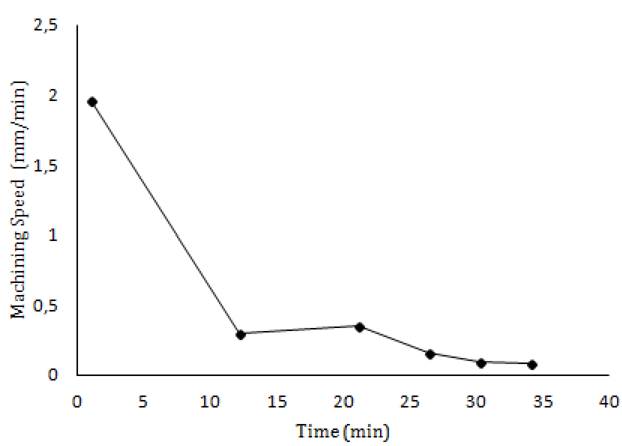

Figure 69 – Machining speed during the drilling operation

The results present bellow are from the analysis of variance *ANOVA*. In order to better understand how to achieve the values presented on Tab.21 and Tab.22 the calculations can be consulted on APPENDIX 2. The calculations present in that section are based on the math relations presented on the previous described sub section *ANOVA* from the section *Methods*.

21.2.1 *ANOVA* results

As mentioned in chapter 18.2, analysis of variance (ANOVA) can be applied in order to better illustrate the significance of the effect of each controlled parameter on the performance characteristics (*MRR, EW, ROC, TAPER*)

Table 21 – Mean S/N ratios for material removal rate, electrode wear, radial over cut, taper

Experiment	S/N ratios (dB)			
	MRR	EW	ROC	T
1	-18,9092	28,8437	28,0498	-13,0736
2	-13,6965	32,9815	22,7236	-7,0331
3	-28,1317	52,5842	29,5424	-11,6107
4	-17,9061	24,3652	27,4664	-11,9271
5	-15,7417	21,9735	22,8433	-10,7754
6	-27,9549	40,5330	35,7385	-16,1000
7	-15,5110	22,5503	23,9331	-10,2458
8	-14,5262	23,8377	25,1796	-7,3306
9	-14,6467	54,9113	19,4259	-1,1707
Overall mean	-18,5582	33,6201	26,1003	-9,9186

The factor effect of a parameter at any level is computed by taking the average of all S/N ratios at the same level. The effect of various factors at different levels for responses *MRR*, *EW*, *ROC* and *TAPER* are shown in Tab.22. Also, the graphical representations of parameters effect at different levels are shown in Fig.70, Fig.71, Fig.72, Fig.73, .

Table 22 – S/N response table for material removal rate (MRR), electrode wear (EW), radial over cut (ROC) and taper (T)

Symbol	Factor	Mean S/N ratios (dB)		
		Level 1	Level 2	Level 3
MMR				
PC	Peak current	-20,2458	-20,5342	-14,8946[a]
SV	Servo voltage	-17,4421	-14,6548[a]	-23,5778
Ton	Pulse on-time	-20,4634	-15,4164[a]	-19,7948
Toff	Pulse off-time	-16,4326[a]	-19,0541	-20,1880
EW				
PC	Peak current	38,1365[a]	28,9573	33,7664
SV	Servo voltage	25,2531	26,2642	49,3429[a]
Ton	Pulse on-time	31,0715	37,4193[a]	32,3694
Toff	Pulse off-time	35,2428[a]	32,0216	33,5957
ROC				
PC	Peak current	26,7719	28,6827[a]	22,8462
SV	Servo voltage	26,4831	23,5822	28,2356[a]
Ton	Pulse on-time	29,6560[a]	23,2053	25,4396
Toff	Pulse off-time	23,4396	27,4651[a]	27,3961
$TAPER$				
PC	Peak current	-10,5725	-12,9342	-6,2490[a]
SV	Servo voltage	-11,7488	-8,3797[a]	-9,6272
Ton	Pulse on-time	-12,1681	-6,7103[a]	-10,8773
Toff	Pulse off-time	-8,3399[a]	-11,1263	-10,2895

[a]Optimum level

The figures bellow represent the optimum parameter level which is the level corresponding to maximum average S/N ratio. The slope of the line into each parameter, from a level to a next level, shows the power of each level variance on the response under study. The power of each level variance and the slope line are directly proportionals.

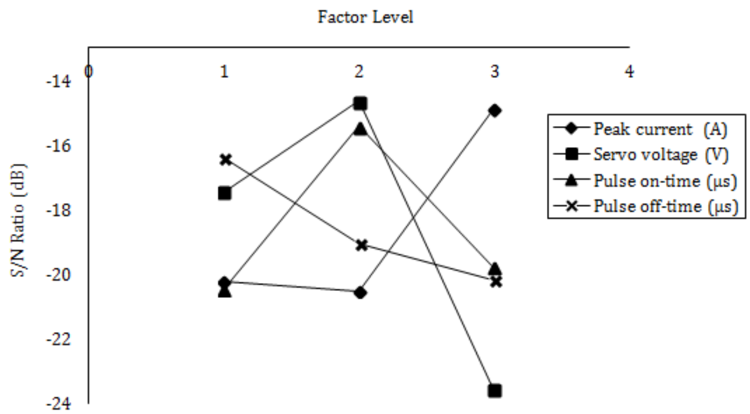

Figure 70 – Effect of factor levels on S/N ratio for material removal rate

Concerning the Fig70 , the optimum parameter level for a maximum value of MRR is $PC_3SV_2Ton_2Toff_1$.

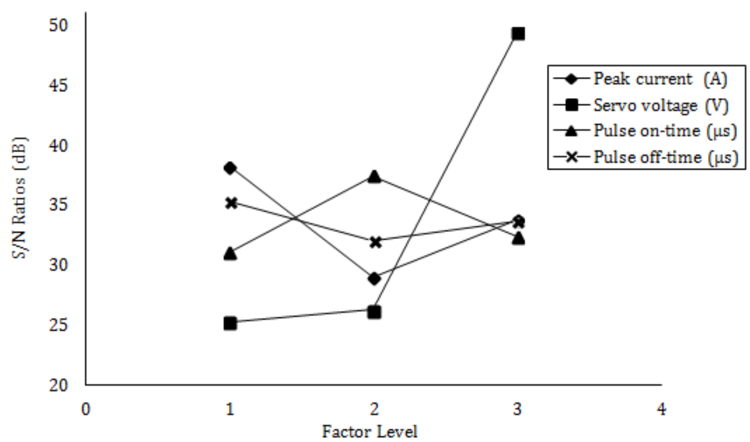

Figure 71 – Effect of factor levels on S/N ratio for electrode wear

The optimum parameter level for a minimum value of EW is $PC_1SV_3Ton_2Toff_1$, as shown on Fig.71.

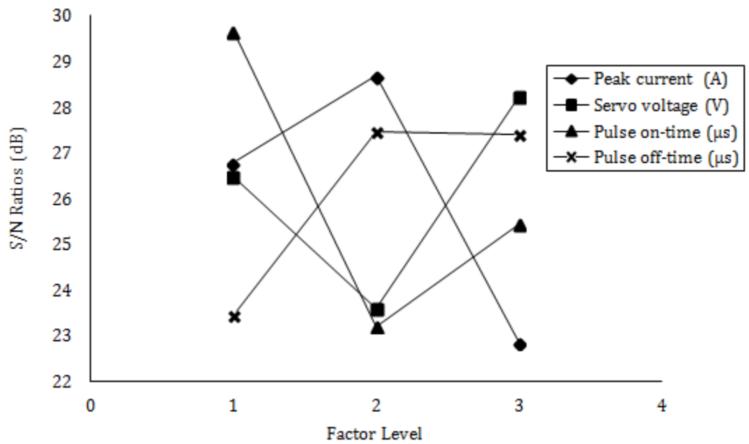

Figure 72 – Effect of factor levels on S/N ratio for radial over cut

Regarding the ROC, the optimum parameter level for a minimum value of this output parameter is $PC_2SV_3Ton_1Toff_2$, as shown of Fig.72.

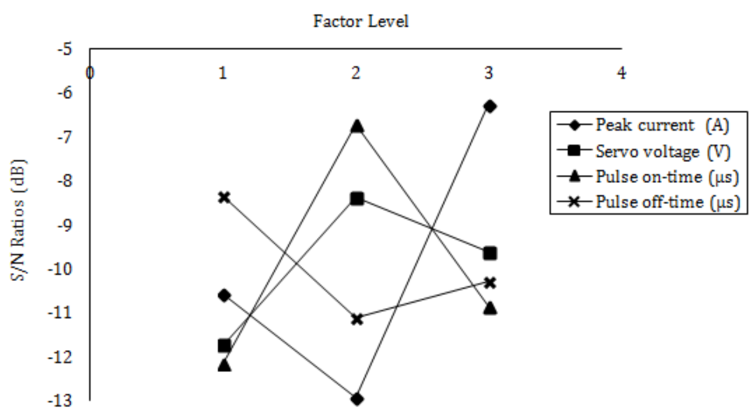

Figure 73 – Effect of factor levels on S/N ratio for taper

The optimum parameter level for a minimum value of $TAPER$ is $PC_3SV_2Ton_2Toff_1$ as shown on Fig.73.

A better way to understand the relative effect of the different parameters can be obtained by the decomposition of the variance, which is commonly called *ANOVA*. This statistical technique can estimate quantitatively the relative contribution that each control factor or parameters have on the overall measured response. The relative significance of factors is often represented in terms of $F - ratio$ or in percentage contribution. Greater the $F - ratio$ more significant will be the factor and also bigger the contribution. The Tab.23 and Fig.74 shows the results of *ANOVA* for MRR, EW, ROC and T.

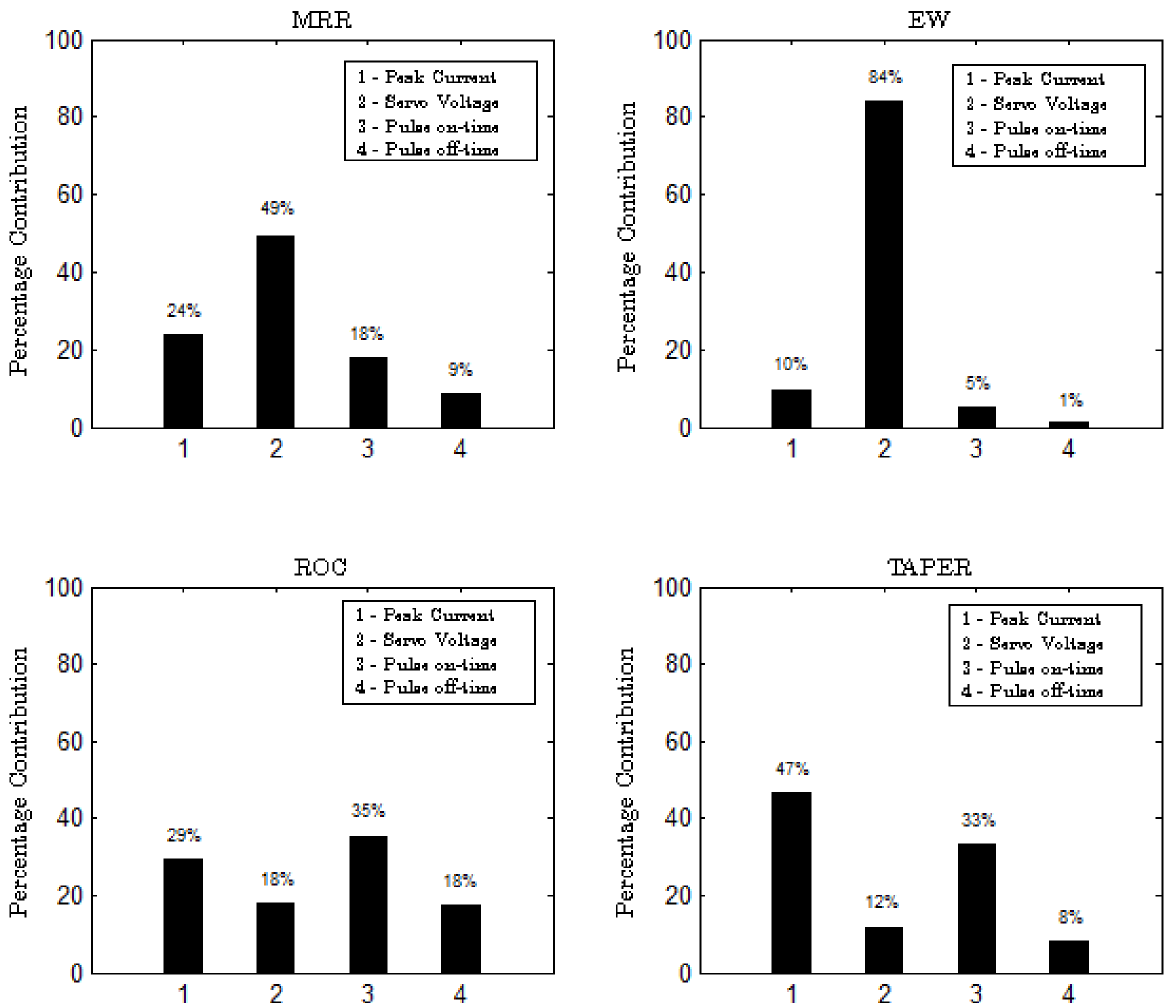

Figure 74 – Contribution of different control factors from $ANOVA$

Table 23 – Results of ANOVA for MMR, EW, ROC and $Taper$

Symbol	Factor	DOF	Sum of sq.	Mean sq.	F	Contr. (%)
MMR						
PC	Peak current	2	60,5230	30,2615	2,7187	23,9308
SV	Servo voltage	2	125,0348	62,5174	5,6167	49,4388
Ton	Pulse on-time	2	45,0891	22,5445	2,0254	17,8282
Toff	Pulse off-time	2	22,2614[a]	11,1307	-	8,8021
Error		-	-	-		
Pooled Error		2	22,2614	11,1307		
Total		8	252,9082	-		100
EW						
PC	Peak current	2	126,4834	63,2417	8,1250	9,5568
SV	Servo voltage	2	1113,9628	556,9814	71,5584	84,1683
Ton	Pulse on-time	2	67,4813	33,7407	4,3348	5,0987
Toff	Pulse off-time	2	15,5672[a]	7,7836	-	1,1762
Error		-	-	-		
Pooled Error		2	15,5672	7,7836		
Total		8	1323,4947	-		100
ROC						
PC	Peak current	2	53,1275	26,5637	1,6674	29,1090
SV	Servo voltage	2	33,1409	16,5704	1,0401	18,1582
Ton	Pulse on-time	2	64,3808	32,1904	2,0206	35,2749
Toff	Pulse off-time	2	31,8628[a]	15,9314	-	17,4579
Error		-	-	-		
Pooled Error		2	31,8628	15,9314		
Total		8	182,5120	-		100
$Taper$						
PC	Peak current	2	68,9605	34,4803	5,6224	46,7683
SV	Servo voltage	2	17,4086	8,7043	1,4194	11,8064
Ton	Pulse on-time	2	48,8170	24,4085	3,9801	33,1072
Toff	Pulse off-time	2	12,2652[a]	6,1326	-	8,3181
Error		-	-	-		
Pooled Error		2	12,2652	6,1326		
Total		8	147,4514	-		100

[a]Pooled error

As previous described the optimum combination level suggests the parameter level combination which will improve the responses values. The Tab.24 shows the improvement , and the percentage of improvement that should appear on the experimental observations. Latter on will be discuss the error of this values, through a comparison with the experimental values obtained on the experiments for the optimum combination level. Is important to note that for ROC is impossible to find the improvement, since that the optimum combination level is an experiment already done on the orthogonal array L_9, more exactly $PC_2SV_3Ton_1Toff_2$.

Table 24 – Improvement values of responses through the optimum combination level

Responses	Experiments	Parameter level	S/N ratio [dB]	Improv. [dB]	Pct. [%]
MRR	Best Exp.	$PC_1SV_2Ton_2Toff_2$	-13,6965	7,9	58
	Opt. comb.	$PC_3SV_2Ton_2Toff_1$	-5,7238		
EW	Best Exp.	$PC_3SV_3Ton_2Toff_1$	54,9113	4,3	8
	Opt. comb.	$PC_1SV_3Ton_2Toff_1$	59,2813		
ROC	Best Exp.	$PC_2SV_3Ton_1Toff_2$	35,7338	-	-
	Opt. comb.	$PC_2SV_3Ton_1Toff_2$	-		
$TAPER$	Best Exp.	$PC_3SV_2Ton_2Toff_1$	-1,1707	1,1	94
	Opt. comb.	$PC_3SV_3Ton_2Toff_1$	0,0767		

21.3 Confirmation test

On Taguchi method the confirmation test is necessary and an important step. Once the optimal combination of EDM parameters is selected, now is time to predict and verify the expected response through the confirmation test.There are two ways to predict this value.

First, through the a Eq.20, finding the optimum S/N ratio value for each output parameter. However to use this method is necessary to previously realize the experiment with the optimal combination of parameters to after make a comparison between the observed and predicted values. The measurements behind this results can be consult on Appendix 6, note that for ROC, the optimum combination level was a experiment previous done on the L9 array, in this case sixth experiment.

Table 25 – Comparison between Optimum and Experimental S/N ratios

Parameters	S/N Ratio [dB)]	
	Optimum ($\hat{\eta}_{opt}$)	Experimental (η_{obs})
MRR	-5,7238	-12,0308
EW	59,2813	56,8933
ROC	35,7385	35,7385
$TAPER$	0,0767	-1,0726

In order to statistically judge the closeness of the predicted ($\hat{\eta}_{opt}$) and observed value of S/N ratio (η_{obs}), the confidence intervals (CIs) values of $\hat{\eta}_{opt}$ for the optimal parameter level combination at 95% confidence band are determined [94]. The Experimental value must fit on the confidence interval to be accepted. As it can be seen in Tab.26 all experimental values obtained from the experiments with optimum combination levels fits on the confidence intervals.

Table 26 – Confirmation of Experimental values into a confidence interval at 95%

Parameters	Confirmation at 95% of confidence			
	CI	Opt - CI	Experimental values	Opt + CI
MRR	7,0457	-12,7695	$<$ -12,0308 $<$	1,3219
EW	5,8919	53,3894	$<$ 56,8933 $<$	65,1732
ROC	8,4293	27,3092	$<$ 35,7385 $<$	44,1678
$TAPER$	5,2298	-5,1531	$<$ -1,0726 $<$	5,3065

Table 27 – Errors of optimum combination level predicted by confirmation test ($\hat{\eta}_{opt}$) Vs. Experimental (η_{obs})

Response	Optimum comb.	Predicted ($\hat{\eta}_{opt}$)		Experimental (η_{obs})		Error [%]
		S/N [dB]		S/N [dB]		
MRR	$PC_3SV_2Ton_2Toff_1$	-5,7238	-	-12,0307	-	-
[mm^3/min]	-	-	0,5173	-	0,2530	106
EW	$PC_1SV_3Ton_2Toff_1$	59,2813	-	56,8933	-	-
[mm^3/min]	-	-	0,0010	-	0,0014	32
ROC	$PC_2SV_3Ton_1Toff_2$	35,7338	-	-	-	-
[mm]	-	-	0,0163	-	-	-
$TAPER$	$PC_3SV_2Ton_2Toff_1$	0,0767	-	-1,0726	-	-
[$degrees$]	-	-	0,9912	-	1,1314	14

21.4 Mathematical Modelling

The experimental data can be used for mathematical processing in order to find a multiple regression equation, which establishes the dependency between the corresponding category of output value and the *EDM* parameters. To achieve these equations, *GW basic* software, based on least square method was used. The best considered equations for *MRR, EW, ROC*, and *TAPER* influences were a polynomial ones. The Gauss sums are presented bellow the equations for each model.

Material removal rate mathematical model

$$MRR = -28,627 - 1.836 \cdot PC + 0,118 \cdot PC^2 + 0,508 \cdot SV - 3,659 \times 10^{-3} \cdot SV^2 + 0,465 \cdot Ton$$

$$-7,540 \times 10^{-3} \cdot Ton^2 - 0,146 \cdot Toff + 1,190 \times 10^{-3} \cdot Toff^2 \tag{30}$$

$$S_{Gauss} = 3,180 \times 10^{-9}$$

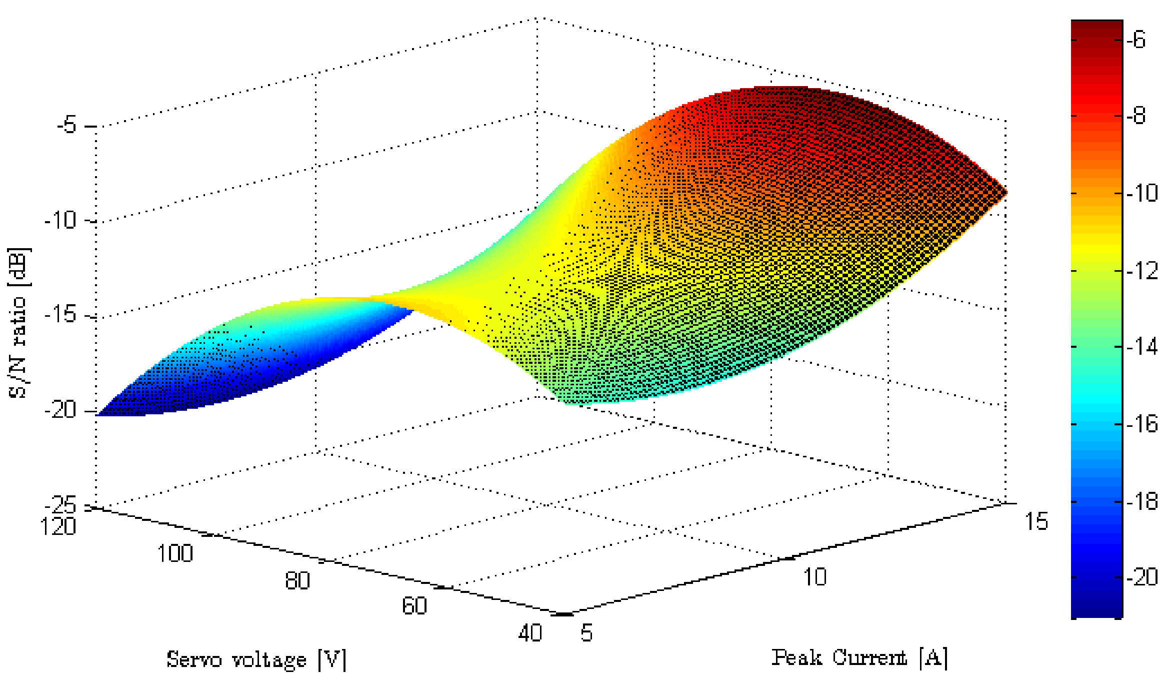

Figure 75 – 3D Graphic peak current Vs servo voltage on *MRR* response

As can be seen on Fig.75, the Eq.30, reveals that the maximum for material removal ratio can be found around the values of 15 A for the *peak current* and 80 V for *servo voltage* as previous predicted on $ANOVA$, Fig.70.

Electrode wear mathematical model

$$EW = 64,021 - 5,533 \cdot PC + 0,259 \cdot PC^2 - 0,739 \cdot SV + 6,583 \times 10^{-3} \cdot SV^2 + 0,640 \cdot Ton$$

$$-9,917 \times 10^{-3} \cdot Ton^2 - 0,195 \cdot Toff + 3,037 \times 10^{-3} \cdot Toff^2 \quad (31)$$

$$S_{Gauss} = 5,216 \times 10^{-8}$$

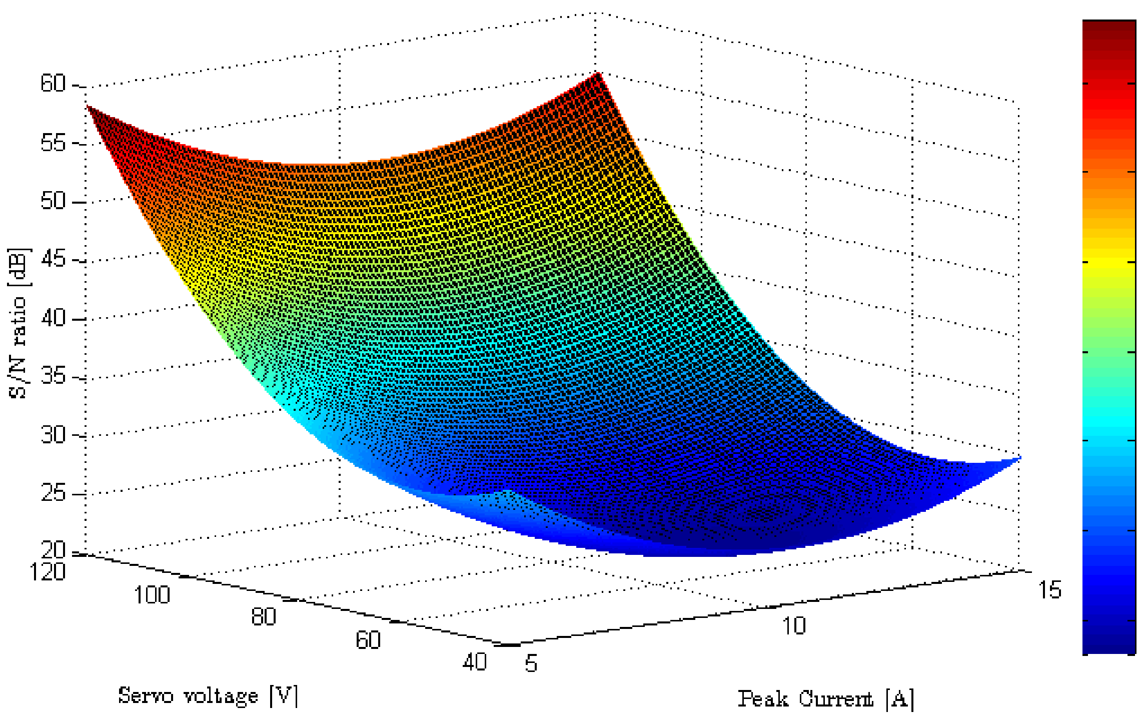

Figure 76 – 3D Graphic peak current Vs servo voltage on EW response

Regarding the Fig.76, the Eq.31, reveals that the minimum value for electrode wear can be found around of *5A* for *peak current* and *120 V* for *servo voltage* as previous mentioned by *ANOVA,* Fig.71

Radial over cut mathematical model

$$ROC = 29,883 + 2,706 \cdot PC - 0,154 \cdot PC^2 - 0,355 \cdot SV + 2,360 \times 10^{-3} \cdot SV^2 - 0,501 \cdot Ton$$

$$+6,948 \times 10^{-3} \cdot Ton^2 + 0,275 \cdot Toff - 3,275 \times 10^{-3} \cdot Toff^2 \quad (32)$$

$$S_{Gauss} = 8,454 \times 10^{-9}$$

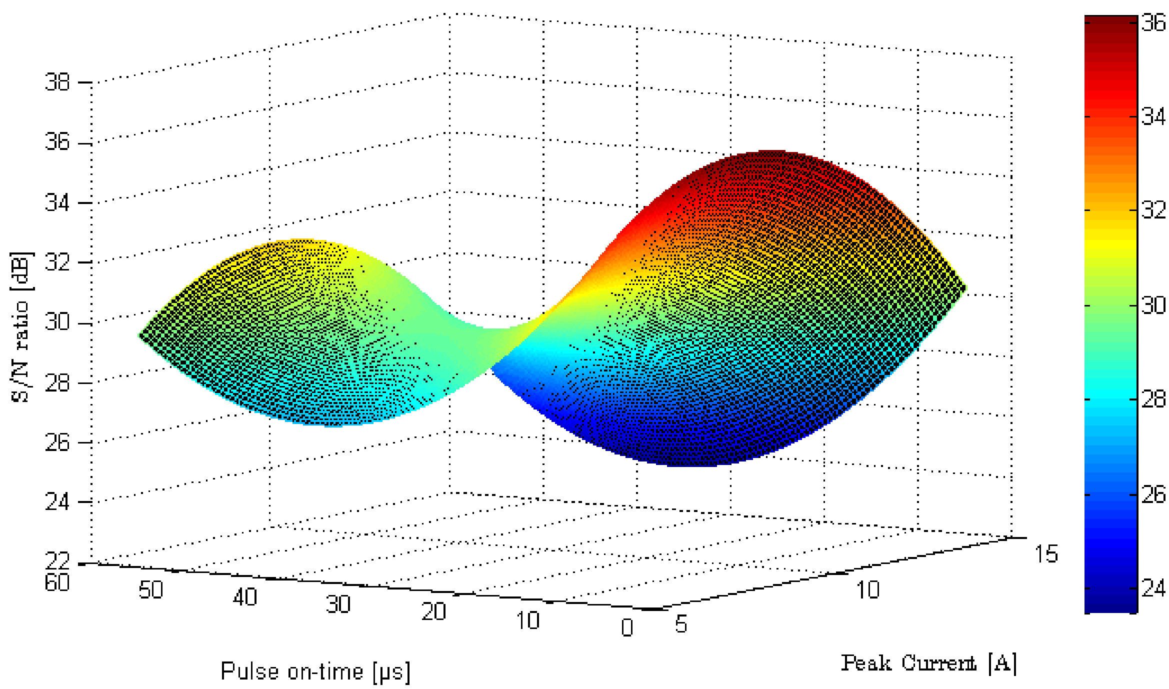

Figure 77 – 3D Graphic peak current Vs pulse on-time on ROC response

Concerning the Fig.77, the Eq.32, it can be observed that the minimum for radial over cut can be found around the values of $8\,A$ for the *peak current* and $30\,\mu s$ for *pulse on-time* as previous predicted by $ANOVA$, Fig.72.

Taper mathematical model

$$TAPER = -10,905 - 3,186 \cdot PC + 0,180 \cdot PC^2 + 0,257 \cdot SV - 1,442 \times 10^{-3} \cdot SV^2 + 0,487 \cdot Ton$$

$$-7,699 \times 10^{-3} \cdot Ton^2 - 0,212 \cdot Toff + 2,898 \times 10^{-3} \cdot Toff^2 \quad (33)$$

$$S_{Gauss} = 4,812 \times 10^{-9}$$

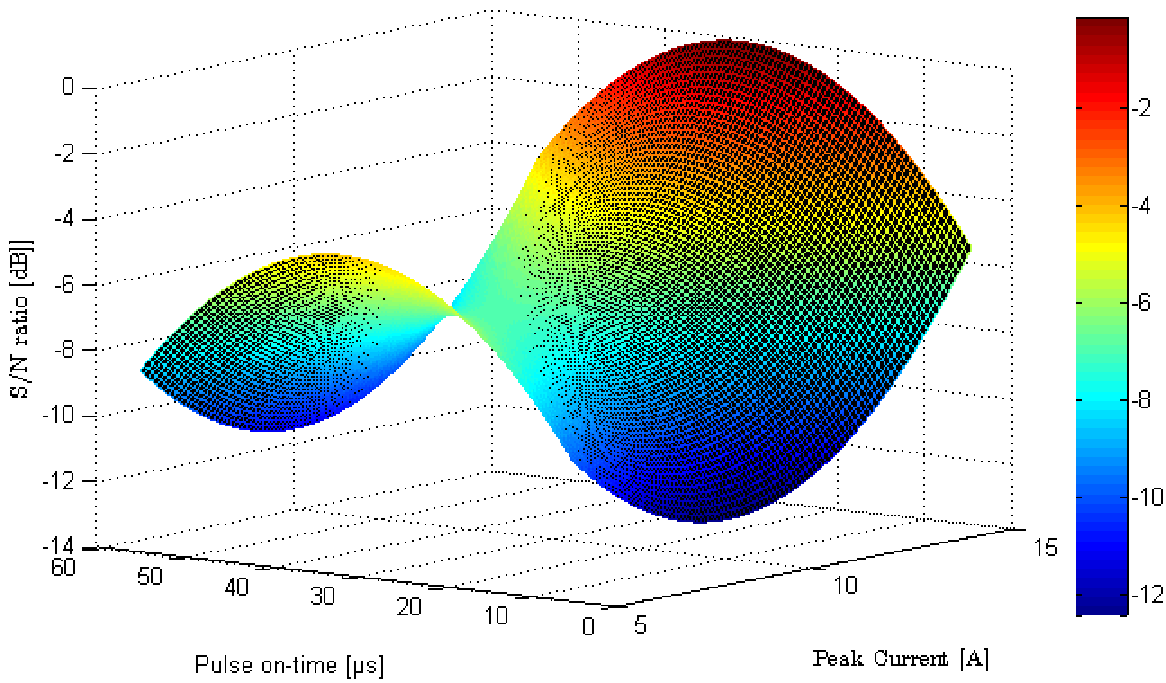

Figure 78 – 3D Graphic peak current Vs pulse on-time on $TAPER$ response

As it can be seen on Fig.78, the Eq.33, the minimum for taper can be found around the values of 15 A for the *peak current* and 30 μs for *pulse on-time* as previous predicted on $ANOVA$, Fig.73.

If some one wishes to compare the predicted values for S/N ratio for *MRR, EW, ROC* and *TAPER*, then the Fig.79, Fig.80, Fig.81, and Fig.82, gives an image for comparing the measured with the predicted ones.

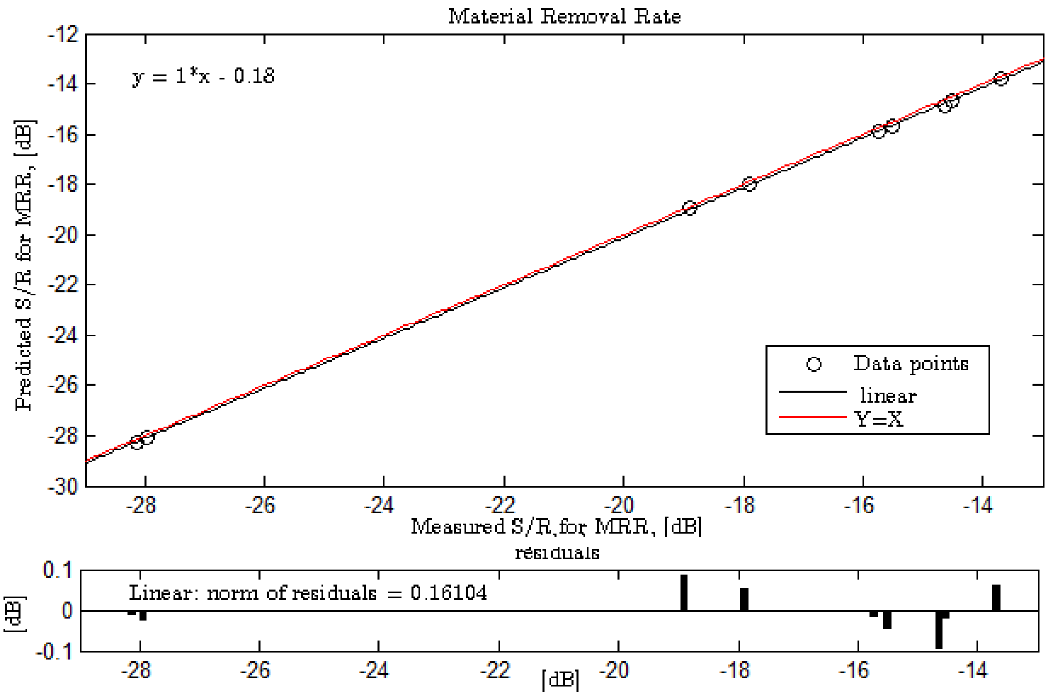

Figure 79 – Comparison of measured and predicted values of S/N ratios for MRR

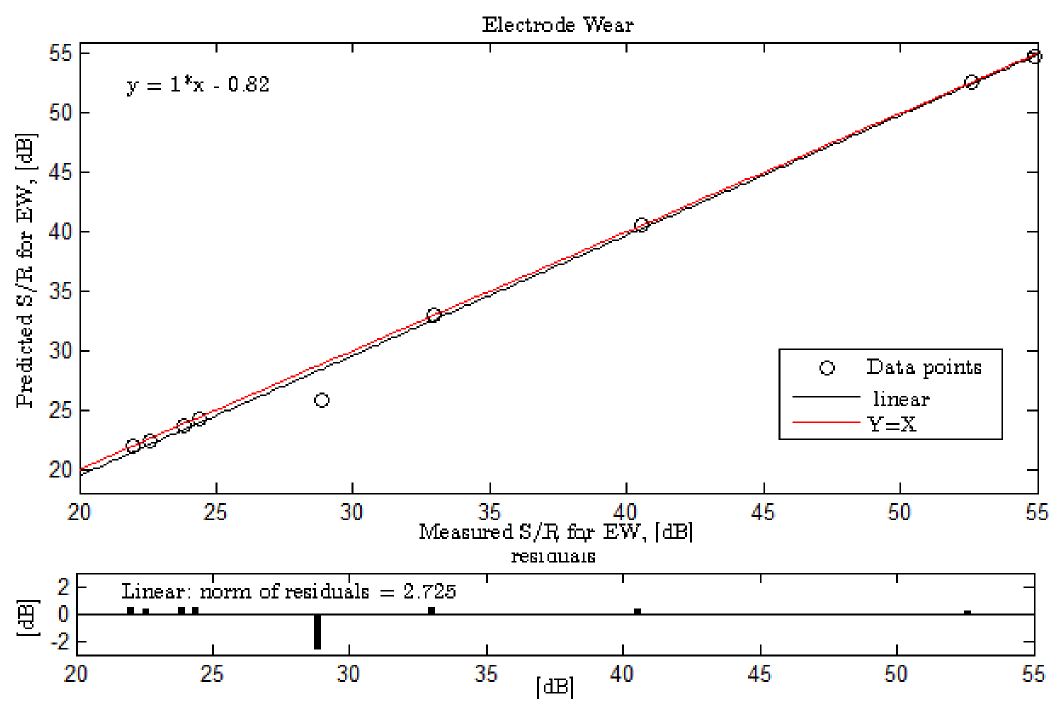

Figure 80 – Comparison of measured and predicted values of S/N ratios for EW

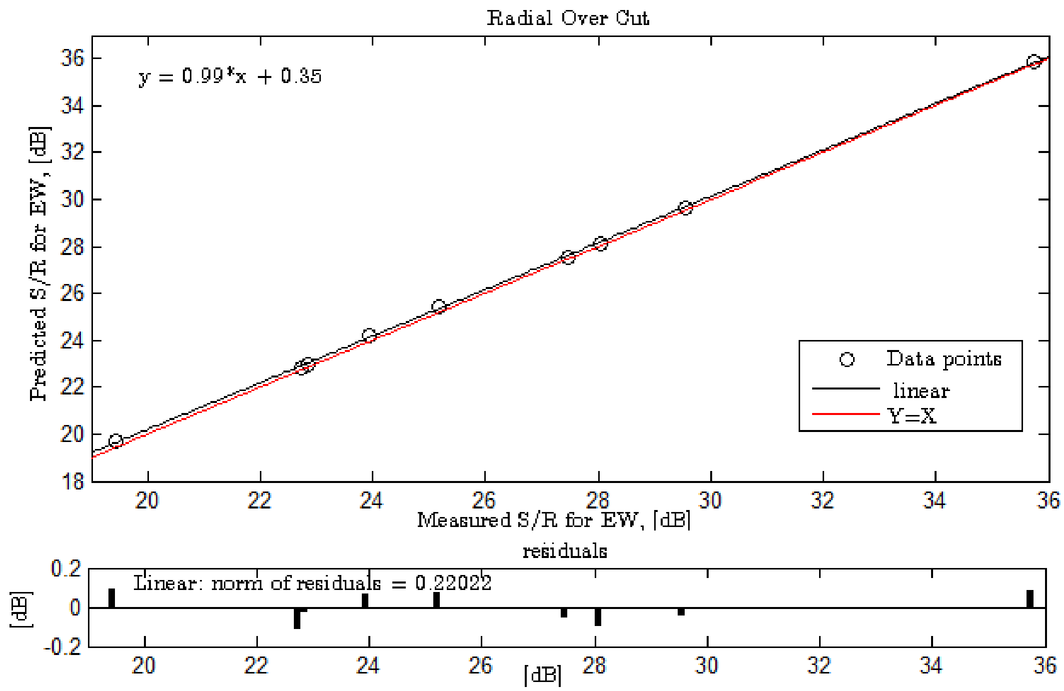

Figure 81 – Comparison of measured and predicted values of S/N ratios for *ROC*

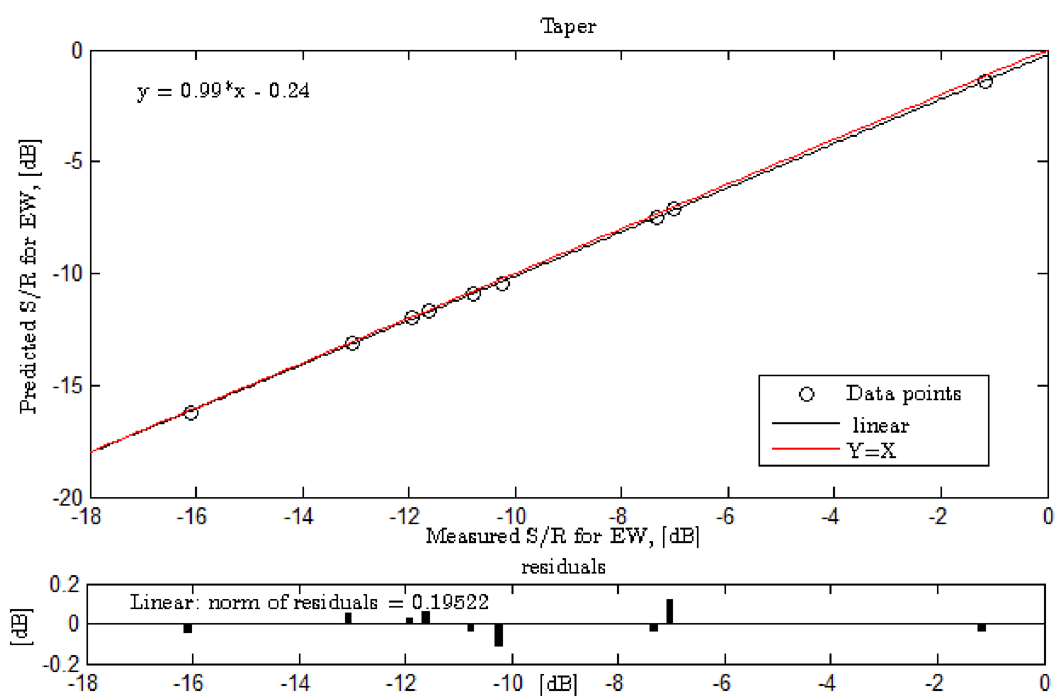

Figure 82 – Comparison of measured and predicted values of S/N ratios for *TAPER*

The Fig.79 , Fig.80, Fig.81, and Fig.82 are the graphical representation of the measured S/N ratios vs. predicted S/N ratios trough mathematical models previously presented. To better understand this proposal a linear regression was made, and also was drawn a $Y = X$ line. Since the results from the measured and predicted values should be very close form each other , they should present themselves very close to a line of a type $Y = X$, and indeed, the linear regression present itself very close from a $Y = X$ line. Also on those figures is represented the residuals from the linear regression.

To obtain the MRR, EW, ROC and $TAPER$ values through the S/N ratios values is necessary to apply the simple relations:

$$MRR = 10^{\frac{\eta_{MRR}}{20}} \tag{34}$$

$$EW = 10^{-\frac{\eta_{EW}}{20}} \tag{35}$$

$$ROC = 10^{-\frac{\eta_{ROC}}{20}} \tag{36}$$

$$TAPER = 10^{-\frac{\eta_{TAPER}}{20}} \tag{37}$$

Thus using the Eq.30, Eq.31, Eq.32, Eq.33, and Eq.34 to predict the S/N ratio value and than Eq.35, Eq.36 and Eq.37 it is possible to determine MRR, EW, ROC and $TAPER$ for arbitrary chosen values of the EDM parameters.

Table 28 – Relative errors - Confirmation test Vs. Mathematical model

Responses	Predicted values		Relative error [%]
	Confirmation test ($\hat{\eta}_{opt}$)	Mathematical model	
MRR [mm^3/min]	0,5173	0,5051	2,4
EW [mm^3/min]	0,0010	0,0012	20
ROC[mm]	0,0163	0,0160	1,9
TAPER[$degrees$]	0,9912	1,0198	2,9

In order to understand and somehow validate the mathematical models, were calculated two types of errors. First, an error based on the difference between the values obtained through the confirmation test ($\hat{\eta}_{opt}$), by Taguchi method and the values obtained by the mathematical models, as shown on Tab.28. The second error was calculated based on the difference between the values from the mathematical models and the real values measured on the experimental work. Both of those errors were calculated based on the real values of the responses, using the Eq.34, 35, 36 and 37.

Table 29 – Average relative errors of predicted responses by mathematical models

Responses	Exp.	Observed values		Errors [%]		
		Eq.	Exp.	Rel. error	Av. error	
					W/ Opt.C.	Final Exp
MRR[mm^3/min]	Exp. 1	0,1127	0,1133	0,5	27	2
	Exp. 5	0,1603	0,1632	1,8		
	Exp. 9	0,1802	0,1852	2,8		
	Opt.C.	0,5051	0,2503	102		-
EW[mm^3/min]	Exp. 1	0,0509	0,0361	41	16	16
	Exp. 5	0,0803	0,0796	0,8		
	Exp. 9	0,0018	0,0017	5,9		
	Opt.C.	0,0012	0,0014	17		-
ROC[mm]	Exp. 1	0,0393	0,0395	0,5	2	2
	Exp. 5	0,0707	0,0720	1,8		
	Exp. 9	0,1032	0,1068	3,5		
	Opt.C.	0,0160	0,0163	1,8		-
TAPER[$degrees$]	Exp. 1	4,5223	4,5048	0,4	4	2
	Exp. 5	3,5179	3,4575	1,7		
	Exp. 9	0,8485	0,8739	3		
	Opt.C.	0,9805	0,8838	11		-

The relative errors of predicted responses through the mathematical models were calculated based on four responses values obtained from experimental measurements and another four responses values obtained from the mathematical models, thus to be able to make an average as shown on Tab.29.

21.5 Discussion

The efficiency of EDM depends on the electrical conductivity of the work material. In spite of the low electrical conductivity and high thermal resistance of the SiC particles, which ultimately reduces the electrical conductivity of the work material, the results obtained indicate that $AlMg10\,5\%\,SiC$ can be machined effectively using EDM. By *Taguchi* method, all considerations on this chapter are only acceptable taking into account the range of levels under study. These data may not generalize the same process with bigger range of parameters.

21.5.1 Material removal rate

Concerning the MRR, it was found that the optimum combination of parameters level was $PC_3SV_2Ton_2Toff_1$, as shown on Fig.70. The parameters with more influence were *servo voltage* (49%) and *peak current* (24%), followed by *pulse on-time* (18%) and *pulse off-time* (9%), as shown on Fig.74. Analyzing the Fig.70, concerning the *servo voltage*, it can be seen that the slope between the first and second level is smaller than between the second and third level. This means that a bigger gap between the electrode and the workpiece doesn't benefit the MRR. On the other hand, with a gap too small the debris can not be properly removed from the gap, which may lead to an accumulation of the same debris on the bottom surface of the electrode tool.

It was observed that the MRR increases with increasing values of discharge energy, attributed to *peak current*, Eq.1. The increased rate of material removed from the work piece is attributed to the higher thermal loading, as a result of higher discharge current value. On the other hand, high values of *pulse on-time* do not increase the material removal rate. MRR was found to be faster at the beginning of the process, and gradually slows down due to the entrapment of SiC particles into the spark gap.

21.5.2 Electrode wear

Regarding the EW, the optimum combination of parameter levels was $PC_1SV_3Ton_2Toff_1$, as shown on Fig.71. The Fig.74 shows that the parameter with more influence was *servo voltage* (84%), followed by *peak current* (10%), *pulse on-time* (5%) and *pulse off-time* (1%). A bigger gap between the electrode and the workpiece allow that the debris can be properly removed from the working area gap, which leads to non-existence of abnormal discharges that usually promotes a bigger electrode wear. Moreover, a better removal of debris results in less of them groped on the electrode, which can often lead to a decrease of the wear.

From the literature,small values of *peak curren*t are directly related with a decreasing of the electrode wear. Smaller energy discharge promoted in part by smaller *peak current* leads to a small amounts of material removed form the electrode tool which leads a smaller electrode wear.

21.5.3 Radial over cut

Regarding the ROC, the optimum combination of parameter levels was $PC_2SV_3Ton_1Toff_2$, as shown on Fig.72. The Fig.74 shows that the parameters with more influence were *pulse on-time* (35%) and *peak current* (29%), followed by *pulse off-time* (18%) and *servo voltage* (18%). Once more the amount of material that is removed from the workpiece is the key to understand these results. Since the parameter *pulse on-time*, present itself with small value on the optimum combination level, it is possible to say that ROC is directly proportional to *pulse on-time*. Smaller values of energy discharge conduct a smaller amount of removed material, which leads a smaller values of ROC. In addition, smaller values of *peak current* are important to achieve smaller values of radial over cut.

To better understand these results a comparison can be made between the parameter levels and the same parameter levels that are required for a EDM finishing operation. Both of them required small values of *peak curren*t and *pulse on-time* to achieve a good precision and accuracy, since smaller amounts of removed material per pulse, thus leads to a good result of roughness on finishing operations and, in this case, good results of radial over cut.

21.5.4 Taper

Concerning the Taper, it was found that the optimum combination of parameter levels was $PC_3SV_2Ton_2Toff_1$, as shown on Fig.73. The parameters with more influence were *peak curren*t (47%) and *pulse on-time* (33%) followed by *servo voltage* (12%) and *pulse off-time* (8%), as shown on Fig.74. Through the literature it is accepted that small values of *peak current* and *pulse on-time* are better to improve the $Taper$, however, most of these studies are based on homogenous materials. In this case the explanation for this outcome lies in the grain size of the SiC particles, since those particles have a larger grain size than the rest of the material that involves them.

In addition, the melting point of those particles is higher than the surrounding material, which leads the surrounding material to melting first than the SiC particles. After that, the silicone particles will be in the gap area, almost intact, and will promote secondary discharges leading to a bigger $Taper$. As a consequence, higher values of discharge energy are needed to avoid this phenomena, and now, is understandable the influence of the *peak current* and *pulse on-time* with bigger values. A bigger discharge energy will have a better melting effect on the SiC, promoting small particles and avoiding "whirlwind effect" of big particles inside the hole.

21.5.5 Comments

In this work, specially in the experimental part, there were some problems related with the electrode tool. As described on section *19- Experimental setup,* after each experiment the tool required some operations to be able to be used again. Within those operations electrode tip were cut and the electrode bottom face was grinded to achieve a plane surface again. The problem occurs during the grinding operation, since this operation is based on abrasion, temperatures rise up very fast, rapidly heating the electrode, leaving the electrode more prone to slight deformations. Even slightly, this deformation has impact on the final results, promoting low circularity of the holes, irregular cross section and irregular bottoms that can affect the responses under study.

The average relative errors predicted through the mathematical model, on the MRR response, shows a bigger value when used the optimum combination level in comparison with the value obtained without optimum combination level, as shown on Fig.29. Also on Fig.27, the error between predicted value by *Taguchi* and the experimental value is bigger regarding the MRR. This difference can be related with measurements errors and with the electrode wear since the best combination for MRR use *peak curren* with $15A$ and this higher value of current intensity not benefit the EW. As a consequence of the wear, the bottom surface of the electrode will lose his flat shape, and will influence the bottom of the hole. Irregulars hole bottoms can induce measurements errors, once that the volume of the hole needed to calculate the MRR response is based on an approximation between a cone frustum and the hole shape. Therefor only the average relative error values that not use the optimum combination level on their calculations, should be used to interpret the quality and efficiency of the mathematical models.

22 Conclusions and recommendations

EDM drilling process is a widely used fabrication technique to produce micro-parts and components needed on industrial, medical, military and aerospace applications. This research, studied the effects of several EDM parameters on a drilling operation of a metal matrix composite material ($AlMg10\,5\%\,SiC$) using the $Taguchi\,method$ for planning and analyzing the experiments and finally the statistic method $Analysis\,of\,variance$ ($ANOVA$) to interpret the results.

The proposal for this research was to study the responses of material removal rate, electrode wear, radial over cut and taper on the EDM drilling operation of MMC. The reinforcement with SiC carbide particles of this material reveals itself as the biggest problem of the process. The Taguchi method was used to plan the experiments, find the optimum combination level for each response in terms of S/N ratios and finally validate the method with the confirmation tests. The $ANOVA$ was used to find out which parameter has the bigger contribution for each response.

According to the experimental results, *Taguchi* method and statistical analysis of *ANOVA*, the following conclusions have been drawn:

- The material removal rate response presents the optimum combination level for *peak current* $15A$, *servo voltage* $80V$, *pulse on-time* $30\mu s$, *pulse off-time* $5\mu s$ and the parameters which have more influence on this response are *servo voltage* and *peak current* with 49% and 24% of contribution.

- Regarding electrode wear response, presents the optimum combination level for *peak current* $5A$, *servo voltage* $120V$, *pulse on-time* $30\mu s$, *pulse off-time* $5\mu s$ and the parameters which have more influence on this response are *servo voltage* and *peak current* with 84% and 10% of contribution.

- The radial over cut response present the optimum combination level for *peak current* $10A$, *servo voltage* $120V$, *pulse on-time* $5\mu s$, *pulse off-time* $30\mu s$ and the parameters which have a bigger contribution are *pulse on-time* and *peak current* with 35% and 29% respectively.

- Concerning the taper response, it shows that the optimum combination level for *peak current* $15A$, *servo voltage* $80V$, *pulse on-time* $30\mu s$, *pulse off-time* $5\mu s$ and the parameters which have more influence on this response are *peak current* and *pulse on-time*

47% and 33% of contribution.

- This experimental work was validated through the confirmation tests, since difference between the $\hat{\eta}_{opt}$ and η_{obs} is within the CI value at 95% of confidence level for all four responses.
- The mathematical models are acceptable since the residual values from the linear regression are small, and the graphical representation S/N measured Vs. S/N predicted shows a behavior close to the line $Y = X$.
- Responses in study can be predicted using the Mathematical models with a average error of 2 % for MRR, 16% for EW, 2% for ROC and 2% for $TAPER$.

In summary, the discharge energy, gap voltage and grain size are the most important characteristics on EDM drilling process of the $AlMg10\,5\%\,SiC$.

As recommendations,

Some improvements on this study can be done such as the choosing a bigger range of levels, in the case of *peak current*, in other hand, a small range of levels for *pulse on-time* and *pulse off-time*. Also the effect of other parameters such as polarity and duty cycle can be study on the next researches. The use of a bigger orthogonal array, for example L_{18} or L_{25}, can be a good improvement to better understand the effect of the parameter levels. In this study, dielectric oil is used as a flushing liquid, dielectric liquid can be changed to different dielectric liquid, such as dielectric water or kerosene, and efficiency on the machined parts can be compared. Other important parameter is the type of flushing. Submerged flushing is used on this investigation as a type of flushing. The type of flushing also can be changed to a different type, such as a normal pressure flushing into the working area or a pressure flushing through the electrode. The shape and material of the electrode tool also can be changed to a tubular shape, and concerning the material, graphite electrodes can be used in order to make a comparison between materials. In addition different output parameters can be studied, such as heat affected zone and surface roughness. Finally based on this research and in the next ones a software based model can be developed to predict the machined hole geometry, dimensions and quality in advance. This model provides us to save waste of time consumed during the sacrificial experiments.

Part III

Appendices

Appendix 1

Equipment

Main components

In general the components in the *EDM* machines can be divided in four main sub systems such the power supply, the subsystem for he working motion and servo-control of the gap size, the electrode tool subsystem and the dielectric fluid subsystem as shown in Fig.83. However different types of process have some differences among them, specially on the electrode tool and working motion subsystem.

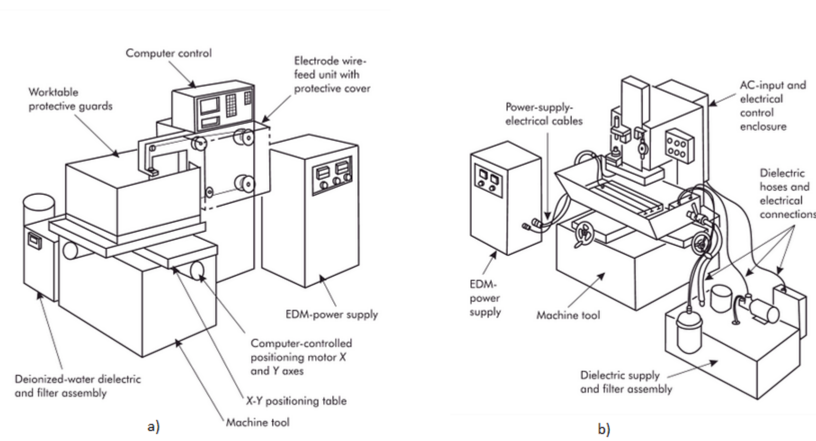

Figure 83 – Schematic representation of EDM setup: a) Wire EDM, b) Die-sinking EDM[1]

Main components Die-sinking *EDM*

The main components by subsystem on a Die-sinking *EDM* Machine are [1, 2, 9, 13, 58, 59]:

- Power Supply (pulse generator, pulse control circuit, power amplifiers, current sensors, transducers)
- Working Motion (*CNC* control system, servo motor, contact sensor)

- Electrode Tool (electrode tool, chucks, clamping, motorized X-Y worktable)
- Dielectric Fluid (dielectric fluid, filters, pumps, dielectric fluid tanks, pipes, nozzles, pressure gauge, valves)

Main components Wire *EDM*

The main components on a wire *EDM* Machine are the the same that on a Die-sinking *EDM* Machine except [60]:

- Electrode Tool (wire, tensiometer, wire break, wire puller, wire supply pool, left and right wire guide, wire guides)

Main components *EDM* drilling

In *EDM* drilling the main components are the same that Die-sinking *EDM* except Dry *EDM* head. This components is attached on the machine and allows the flushing with compressed air trough the electrode tool. This component can be seen in the previous section, Dry *EDM*.

Types of equipments

Die-sinking *EDM*

Wire *EDM*

*EDM***drilling**

Market

Machine Producers

The main producers are: Sodick, MAKINO, Mitsubishi Electric Eroding Systems, AgieCharmilles, 600 Group, Doosan Infracore Machine Tools, KNUTH Machine Tools, ONA electro erosión, EXERON, KENT USA, ANG International, MAXSEE INDUSTRY CO. LTD., ARISTECH, Anotronic LTD., CHMER, Zimmer Kreim, POSALUX, Current EDM , OSCAR MAX EDM, NEUAR, CREATOR PRECISION CO. LTD., OPS INGERSOLL, SARIX , WINBRO GROUP, JOEMARS, HEUN, AccuteX and Top-One.

Machine equipments Producers

Wires

- Bedra Intelligent wires (Wire for high speed precision wire electrical discharge machining)
- PAPS Pungkuk EDM Wire Manufacturing CO., Ltd. (wire for high power EDM)
- MMTL Ningbo Powerway Materialise Co., Ltd. (Zinc-coated wire for wire EDM)

Programing Software

- Gibbs and Associates (Wire EDM programming software)
- TEBIS (Wire EDM programming software)

Clampings and Chucks

- EROWA (Clamping system for wire EDM machine)
- F-Tool International AG F-Tool International AG (Clamping system for wire EDM machine)
- Wen Technology (Chuck for EDM machine)
- BRAILON MAGNETICS (Chuck for EDM machine)

Electrodes

- RABOURDIN INDUSTRIE (Copper electrode for EDM)
- Holepop.com (Brass electrode for EDM)
- SLG GROUP The carbon company (Graphite for EDM electrodes)

Dielectric Oils

- IGOL Lubrificants (Dielectric oil)
- MOTUL TECH (Dielectric oil)
- Hangsterfer's (Dielectric oil)

Others

- LOSMA (Fume extractor for EDM)
- SCHMIDT Control instruments (Tension meter for wire EDM)

Figure 84 – Logos of the main brands (machines and machines components)

Appendix 2

S/N ratios

To better understand the values on the Tab.21, the following calculations are a explanation of the first values,

Value of S/N ratio for MRR, first experiment,

With the Eq.13 and the final results to MRR, presents on Tab.20,

$$S/N\,ratio\,MRR = -10log_{10}\left(\frac{1}{9}\left[\left(\frac{1}{0,1134}\right)^2\right]\right) = -18,9092\ [dB]$$

Value of S/N ratio for EW, first experiment,

With the Eq.14 and the final results to EW, presents on Tab.20,

$$S/N\,ratio\,EW = -10log_{10}\left(\frac{1}{9}\left[(0,0361)^2\right]\right) = 28,8437\ [dB]$$

Value of S/N ratio for ROC, first experiment,

With the Eq.14 and the final results to ROC, presents on Tab.20,

$$S/N\,ratio\,ROC = -10log_{10}\left(\frac{1}{9}\left[(0,0396)^2\right]\right) = 28,0497\ [dB]$$

Value of S/N ratio for T, first experiment,

With the Eq.14 and the final results to T, presents on Tab.20,

$$S/N\,ratio\,T = -10log_{10}\left(\frac{1}{9}\left[(4,5049)^2\right]\right) = -13,0736\ [dB]$$

Mean of S/N ratio

The values present on Tab.22, for each output, are the mean of S/N ratio for each parameter for each level, as described below.

Example for MRR,

Values of PC for level 1 are the average of all values of S/N ratios for MRR, with a parameter to be studied, in this case peak current, and with level 1.

Therefore,

$$= \frac{-18,9092 + (-13,6965) + (-28,1317)}{3} = -20,2458\ [dB]$$

Values of V for level 2 are the average of all values of S/N ratios for MRR, with a parameter to be studied, in this case voltage, and with level 2.

Therefore,

$$= \frac{-13,6965 + (-15,7417) + (-14,5202)}{3} = -14,6548\ [dB]$$

Values of Ton for level 3 are the average of all values of S/N ratios for MRR, with a parameter to be studied, in this pulse on-time, and with level 3.

Therefore,

$$= \frac{-28,1317 + (-15,7417) + (-15,5110)}{3} = -19,7948\ [dB]$$

Values of $Toff$ for level 2 are the average of all values of S/N ratios for MRR, with a parameter to be studied, in this case pulse off-time, and with level 2.

Therefore,

$$= \frac{-13,6965 + (-27,9549) + (-15,5110)}{3} = -19,0541\ [dB]$$

Contribution

The calculation of the contribution of each parameter into a specific output follow an specific order, shown below.

First is necessary to calculate the S/R ratio average ($\overline{y}$) for each output, in this example the MRR, using the Eq.16.

$$\overline{y} = [-18,9092 + (-13,6965) + (...) + (-14,5262) + (-14,6467)]\,/9 = -18,5582$$

Then, follows the value for total sum of squares (SS_T), and this value is calculated by the Eq.15, as the following steps,

$$SS_T = (-18,9092 - (-18,5582))^2 + (-13,6965 - (-18,5582))^2 + (...)$$

$$+(-14,6467 - (-185582))^2) = 252,9082$$

The following step is the calculation of sum of squares due each process parameter(SS_P), with Eq.17, as shown on the following steps:

First, sum of the S/N ratios results involving one parameter and one level, (SY_1, SY_2, SY_3), for example, PC, and level 1,2,3 for MRR, are:

$$SY_1 = (-18,9092) + (-13,6965) + (-28,1317)\text{=-60,7374}$$

$$SY_2 = (-17,9061) + (-15,7417 + (-27,9549)\text{=-61,6027}$$

$$SY_3 = (-15,5110) + (-14,5262) + (-14,6467)\text{=-44,6839}$$

Second, sum of $(SY_{1,2,3})^2$ times the number of the each level repeats on each parameter,in this case three times for each one, as following equation:

$$\frac{(-60,7374)^2}{3} + \frac{(-61,6027)^2}{3} + \frac{(44,6839)^2}{3} = 3160,1920$$

Third, with Eq.17, the square of the sum of MRR values times number of experiments, in this case nine experiments,

$$\frac{1}{9}\left[-18,9092 + (-13,6965) + (...) + (-14,5262) + (-14,6467)\right]^2 = 3099,669$$

Finally, with Eq.17, the SS_Pvalue for MRR, and the contribution of peak current is:

$$SS_P = 3160,1920 - 3099,669 = 60,5229$$

The value of mean square (V_P) is a ratio between SS_P, previous calculated, and the degrees of freedom for each parameter, in this case 2.

The contribution value is a percentage of a ratio between the sum of square due each parameter (SS_P) and total sum of squares for each output (SS_T) in this case MRR. mm^3

Appendix 3

Table 30 – Measurements of the top diameter hole on preliminary experiments

Experiment	Top diameter measurements (mm)		
	6 points	3 points	average
1	1,667	1,641	1,6540
2	1,563	1,588	1,5755
3	1,528	1,537	1,5325
4	1,497	1,512	1,5045
5	1,467	1,472	1,4695

Table 31 – Measurements of the bottom diameter hole on preliminary experiments

Experiment	Bottom diameter measurements (mm)		
	1º measurement	2º measurement	average
1	1,073	1,047	1,0600
2	1,440	1,461	1,4505
3	1,369	1,337	1,3530
4	1,357	1,392	1,3745
5	1,077	1,070	1,0735

Table 32 – Measurements of hole length on preliminary experiments

Experiment	Hole length measurements (mm)		
	1º measurement	2º measurement	average
1	2,030	2,055	2,043
2	1,628	1,637	1,633
3	4,678	4,676	4,677
4	2,038	2,058	2,048
5	3,930	3,955	3,943

Table 33 – Measurements of the electrode lost weight on he preliminary experiments

Experiment	Operation	Measurements (mm)				Lost weight (mm)
		1º	2º	3º	average	
1	Before	2,0313	2,0313	2,0314	2,0313	0,0006
	After	2,0307	2,0306	2,0308	2,0307	
2	Before	2,0274	2,0273	2,0275	2,0274	0,0004
	After	2,0269	2,0269	2,0269	2,0269	
3	Before	2,0251	2,0251	2,0252	2,0251	0,0024
	After	2,0228	2,0227	2,0226	2,0227	
4	Before	2,0222	2,0222	2,0222	2,0222	0,0005
	After	2,0217	2,0217	2,0217	2,0217	
5	Before	2,0207	2,0206	2,0206	2,0207	0,0018
	After	2,0189	2,0188	2,0188	2,0189	

Appendix 4

Table 34 – Measurements of top hole diameters on the final experiments

Experiment	Top diameter measurements (mm)		
	6 points	3 points	average
1	1,475	1,470	1,473
2	1,535	1,544	1,540
3	1,458	1,462	1,460
4	1,475	1,481	1,478
5	1,536	1,539	1,538
6	1,430	1,422	1,426
7	1,535	1,506	1,521
8	1,508	1,499	1,504
9	1,612	1,602	1,607

Table 35 – Measurements of bottom hole diameters on the final experiments

Experiment	Bottom diameter measurements (mm)		
	1º measurement	2º measurement	average
1	0,871	0,988	0,930
2	1,100	1,179	1,140
3	1,325	1,358	1,342
4	0,936	0,980	0,958
5	0,959	1,038	0,999
6	1,164	1,224	1,194
7	0,975	1,002	0,989
8	1,097	1,118	1,108
9	1,455	1,480	1,468

Table 36 – Measurements of hole length on the final experiments

Experiment	Hole length measurements (mm)		
	1º measurement	2º measurement	average
1	3,445	3,447	3,446
2	5,084	5,109	5,097
3	0,879	0,902	0,891
4	3,756	3,779	3,768
5	4,452	4,469	4,461
6	1,011	1,063	1,037
7	4,666	4,694	4,680
8	4,850	4,901	4,876
9	3,502	3,482	3,492

Table 37 – Measurements of the electrode lost weight on he final experiments

Experiment	Operation	Measurements (mm)				Lost weight (mm)
		1º	2º	3º	average	
1	Before	0,93104	0,93104	0,93101	0,93103	0,01113
	After	0,91989	0,91992	0,91990	0,91990	
2	Before	0,83927	0,83925	0,83926	0,83926	0,00691
	After	0,83253	0,83232	0,83220	0,83235	
3	Before	0,73912	0,73933	0,73935	0,73927	0,00072
	After	0,73847	0,73856	0,73860	0,73854	
4	Before	0,62293	0,62291	0,62292	0,62292	0,01863
	After	0,60428	0,60428	0,60430	0,60429	
5	Before	0,50271	0,50271	0,50264	0,50269	0,02454
	After	0,47810	0,47821	0,47813	0,47815	
6	Before	0,96907	0,96907	0,96905	0,96906	0,00290
	After	0,96609	0,96626	0,96615	0,96617	
7	Before	0,87071	0,87073	0,87047	0,87064	0,02296
	After	0,84764	0,84769	0,84769	0,84767	
8	Before	0,66135	0,66130	0,66136	0,66134	0,01980
	After	0,64155	0,64150	0,64156	0,64154	
9	Before	0,52757	0,52753	0,52753	0,52754	0,00055
	After	0,52704	0,52692	0,52701	0,52699	

Appendix 5

Table 38 – All parameters used on the final experiments

Run	PL	ON	OFF	IP	SV	S	V	HP	PP	C	J	UP	DN
1	+	5	5	001.4	40	42	21	0	10	4	5	11	20
2	+	30	30	001.4	80	42	21	0	10	4	5	11	20
3	+	55	55	001.4	120	42	21	0	10	4	5	11	20
4	+	30	55	003.2	40	42	21	0	10	4	5	11	20
5	+	55	5	003.2	80	42	21	0	10	4	5	11	20
6	+	5	30	003.2	120	42	21	0	10	4	5	11	20
7	+	55	30	004.6	40	42	21	0	10	4	5	11	20
8	+	5	55	004.6	80	42	21	0	10	4	5	11	20
9	+	30	5	004.6	120	42	21	0	10	4	5	11	20

Appendix 6

Results of confirmation tests:

First experiment was to confirm MRR and $TAPER$, since the optimum combination of levels was equal for both of them.

Table 39 – Top diameters of the holes on confirmation test of MRR and $TAPER$

Conf. EXp.	Measurements (mm)		Average (mm)
	3 points	6 points	
Diameters	1,575	1,541	1,556
	1,563	1,550	

Table 40 – Bottom diameters and hole length of confirmation test for MRR and $TAPER$

Dimensions	Measurements (mm)			Average (mm)
	1	2	3	
Bottom hole diameter	1,324	1,356	1,338	1,347
Hole length	5,262	5,282	5,297	5,289

Second experiment was to confirm the EW.

Table 41 – Lost weight of the electrode tool on the confirmation test

Operation	Measurements (mm)			Lost weight
	1º	2º	3º	
Before	0,34791	0,34789	0,34788	0,00044
After	0,34750	0,34745	0,34742	

Appendix 7

Table 42 – Statistic table for F distribution at 95%

F Distribution: Critical Values of F (5% significance level)

ν_1 / ν_2	1	2	3	4	5	6	7	8	9	10	12	14	16	18	20
1	161.45	199.50	215.71	224.58	230.16	233.99	236.77	238.88	240.54	241.88	243.91	245.36	246.46	247.32	248.01
2	18.51	19.00	19.16	19.25	19.30	19.33	19.35	19.37	19.38	19.40	19.41	19.42	19.43	19.44	19.45
3	10.13	9.55	9.28	9.12	9.01	8.94	8.89	8.85	8.81	8.79	8.74	8.71	8.69	8.67	8.66
4	7.71	6.94	6.59	6.39	6.26	6.16	6.09	6.04	6.00	5.96	5.91	5.87	5.84	5.82	5.80
5	6.61	5.79	5.41	5.19	5.05	4.95	4.88	4.82	4.77	4.74	4.68	4.64	4.60	4.58	4.56
6	5.99	5.14	4.76	4.53	4.39	4.28	4.21	4.15	4.10	4.06	4.00	3.96	3.92	3.90	3.87
7	5.59	4.74	4.35	4.12	3.97	3.87	3.79	3.73	3.68	3.64	3.57	3.53	3.49	3.47	3.44
8	5.32	4.46	4.07	3.84	3.69	3.58	3.50	3.44	3.39	3.35	3.28	3.24	3.20	3.17	3.15
9	5.12	4.26	3.86	3.63	3.48	3.37	3.29	3.23	3.18	3.14	3.07	3.03	2.99	2.96	2.94
10	4.96	4.10	3.71	3.48	3.33	3.22	3.14	3.07	3.02	2.98	2.91	2.86	2.83	2.80	2.77
11	4.84	3.98	3.59	3.36	3.20	3.09	3.01	2.95	2.90	2.85	2.79	2.74	2.70	2.67	2.65
12	4.75	3.89	3.49	3.26	3.11	3.00	2.91	2.85	2.80	2.75	2.69	2.64	2.60	2.57	2.54
13	4.67	3.81	3.41	3.18	3.03	2.92	2.83	2.77	2.71	2.67	2.60	2.55	2.51	2.48	2.46
14	4.60	3.74	3.34	3.11	2.96	2.85	2.76	2.70	2.65	2.60	2.53	2.48	2.44	2.41	2.39
15	4.54	3.68	3.29	3.06	2.90	2.79	2.71	2.64	2.59	2.54	2.48	2.42	2.38	2.35	2.33
16	4.49	3.63	3.24	3.01	2.85	2.74	2.66	2.59	2.54	2.49	2.42	2.37	2.33	2.30	2.28
17	4.45	3.59	3.20	2.96	2.81	2.70	2.61	2.55	2.49	2.45	2.38	2.33	2.29	2.26	2.23
18	4.41	3.55	3.16	2.93	2.77	2.66	2.58	2.51	2.46	2.41	2.34	2.29	2.25	2.22	2.19
19	4.38	3.52	3.13	2.90	2.74	2.63	2.54	2.48	2.42	2.38	2.31	2.26	2.21	2.18	2.16
20	4.35	3.49	3.10	2.87	2.71	2.60	2.51	2.45	2.39	2.35	2.28	2.22	2.18	2.15	2.12
21	4.32	3.47	3.07	2.84	2.68	2.57	2.49	2.42	2.37	2.32	2.25	2.20	2.16	2.12	2.10
22	4.30	3.44	3.05	2.82	2.66	2.55	2.46	2.40	2.34	2.30	2.23	2.17	2.13	2.10	2.07
23	4.28	3.42	3.03	2.80	2.64	2.53	2.44	2.37	2.32	2.27	2.20	2.15	2.11	2.08	2.05
24	4.26	3.40	3.01	2.78	2.62	2.51	2.42	2.36	2.30	2.25	2.18	2.13	2.09	2.05	2.03
25	4.24	3.39	2.99	2.76	2.60	2.49	2.40	2.34	2.28	2.24	2.16	2.11	2.07	2.04	2.01
26	4.22	3.37	2.98	2.74	2.59	2.47	2.39	2.32	2.27	2.22	2.15	2.09	2.05	2.02	1.99
27	4.21	3.35	2.96	2.73	2.57	2.46	2.37	2.31	2.25	2.20	2.13	2.08	2.04	2.00	1.97
28	4.20	3.34	2.95	2.71	2.56	2.45	2.36	2.29	2.24	2.19	2.12	2.06	2.02	1.99	1.96
29	4.18	3.33	2.93	2.70	2.55	2.43	2.35	2.28	2.22	2.18	2.10	2.05	2.01	1.97	1.94
30	4.17	3.32	2.92	2.69	2.53	2.42	2.33	2.27	2.21	2.16	2.09	2.04	1.99	1.96	1.93
35	4.12	3.27	2.87	2.64	2.49	2.37	2.29	2.22	2.16	2.11	2.04	1.99	1.94	1.91	1.88
40	4.08	3.23	2.84	2.61	2.45	2.34	2.25	2.18	2.12	2.08	2.00	1.95	1.90	1.87	1.84
50	4.03	3.18	2.79	2.56	2.40	2.29	2.20	2.13	2.07	2.03	1.95	1.89	1.85	1.81	1.78
60	4.00	3.15	2.76	2.53	2.37	2.25	2.17	2.10	2.04	1.99	1.92	1.86	1.82	1.78	1.75
70	3.98	3.13	2.74	2.50	2.35	2.23	2.14	2.07	2.02	1.97	1.89	1.84	1.79	1.75	1.72
80	3.96	3.11	2.72	2.49	2.33	2.21	2.13	2.06	2.00	1.95	1.88	1.82	1.77	1.73	1.70
90	3.95	3.10	2.71	2.47	2.32	2.20	2.11	2.04	1.99	1.94	1.86	1.80	1.76	1.72	1.69
100	3.94	3.09	2.70	2.46	2.31	2.19	2.10	2.03	1.97	1.93	1.85	1.79	1.75	1.71	1.68
120	3.92	3.07	2.68	2.45	2.29	2.18	2.09	2.02	1.96	1.91	1.83	1.78	1.73	1.69	1.66
150	3.90	3.06	2.66	2.43	2.27	2.16	2.07	2.00	1.94	1.89	1.82	1.76	1.71	1.67	1.64
200	3.89	3.04	2.65	2.42	2.26	2.14	2.06	1.98	1.93	1.88	1.80	1.74	1.69	1.66	1.62
250	3.88	3.03	2.64	2.41	2.25	2.13	2.05	1.98	1.92	1.87	1.79	1.73	1.68	1.65	1.61
300	3.87	3.03	2.63	2.40	2.24	2.13	2.04	1.97	1.91	1.86	1.78	1.72	1.68	1.64	1.61
400	3.86	3.02	2.63	2.39	2.24	2.12	2.03	1.96	1.90	1.85	1.78	1.72	1.67	1.63	1.60
500	3.86	3.01	2.62	2.39	2.23	2.12	2.03	1.96	1.90	1.85	1.77	1.71	1.66	1.62	1.59
600	3.86	3.01	2.62	2.39	2.23	2.11	2.02	1.95	1.90	1.85	1.77	1.71	1.66	1.62	1.59
750	3.85	3.01	2.62	2.38	2.23	2.11	2.02	1.95	1.89	1.84	1.77	1.70	1.66	1.62	1.58
1000	3.85	3.00	2.61	2.38	2.22	2.11	2.02	1.95	1.89	1.84	1.76	1.70	1.65	1.61	1.58

Appendix 8

Table 43 – All mesasures used do determine the density of the electrode tool

Piece	Dimens.	Measurements				Calculations		Average
		1	2	3	Average	Volume	Density	mm^3/g
	diameter (mm)	1,39	1,39	1,4	1,393			
A	length (mm)	72,11	72,1	72,1	72,103	109,884	0,0088	
	weight (g)	0,96945	0,96941	0,96931	0,969			0,00882
	diameter (mm)	1,39	1,39	1,4	1,393			
B	length (mm)	28,05	28,06	28,06	28,056	42,757	0,00881	
	weight (g)	0,37705	0,37701	0,37711	0,377			

Appendix 9

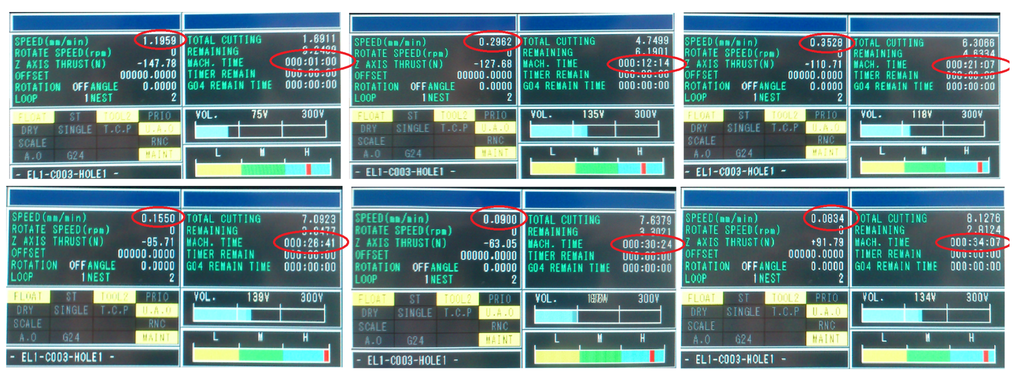

Figure 85 – Machining speed variation on experiment time duration

References

[1] Elman C. Jonson , *(EDM) Electrical Discharge Machining*,2001

[2] Sharanjit Singh and Arvind Bhardwaj , *Review to EDM by Using Water and Powder-Mixed Dielectric Fluid*, Journal of Minerals & Material Characterization & Engineering, vol.10 No.2 pp.199-230,2011

[3] Arbise Machine , Inc., History of EDM, Access at http://www.atlantaedm.com/articles/a8-history-of-edm.php, 21/11/2012

[4] Tebui, W., Boujelbene, M., Bayaraktar, E., Salem, S. Ben., *Parametric Approach Model For Determining Electrical Discharge Machining(EDM) Conditions: Effect of Cutting Parameters on the Surface Integrity*, The Arabian Journal for Science and Engineering volume 34 , Number 1 C

[5] Ho, K.H., Newman, S.T., *State of art electrical discharge machining(EDM)*, International Journal of Machine Tools & Manufacture *43(2003) 1287-1300*

[6] Guitraue, E., Bud, The EDM Handbook, 1997

[7] Sommer, Carl, Non-Traditional Machining Handbook, 2000

[8] Jia Tao,C.C. Kao., Tao, Jia., Shih,Albert J.,(2007), *Near dry electrical discharge machining*, International Journal of Machine & Tool Manufacture 47 (2007) 2273-2281

[9] Slatineanu, Laurentiu, Nagit, Gheorghe, Dodun, Oana, Coteata, Margareta, Chinesta, Francisco, Gonçalves-Coelho, António, Pamies Teixeira, Jorge, San Juan, Manuel, Santo, Loredana, Santos, Francisco, *Non-Traditional Manufacturing Processes*, 2004

[10] ***, Technology of spark erosion, access at http://www.edm-products.com/Dielectrics/ifase/ifase_5.htm, 15/11/2012,

[11] Galindéz, José, Lacalle, Luis, Mentaxaka, Aitzol, *Electroerosión: processo, máquinas y aplicaciones*

[12] Kumar, Vinod, Singh , Jagdeep, *Investigation on the Material Removal Mechanism and the Thermal Aspects in the Electrical Discharge Machining Process*, International Journal Of Engineering and Technology Volume 2 No 9, September , 2012

[13] Sommer, Carl,Sommer, Steve, Complete EDM Handbook, 2005

[14] Amorim , Fred L., Weingaertner, Walter L., *The behavior of graphite and copper electrodes on the finish die-sinking electrical discharge machining (EDM) of AISI P20 tool steel*, Journal of the Brazilian society of Mechanical Sciences and Engineering, vol.29 no. 4 Rio de Janeiro Oct./Dec. 2007

[15] Pandley, Anand, Singh Shakar, *Current research trends in variants of Electrical Discharge Machining: A review,* International Journal of Engineerung Science and Technology Vol.2(6), 2010, 2172-2191

[16] ***,Fundamentals of EDM, access at http://www.slideshare.net/vjtiprod/lecture-2-edm-wedm-and-medm#btnNext, 25/11/2012

[17] Uno, Yoshiyuki, Nakajima, Toshikatsu, Okada, Minoru, *The Effect of Electrode Polarity on Electrical Discharge Machining Performance in Water,* Memoirs of the Faculty of Engineering, Okayama University, Vol.26.No1, November, 1991

[18] Zhao, Wei, *Discussion on the Polarity Effect of EDM,* Advanced of Materials Research, Vols,154-155, 2011

[19] Khan, D. Ahmad, Hameedullah, Mohammad, *Effect of Tool Polarity on the Machining Characteristics in Electrical Discharge Machining of Silver Stell and Statistical Modelling of the Process,* International Journal of Engineering Science and Technology Vol. 3 No 6 , June , 2011

[20] Qu, Jun, Shih, Albert J., Scattergood, Ronald O., Luo, Jie, *Abrasive micro-blasting to improve surface integrity of elctrical discharge machined WC-CO composite,* Journal of Materials Processing Technology 166 , 440-448, 2005

[21] Chourdhary, Rajesh, H Kumar & R K Garg, *Analysis and evaluation of heat affected zones in electric discharge machining of EN-31 die stell,* Indian Journal of Engineering & Materials Sciences Vol 17, April 2010

[22] Qu, Jun, Riester, L., Shih,A.J., Scattergood,R.O., Lara-Curzio, E., Watkins, T.R., *Nanoindentation characterization of surface layers of electrical discharge machined WC/Co,*Materials Science and Engineering A344 (2003) 125/131

[23] Liu, C., Lee, H. T., *Optimizing the EDM hole-drilling strain gage method for the measurement of residual stress,*Journal of Materials Processing Technology 209 (2009) 5626-5635

[24] Rao, G., Satyanarayana, S., Praven, M., *Influence of Machining Parameters on Electric Discharge Machining of Maraging Steels – An Experimental Investigation,* Proceedings of the World Congress on Engineering 2008 Vol II WCE 2008, July 2 - 4, 2008

[25] Lin, J., Wang, K., Yan, B., Tarng, Y.,*Optimization of the electrical discharge machining process based on the Taguchi method with fuzzy logics,* Journal of Materials Processing Technology,2000

[26] Ho, K., Newman, S., Rahimifard, S., Allen, R., *State of the art in wire electrical discharge machining (WEDM),* International Journal of Machine Tools & Manufacture 44 (2004) 1247–1259

[27] Kozak, Jerzy, Rajurkar, Kamlakar P.,Chandarana, Niraj,*Machining of low electrical conductive materials by wire electrical discharge machining (WEDM),* Journal of Materials Processing Technology 149 (2004) 266–271

[28] Hasçalýk, Ahmet, Çaydas, Ulas,*Experimental study of wire electrical discharge machining of AISI D5 tool steel,*Journal of Materials Processing Technology 148 (2004) 362–367

[29] GarethW,Electro-discharge wire cutting (EDWC), access at http://www.mechanicaldesignforum.com/content.php?16-Electro-discharge-wire-cutting-(EDWC), 28/11/2012

[30] Boopathi, S., Sivakumar, K., *Experimental Comparative Study of Near-Dry Wire-Cut Electrical Discharge Machining (WEDM),*European Journal of Scientific Research ISSN 1450-216X Vol.75 No.4 (2012), pp. 472-481

[31] Tao, Jia, Shih, Albert, J., Ni, Jun, *Experimental Study of the Dry and Near-Dry Electrical Discharge Milling Processes,*Journal of Manufacturing Science and Engineering,Vol.130, February 2008

[32] Zhang, Yanzhen, Liu, Yonghong, Shen, Yang, Ji, Renjie, Cai, Baoping, Li, Hang, Wang, Fei, *A Review of the Current Understanding and Technology of Powder Mixed Electrical Discharge Machining (PMEDM),* International Conference on Mechatronics and Automation August 5 - 8, Chengdu, China, 2012

[33] Kansal, H.K., Singh, Sehijpal, Kumar, Pradeep, *Technology and research developments in powder mixed electric discharge machining (PMEDM),*Journal of Materials Processing Technology 184 (2007) 32–41

[34] Peças, Paulo, Henriques, Elsa, *Effect of the powder concentration and dielectric flow in the surface morphology in electrical discharge machining with powder-mixed dielectric (PMD-EDM),* Int J Adv Manuf Technol (2008)

[35] Lin, Yan-Cheng, Hwang, Lih-Ren, Cheng, Chao-Hsu, Su, Pao-Lin,*Effects of electrical discharge energy on machining performance and bending strength of cemented tungsten carbides,* journal of materials processing technology 2 0 6 (2 0 0 8) 491–499

[36] Obaciu, Gheorghe, *Sisteme si Techologii Pentru Prelucrari Prin Erozivne Electrica,* 2000

[37] Mahendran, S., Devarajan. T., Majdi, A., *A Review of Micro-EDM,* Proceedings of the International MultiConference of Engineers and Computers Scientists 2010 Vol II

[38] IIT Kharagpur, Module 9 Non Conventional Machining, Access at http://nptel.iitm.ac.in/courses/Webcourse-contents/IIT%20Kharagpur/Manuf%20Proc%20II/pdf/LM-39.pdf , 03/12/2012

[39] Abdulkaren, S., Khan, A., Zain, Z., *Effect of Machining Parameters on Surface roughness During Wet and Dry Wire-EDM of Stainless Steel,* Journal of Applied Sciences, 2011

[40] Cheke, P., Khedekar, D., Pawar, R., Kadam, M., *Comparative Performance of Wet and Near-Dry EDM Process for Machining of Oil Hardened Non Sinking Steel Material,* International Journal of Mechanical Engineering and Technology (IJMET), Vol. 3, Issue 2, May-August (2012)

[41] Besliu, Irina, Coteata, Margareta, *Characteristics of the Dry Electrical Discharge Machining,* Nonconventional Technologies Review - no.2/2009

[42] Roger Kern, Sinker Electrode Material Selection, Access at http://www.edmtodaymagazine.com/AAweb_2011/edm_flips/TechTipsM-J-8/TechTipsM-J-8.html, 5/12/2012

[43] Çogun, Can, Akaslan, S., *The Effect of Machining Parameters on Tool Electrode Edge Wear and Machining Performance in Electrical Discharge Machining (EDM),* KSME International Journal, Vol.16, No. 1

[44] Ozgedik, Ali, Cogun, Can, *An Experimental Investigation of Tool Wear in Electric Discharge Machining,* Int. J. Adv. Manufacturing Technology, 2006

[45] Ali, Ahsan, Haque, Md., *A study of Electrode Shape Configuration on the Performance of Die Sinking EDM,* International Journal of Mechanical and Materials Engineering (IJMME), Vol. 4 (2009), No. 1

[46] Aerospace Techniques Inc., *Medical*, Access at http://www.aerospacetechniques.com/medical.htm, 16/01/2013

[47] Milco Wire EDM, *Military EDM*, Access at http://www.milcowireedm.com/military-edm.htm, 16/01/2013

[48] Andreasen S., *C& H Machine And EDM SERVICES*, Access at http://www.c-hmachine.com/military-machining, 16/01/2013

[49] Janmance, P., Muttamara, A., *A Study of Hole Drilling on Stainless Steel AISI 431 by EDM Using Brass Tube Electrode,* International Transaction Journal of Engineering, Management, & Applied Sciences & Technologies, 2011

[50] Bamberg E., Heamawatanachai, S., *Orbital electrode actuation to improve efficiency of drilling micro-holes by micro-EDM,* Journal of materials processing technology 209 (2009)

[51] Diver, C., Atkinson, J., Helml, H., Li, L., *Micro-EDM drilling of tapered holes for industrial applications,* Journal of Materials Processing Technology 149 (2004)

[52] Chiang, H., Wang, J., *An analysis of overcut variation and coupling effects of dimensional variable in EDM process,* International Journal Advanced Manufacturing Technologies (2011)

[53] Advanced EDM Technology, *Microhole & Fasthole EDM Prototype Parts & Production Machines*, Access at http://www.aaedmcorp.com/applications.html, 20/01/2013

[54] Global Plastic Injection Molding, *Plastic Injection Molding and Mold Making*, Access at http://www.global-plastic-injection-molding.com/EDM-and-injection-molding.html, 20/01/2013

[55] SGL GROUP, *EDM apllications*, Access at http://www.sglgroup.com/cms/international/applications/plastics/applications/electrical-discharge-machining-edm.html?___locale=en, 20/01/2013

[56] Departement of Mechanical Engineering of the University of the Basque Country, Access at http://www.ehu.es/manufacturing/en-lineas-electroerosion-penetracion.php, 20/01/2013

[57] ZXTECH Rapid Prototyping Co.,Ltd. Access at http://zxtechrapidprototype.word press.com/2011/08/04/rapid-prototyping-technique-edm-electrical-discharge-machining/ , 20/01/2013

[58] Srivastava, V., Pandley, P., *Effect of process parameters on the performance of EDM process with ultrasonic assisted cryogenically cooled electrode,* Journal of Manufacturing Process, 2012

[59] Lin, Y., Lih-Ren, H., Chao-Hsu, C., Pao-Lin, S., *Effects of electrical discharge energy on machining performance and bending strength of cemented tungsten carbides,* Journal of Materials Processing Technology, 2006

[60] Eberhard, B., Dinesh, R., *Experimental investigation of wire electrical discharge machining of gallium-doped germanium,* Journal of Materials Processing Technology, 2008

[61] Sourabh, S., Choudhury, S., *Experimental investigation and empirical modeling of the dry electric discharge machining process,* International Journal of Machine Tools & Manufacture, 2009

[62] Joshi, S., Govindan, P., Malshe, A., Rajurkar, K., *Experimental characterization of dry EDM performed in a pulsating magnetic field,* ECIRP Annals - Manufacturing Technology, 2011

[63] Govindan, P., Joshi, S., *Analysis of micro-cracks on machined surfaces in dry electrical discharge machining,* Journal of Manufacturing Processes, 2012

[64] Ming, P., Zhu, D., Zeng, Y., Hu, Y., *Wear resistance of copper EDM tool electrode electroformed from copper sulfate baths and pyrophosphate baths*, International Journal Advanced Manufacturing Technology, 2010

[65] Kingred Electrical And Mechanical Technology Co., Ltd., *Applications of wire cut EDM machining*, Access at http://www.kingedms.com/blog/index.php/2011/11/application-of-wire-cut-edm-machining, 22/01/2013

[66] Retecon Lta., Access at http://www.retecon.co.za/gf-agiecharmilles, 20/01/2013

[67] Hozbon Motzer, *Medical devices*, Access at http://www.hobsonmotzer.com/Content/Industries_Served.asp, 23/01/2013

[68] Liu, K., Reynaerts, D., Lauwers, B., *Influence of the pulse shape on the EDM performance of Si3N4–TiN ceramic composite,* CIRP Annals - Manufacturing Technology, 2009

[69] Wire Cut Company, Inc, *EDM Machining Services*, Access at http://www.wirecutcompany.com, 23/01/ 2013

[70] Curtis Industries, Inc., *EDM notch reference standards*, Access at http://www.curtis-test.com/edm.htm, 23/01/2013

[71] Peterson Enterprises, *EDM products*, Access at http://petersonenterprises.com/processes products/machining/edm, 23/0172013

[72] Amorim, F., WEingaertner, W., *The behavior of graphite and copper electrodes on the finish die-sinking electrical discharge machining (EDM) of AISI P20 tool steel,* Journal of the Brazilian Society of Mechanical Sciences and Engineering, 2007

[73] Canadian Industrial Machinery, *Understanding non contact drilling*, Access at http://www.cimindustry.com/article/edm/edm-hole-drilling, 25/01/2013

[74] ZK simply genius, *Processing examples for the automotive industry*, Access at http://www.zk-system.com/products/genius-edm-systems/processing-examples/#fahrzeug, 27/01/2013

[75] Anon., *Micro Drilling using EDM and Advantages over Other Micro Drilling Technologies*, Access at http://zycon.hubpages.com/hub/Micro-Drilling-Using-EDM-and-Advantages-Over-Other-Micro-Drilling-Technologies, 27/072013

[76] Lee, H., Tai, T., *Relationship between EDM parameters and surface crack formation,* Journal of Materials Processing Technology, 2003

[77] Direct Industry catalog search , *Die Sinking EDM FO 350 MS - Mikron Agie Charmilles* , Access at http://pdf.directindustry.com/pdf/mikron-agie-charmilles/die-sinking-edm-fo-350-ms/14977-167192-_3.html, 03/02/2013

[78] Direct Industry catalog search, *GF AC Portfolio - Mikron Agie Charmilles* , Access at http://pdf.directindustry.com/pdf/mikron-agie-charmilles/gf-ac-portfolio/14977-307097-_45.html, 03/02/2013

[79] Direct Industry catalog search, *BA Series catalogue - Mitsubishi EDM,* Access at http://pdf.directindustry.com/pdf/mitsubishi-edm/ba-series-catalogue/26539-276295-_4.html, 03/02/2013

[80] Direct Industry catalog search, *Makino Europes Customer Magazine - MAKINO* , Acess at http://pdf.directindustry.com/pdf/makino/makino-europe-s-customer-magazine/22025-318875-_7.html, 03/02/2013

[81] Sarix 3D μEDM Milling, *Catalog High Precision 3D micro EDM milling machines*

[82] Anon., *Estatistica da técnologia EDM nos diversos ramos da engenharia*, Access at http://engenharianano tcnologica.blogspot.ro, 03/02/2013

[83] Sodick, *Company Information*, Access at http://www.sodick.com/ourcompany/company information, 05/02/2013

[84] Wysk, R., Niebel, *B., M, Manufacturing Processes: Integrated Product and Process Design: McGraw Hill, New York*, 2000, Access at http://www.mne.psu.edu/simpson/courses/ie466/ie466.robust.handout.pdf, 28/05/2013

[85] Kang, J., Hadfield, M., *Parameter optimization by Taguchi Methods for finishing advanced ceramic balls using a novel eccentric lapping machine*, Bournemouth University, School of Design, Engineering & Computing

[86] Vidal, C., Infante, V., Peças, P., Vilaça, P., *Applications of Taguchi Method in the Optimization of Friction Stir Welding parameters of an Aeronautic Aluminium Alloy, Departamento de Engenharia Mecânica, Instituto Superior Técnico, Lisboa, Portugal*

[87] Cymat Technologies Lda, *Aluminum Foam Technology Applied to Automotive Design,* www.cymat.com

[88] Singh, P., Raghukandan, K., *Electric discharge machining of Al–10%SiCP as-cast metal matrix composites*, Journal of Materials Processing Technology, 2004.

[89] Yan, B., Wang, C., *The machining characteristics of Al2O3/6061Al composite using rotary electro-discharge machining with a tube electrode,* Journal of Materials Processing Technology 95, 1999.

[90] Iosub, A., Axinte, E., Negoescu, F., A *study about micro-drilling by electrical discharge method of an Al/SiC hybrid composite*, International Journal of Academic Research, 2010.

[91] Mohan, B., Rajadurai, A., E*lectric discharge machining of Al–SiC metal matrix composites using rotary tube electrode,* Journal of Materials Processing Technology, 2004.

[92] Lin, Y., Chen, Y., Wang, D., *Optimization of machining parameters in magnetic force assisted EDM based on Taguchi method, journal of materials processing technology, 2009.*

[93] Lanfried, R., Kern, F., Gadow, R., *Electrical Discharge Machining of Alumina-Zirconia-TiC Composite with varying zirconia content,* Key Engineering Materials, 2013

[94] Madic, M., Radovanovic, M., Slatineanu, L., *Surface Roughness Optimization in* CO_2 *Laser Cutting by Using Taguchi Method,* U.P.B. Sci. Bull., Series D, 2013

[95] Roy, R., *Design of Experiments Using the Taguchi Approach: 16 Steps to Product and Process Improvement*

[96] Roy., R. *A Primer on the Taguchi Method,* Society of Manufacturing Engineers.

[97] Anon., *Design of experiments via Taguchi methods: orthogonal arrays,* Access at https://controls.engin.umich.edu/wiki/index.php/Design_of_experiments_via_taguchi_methods:_orthogonal_arrays, 05/06/2013